

January 2012

Crystal Engineering of Multi-Component Crystal Forms: The Opportunities and Challenges in Design

Heather Dawn Marie Clarke

University of South Florida, hdclarke@mail.usf.edu

Follow this and additional works at: <http://scholarcommons.usf.edu/etd>



Part of the [American Studies Commons](#), and the [Chemistry Commons](#)

Scholar Commons Citation

Clarke, Heather Dawn Marie, "Crystal Engineering of Multi-Component Crystal Forms: The Opportunities and Challenges in Design" (2012). *Graduate Theses and Dissertations*.
<http://scholarcommons.usf.edu/etd/4013>

This Dissertation is brought to you for free and open access by the Graduate School at Scholar Commons. It has been accepted for inclusion in Graduate Theses and Dissertations by an authorized administrator of Scholar Commons. For more information, please contact scholarcommons@usf.edu.

Crystal Engineering of Multi-Component Crystal Forms: The Opportunities and
Challenges in Design

by

Heather D. Clarke

A dissertation submitted in partial fulfillment
of the requirements for the degree of
Doctor of Philosophy
Department of Chemistry
College of Arts and Sciences
University of South Florida

Major Professor: Michael J. Zaworotko, Ph.D.
Wayne C. Guida, Ph.D.
Brian D. Moulton, Ph.D.
Ning Shan, Ph.D.

Date of Approval:
April 6, 2012

Keywords: Pharmaceutical cocrystal, crystalline hydrates, polymorphs, supramolecular
chemistry and nutraceuticals

Copyright © 2012, Heather D. Clarke

Dedication

Now to Him who is able to do immeasurably more than all we ask or imagine, according to His power that is at work within us, to Him be glory in the church and in Christ Jesus throughout all generations, for ever and ever! Ephesians 3:20-21

Acknowledgement

I thank the Lord for sustaining and leading me throughout this program. My deepest gratitude goes to Professor Michael J. Zaworotko for his guidance and mentorship. Your leadership has enabled me to grow and mature scientifically. To the members of my committee, Dr. Wayne Guida, Dr. Brian Moulton and Dr. Ning Shan, I am grateful for your significant contribution in my growth and development.

To the members of the cocrystal and MOF lab, I would like to say thank you for the fruitful discussions. I am grateful to Dr. Kapildev K. Arora, Dr. Łukasz Wojtas for their help with single crystal X-ray crystallography. I thank the Department of Chemistry for their support throughout the years. To Aunty Molly, you have instilled in me to pursue “excellence in all things!” Lastly, to my husband, Zak you have been with me through the valley and encouraged me throughout, I want you to know that I couldn’t have completed this without you.

Table of Contents

List of Tables	iv
List of Figures	v
Abstract	viii
Chapter 1: Introduction	
1.1 Relevance of crystal form in pharmaceutical science	1
1.2 Drug Dissolution and Bioavailability	3
1.3 Types of Crystal Forms	5
1.3.1 Hydrates and Solvates	5
1.3.2 Polymorphs	5
1.3.3 Salts	6
1.3.4 Pharmaceutical cocrystals	7
1.4 Supramolecular Chemistry	9
1.5 Crystal Engineering	11
1.6 Graph Set Analysis and Supramolecular Synthon	12
1.7 Cambridge Structural Database	13
1.8 Cocrystal	15
1.8.1 Definition	15
1.8.2 History	16
1.8.3 Designing cocrystals	17
1.8.4 Cocrystal synthesis	17
1.9 Impact of Pharmaceutical Cocrystals	19
1.9.1 Solubility	19
1.9.2 Bioavailability	21
1.9.3 Hydration Stability	22
1.9.4 Mechanical properties	23
1.10 Overview of Dissertation	23
1.11 References	26

Chapter 2: A Crystal Engineering Study of Gallic Acid and Ferulic Acid as Cocrystal Formers

2.1	Introduction	34
2.2	Materials and Methods	37
	2.2.1 Materials	37
	2.2.2 Preparation of cocrystals	38
	2.2.3 Methods	40
2.3	Results	49
2.4	Discussion	59
2.5	Conclusion	62
2.6	References	63

Chapter 3: Crystal Engineering of Isostructural Quaternary Multi-Component Crystal Forms of Olanzapine.

3.1	Introduction	68
3.2	Materials and Methods	70
	3.2.1 Materials	70
	3.2.2 Preparation of cocrystals	71
	3.2.3 Methods	72
3.3	Results	74
3.4	Discussion	77
3.5	Conclusion	87
3.6	References	88

Summary	94
---------	----

Appendix 1: Copyright Approval	98
--------------------------------	----

Appendix 2: Publication 1: Structure-Stability Relationships in Cocrystal Hydrates: Does the Promiscuity of Water Make Crystalline Hydrates the Nemesis of Crystal Engineering?	103
---	-----

Appendix 3: Publication 2: Polymorphism in Multiple Component Crystals: Forms III and IV of Gallic Acid Monohydrate.	120
--	-----

Appendix 4: Supplementary Information: A Crystal Engineering Study of Gallic Acid and Ferulic Acid as Cocrystal Formers.	124
--	-----

List of Tables

Table 1.1:	Strength of Non-covalent Interactions.	10
Table 2.1	Crystallographic data and structure refinement parameters for the cocrystals presented herein.	45
Table 2.2	Selected hydrogen bond distances and parameters of cocrystals.	47
Table 2.3	Comparison of supramolecular homosynthon versus supramolecular heterosynthon of carboxylic acids with primary and secondary amides.	48
Table 3.1	Refcodes for crystal structures of olanzapine deposited in the CSD.	76
Table 3.2	Crystal forms of olanzapine that exhibits packing A.	80
Table 3.3	Crystal forms of olanzapine that exhibits packing B.	80
Table 3.4	Crystal forms of olanzapine that exhibits packing C.	80
Table 3.5	Crystal forms of olanzapine that exhibits packing D.	81
Table 3.6	CSD statistics of crystal forms containing four distinct molecular chemical entities	86

List of Figures

Figure 1.1:	Steps in the selection of crystal form in the development of the API.	1
Figure 1.2:	Schematic representation of the types of crystal forms exhibited by APIs.	2
Figure 1.3:	Reasons why new drug candidates fail in development.	3
Figure 1.4:	Comparison of BCS classification of marketed drugs and new drug candidates.	3
Figure 1.5:	The Biopharmaceutical Classification System (BCS)	4
Figure 1.6:	Illustration of (a) carboxylic acid supramolecular homosynthon and (b) amide supramolecular homosynthon.	14
Figure 1.7:	Illustration of (a) carboxylic acid-amide supramolecular heterosynthon and (b) carboxylic acid-aromatic nitrogen supramolecular heterosynthon.	15
Figure 1.8:	Interaction between 9-methyladenine and 1-methylthymine molecules.	16
Figure 1.9:	Dissolution profile of pharmaceutical cocrystals of itraconazole.	20
Figure 1.10:	Dissolution profile of pharmaceutical cocrystals of fluoxetine HCl.	22
Figure 2.1:	Cocrystal formers used herein, abbreviated as follows: INZ, ADN, DMP, TBR, URE, GAH.	37
Figure 2.2:	High-resolution synchrotron powder diffraction data (dots) and Rietveld fit of the data for GALADN . The lower trace is the difference, measured minus calculated, plotted to the same vertical scale.	44
Figure 2.3:	(a) Crystal packing in GALINZ reveals form H-bonded tapes that are sustained by $\text{COOH} \cdots \text{N}_{\text{basic}}$ supramolecular heterosynthons (b) Illustration of bilayers of GALINZ sheets.	49

Figure 2.4:	(a) Phenolic homodimers of GAL molecules acts as a donor and an acceptor to DMP molecules (b) $R^3_3(9)$ trimeric motif involving two GAL molecules and a DMP molecule (c) Crystal packing in GALDMP reveals a 2D network of GAL and DMP molecules.	51
Figure 2.5:	Crystal packing in GALADN reveals form H-bonded interactions between the carboxylic acid moiety of GAL molecules and the aminopyridine moiety of ADN molecules.	52
Figure 2.6:	Crystal packing in GALURE reveals molecular tapes of heterodimers of GAL and URE molecules.	53
Figure 2.7:	(a) Crystal packing in GALGAH reveals undulating tapes sustained by dimers of GAL molecules linked by GAH molecules to form sheets (b) Illustration of sheets interconnected by homodimers of GAH molecules.	54
Figure 2.8:	(a) Crystal packing in FERADN reveals two point recognition supramolecular heterosynthons between the acid moiety of FER molecule and the amine and the basic nitrogen moiety of the ADN molecule (b) Crystal packing of FERADN is that of a 3D interpenetrated network.	55
Figure 2.9:	(a) Crystal packing in FERINZ sustained by $COOH \cdots N_{basic}$ supramolecular heterosynthons (b) Herring bone pattern of FERINZ .	56
Figure 2.10:	Crystal packing in FERURE reveals amide-amide supramolecular homosynthons between URE molecules to generate tapes that are interconnected by FER molecules.	57
Figure 2.11:	Crystal packing in FERGAH reveals molecular tapes of amide-amide supramolecular homosynthons between GAH molecules interconnected by FER molecules.	58
Figure 2.12:	Crystal packing of FERTBR · H₂O reveals that FERTBR heterodimers are connected by water molecules.	59
Figure 3.1:	Chemical structures of olanzapine and cocystal formers used herein.	71
Figure 3.2:	Crystal packing view along <i>a</i> axis of (a) OLANAM.IPA.4H₂O , (b) OLASAM.IPA.4H₂O and (c) OLAPBNZ.IPA.4H₂O exhibiting a tetrameric catemer of water molecules that is hydrogen bonded to four OLA molecules. The tetrameric catemer of water molecules offers 4 hydrogen bond donors and 2 hydrogen bond acceptors to complement a pair of olanzapine molecules. The isopropyl acetate	75

and the cocrystal former (**NAM**, **SAM** or **PHBNZ**) hydrogen bond to each side of the tetrameric catemer of water molecules.

- Figure 3.3: Crystal packing view along *c* axis of **OLANAM.IPA.4H₂O**, (b) **OLASAM.IPA.4H₂O** and (c) **OLAPHBNZ.IPA.4H₂O** showing how the tetrameric catemers of water molecules are terminated by the cocrystal former (**NAM**, **SAM** or **PHBNZ**). The **NAM**, **SAM** and **PHBNZ** molecules form dimers to extend the structure. In each case, two olanzapine molecules are omitted for clarity. 75
- Figure 3.4: Crystal packing of **OLANAM.IPA.4H₂O**, (b) **OLASAM.IPA.4H₂O** and (c) **OLAPHBNZ.IPA.4H₂O** showing a herring bone pattern of pairs of olanzapine enantiomers hydrogen bonded to four water molecules. **NAM**, **SAM**, **PHBNZ** and isopropyl acetate molecules omitted for clarity. 76
- Figure 3.5: Crystal packing of olanzapine anhydrate form I showing olanzapine enantiomers sustained by NH⁺⋯N hydrogen bond interactions along the *c* axis. 77
- Figure 3.6: Two types of supramolecular heterosynthons exhibited in crystal structures of olanzapine dihydrate. 79
- Figure 3.7: (a) Crystal structure of olanzapine dihydrate form D exhibiting packing A where a cyclic tetramer of water molecules hydrogen bonds to four olanzapine molecules along the *b* axis. (b) Sheets of olanzapine molecules eclipse one another; water molecules deleted for clarity. 81
- Figure 3.8: Crystal packing of (a) olanzapine dihydrate form B (b) olanzapine sesquihydrate form II and (c) olanzapine methanol solvate exhibiting packing B, wherein the solvent molecules are arranged such that they hydrogen bond to four olanzapine molecules. (d) Illustrates sheets that are arranged in a herring bone pattern and stack in an eclipsed manner; solvent molecules deleted for clarity. 82
- Figure 3.9: Crystal forms of (a) olanzapine sesquihydrate form I (b) olanzapine DMSO solvate and (c) olanzapine methanol monohydrate exhibiting packing C where the solvent molecules form bridges to hydrogen bond to four olanzapine molecules. (d) Illustrates adjacent sheets that stack in a staggered manner; solvent molecules deleted for clarity. 83
- Figure 3.10: Packing D exhibiting olanzapine cation interacts with nicotinate and benzoate anions via charge assisted NH⁺⋯COO⁻ hydrogen bonds along the *a* axis. 84

Abstract

There is heightened interest to diversify the range of crystal forms exhibited by active pharmaceutical ingredients (APIs) in the pharmaceutical industry. The crystal form can be regarded as the Achilles' heel in the development of an API as it directly impacts the physicochemical properties, performance and safety of the API. This is of critical importance since the crystal form is the preferred method of oral drug delivery by industry and regulatory bodies. The ability to rationally design materials is a lucrative avenue towards the synthesis of functional molecular solids with customized physicochemical properties such as solubility, bioavailability and stability. Pharmaceutical cocrystals have emerged as a new paradigm in pharmaceutical solid form development because they afford the discovery of novel, diverse crystal forms of APIs, generate new intellectual property and modify physicochemical properties of the API. In addition, pharmaceutical cocrystals are amenable to design from first principles of crystal engineering.

This dissertation focuses on the crystal engineering of multi-component crystal forms, in particular pharmaceutical cocrystals and crystalline hydrates. It addresses: (i) the factors involved in the selection of cocrystal formers (ii) design strategies for APIs that exhibit complexity, (iii) the role of water molecules in the design of multi-component crystal forms and (iv) the relationship between the crystal structure and thermal stability of crystalline hydrates.

In general, cocrystal former libraries have been limited to pharmaceutically acceptable substances. It was investigated to expand this library to include substances with an acceptable toxicity profile such as nutraceuticals. In other words, can nutraceuticals serve as general purpose cocrystals formers? The model compounds, gallic acid and ferulic acid, were selected since they possess the functional moieties carboxylic acids and phenols, that are known to form persistent supramolecular synthons with complementary functional groups such as basic nitrogen and amides. The result yielded pairs of cocrystals and revealed the hierarchical nature of hydrogen bonding between complementary functional groups.

In general, pharmaceutical cocrystals have been designed by determining the empirical guidelines regarding the hierarchy of supramolecular synthons. However, this approach may be inadequate when considering molecules that are complex in nature, such as those having a multiplicity of functional groups and/or numerous degrees of conformational flexibility. A crystal engineering study was done to design multi-component crystal forms of the atypical anti-psychotic drug olanzapine. The approach involved a comprehensive analysis and data mining of existing crystal structures of olanzapine, grouped into categories according to the crystal packing exhibited. The approach yielded isostructural, quaternary multi-component crystal forms of olanzapine. The crystal forms consist of olanzapine, the cocrystal former, a water molecule and a solvate.

The role of water molecules in crystal engineering was addressed by investigating the crystal structures of several cocrystals hydrates and their related thermal stability.

The cocrystal hydrates were grouped into four categories based upon the thermal stability they exhibit and it was concluded that no structure/stability correlations exist in any of the other categories of hydrate. A Cambridge Structural Database (CSD) analysis was conducted to examine the supramolecular heterosynthons that water molecules exhibit with two of the most relevant functional groups in the context of active pharmaceutical ingredients, carboxylic acids, and alcohols. The analysis suggested that there is a great diversity in the supramolecular heterosynthons exhibited by water molecules when they form hydrogen bonds with carboxylic acids or alcohols. This finding was emphasized by the discovery of two polymorphs of gallic acid monohydrate to it the first tetramorphic hydrate for which fractional coordinates have been determined. Analysis of the crystal structures of gallic acid monohydrate polymorphs revealed that forms I and III exhibit the same supramolecular synthons but different crystal packing and forms II and IV exhibit different supramolecular synthons. Therefore, the promiscuity of water molecules in terms of their supramolecular synthons and their unpredictable thermal stability makes them a special challenge in the context of crystal engineering.

Chapter 1: Introduction

1.1 Relevance of crystal form in pharmaceutical science

The selection of crystal form is a critical step in pharmaceutical development. Indeed, crystallization is generally used as a separation or purification method in the production of substances due to its high stability and ease in processing. The vast majority of active pharmaceutical ingredients (APIs) are isolated in the solid form and the selection of crystal form is invariably considered to be the first step in formulation development (Fig. 1.1). Therefore, the control of the crystal form and the size and shape of the crystal become of paramount interest. The crystal form influences downstream process applications such as filtration, drying, milling, granulation and tableting. More importantly, physicochemical properties such as bioavailability, solubility and dissolution rate are strongly dependent on the crystal form of the API.

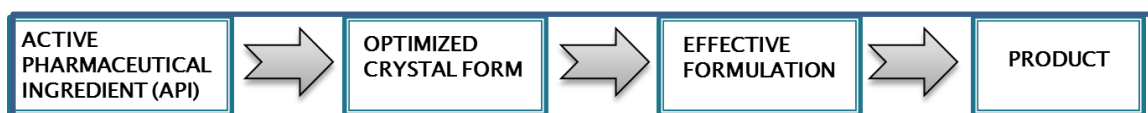


Figure 1.1: Steps in the selection of crystal form in the development of the API.

The ubiquitous nature of APIs i.e. they contain multiple hydrogen bonding sites makes them inherently predisposed to form multiple crystal forms. These crystal forms include but are not limited to salts, hydrates, solvates, polymorphs and pharmaceutical

cocrystals (Fig.1.2). The diversity of crystal forms of an API creates opportunities to customize the physicochemical properties of that API. High-throughput screening has been generally used to explore crystal forms of APIs since it accelerates the discovery of diverse crystal forms and provides an understanding of the factors that govern crystallization.¹ However, *in vitro* screening in solvents such as dimethyl sulfoxide and polyethylene glycol to identify as many hits as possible resulted in new drug candidates exhibiting poor aqueous solubility and/or dissolution rate.² As bioavailability is a function of solubility, poor oral bioavailability has become characteristic of many new drug candidates.^{3,4} In fact, drug candidates with poor bioavailability are the primary reason why 41% of new drug candidates fail in preclinical and clinical development (Fig. 1.3)⁵ and 90% of new drug candidates fall into BCS class II and class IV (Figure 1.4).⁶ Therefore, from a crystal engineering perspective, the design of pharmaceutical solids with desired physicochemical properties becomes relevant.

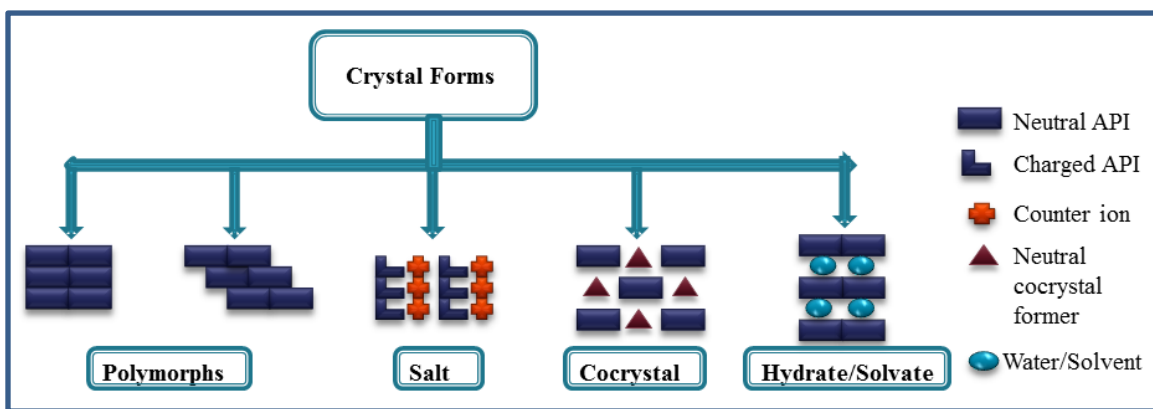


Fig. 1.2: Schematic representation of the types of crystal forms exhibited by APIs.

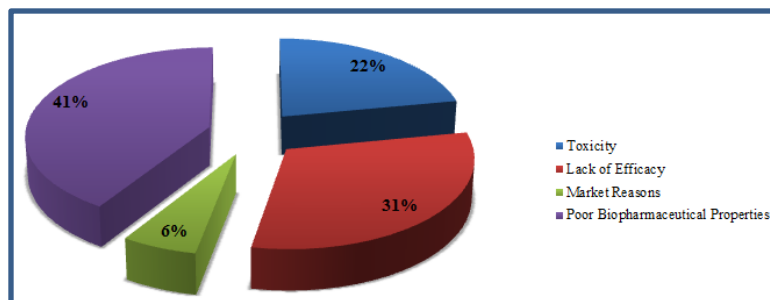


Figure 1.3: Reasons why new drug candidates fail in development.

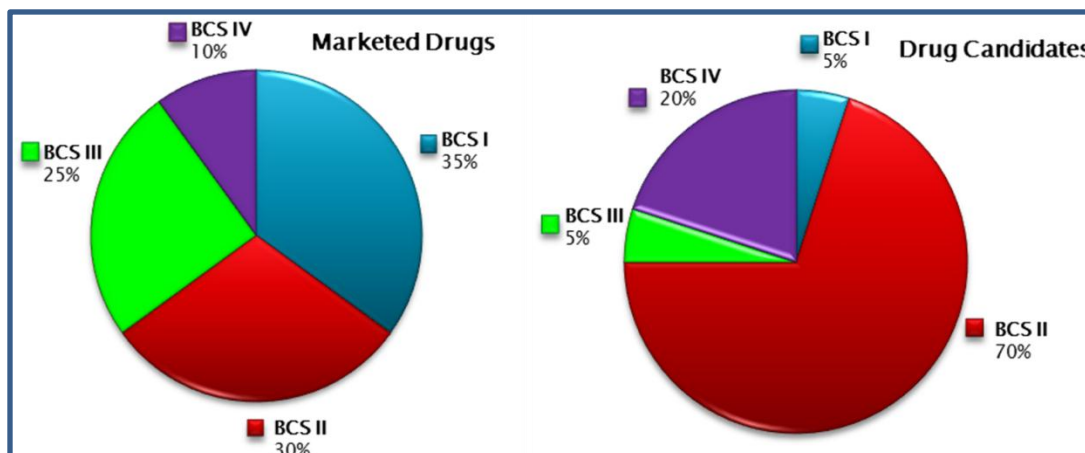


Figure 1.4: Comparison of BCS classification of marketed drugs and new drug candidates.

1.2 Drug Dissolution and Bioavailability

Drug dissolution was first modeled by Noyes and Whitney. They proposed the Noyes and Whitney equation where the rate of dissolution is proportional to the difference between the solution concentration at time t and the equilibrium solubility.⁷ This equation was later modified to become the Noyes-Whitney-Nernst equation and denoted that, with all other parameters being constant, the rate of drug dissolution is proportional to the thermodynamic solubility of the drug.⁸ Amidon and coworkers developed the

Biopharmaceutical Classification System (BCS) which proposes that the bioavailability of the API is a function of solubility or dissolution rate and membrane permeability.⁹ According to the BCS system, APIs are categorized into four categories: (1) high permeability, high solubility; (2) high permeability, low solubility; (3) permeability, high solubility and (4) low permeability, low solubility (Figure 1.5). A drug substance is considered highly soluble when the highest dose strength is soluble in ≤ 250 ml water over a pH range of 1 to 7.5 and highly permeable when the extent of absorption in humans is determined to be $\geq 90\%$ of an administered dose, based on mass-balance or in comparison to an intravenous reference dose.

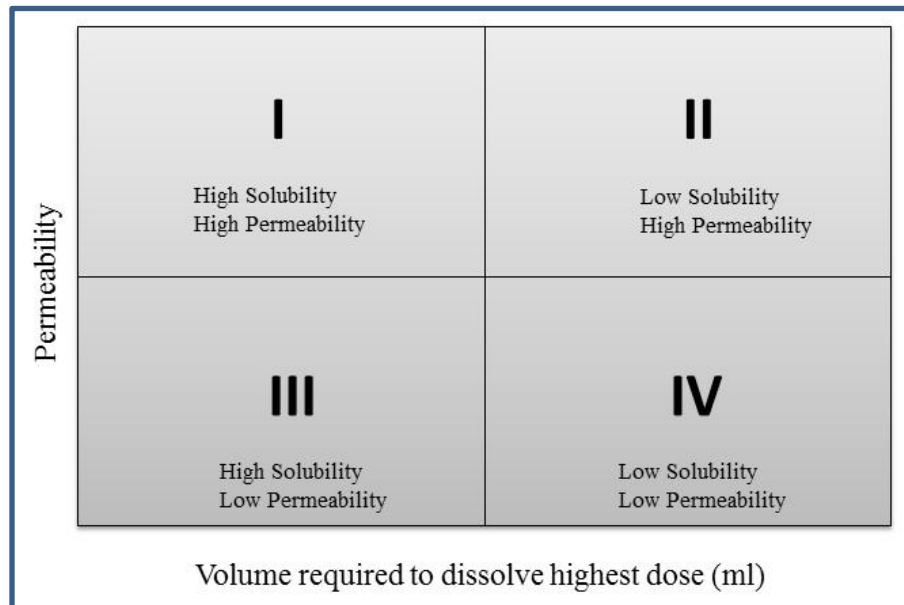


Fig. 1.5: The Biopharmaceutical Classification System (BCS)

1.3 Types of Crystal Forms

1.3.1 Hydrates and Solvates

Solvates are molecular complexes where one or more solvent molecules are incorporated within the crystal lattice in stoichiometric proportions. It is referred to as a hydrate when the solvent of crystallization is a water molecule.¹⁰ Hydrates represent about 10% of the structures archived in the CSD¹¹ and it has been suggested that approximately 33% of organic compounds form hydrates, whereas solvates are less prevalent (10%).¹² The adventitious nature of the water molecule allows it to be easily incorporated within the crystal lattice due to its size and versatile hydrogen bonding capabilities. The water molecule can act as a guest where the water molecule is not firmly bound within the crystal structure or the water molecule can play an integral role to stabilize the crystal structure where there is an imbalance in the number of hydrogen bond and donors.¹³ APIs are prone to hydrate formation due to their inherent nature, i.e. they possess many hydrogen bond donors and acceptors and it is estimated that approximately one third of APIs are capable of forming hydrates during pharmaceutical manufacturing.¹⁴ Stability is a matter of concern for pharmaceutical hydrates because they can undergo solid phase transition under storage conditions and therefore alter the physicochemical properties.

1.3.2 Polymorphs

Polymorphism refers to the ability of a compound to exist in more than one crystal form. The earliest reported polymorphic compound was benzamide discovered in

1832 by Wöhler and Liebig. The phenomenon of polymorphism is a scientific challenge in the pharmaceutical industry and its adverse effects is revealed in the prominent examples of rantidine hydrochloride and ritonavir.^{15,16} The relevance of polymorphism was heightened by the patent litigation between Glaxo and Novopharm, where Glaxo sued for the infringement of its patent of a form II polymorph of rantidine hydrochloride. In addition to legal and regulatory implications, polymorphism also affects the physicochemical properties of an API such as dissolution rate. This is exemplified by the API ritonavir where after the launch of the drug ritonavir by Abbot Laboratories, a more stable, previously unknown form II was discovered. The dissolution properties of the latter were significantly different in comparison to the previous form forcing the company to reformulate the API resulting in a loss of sales. Polymorphism can be divided into two classes: packing polymorphism and conformation polymorphism. Packing polymorphism occurs when rigid molecules exhibit more than one packing arrangement caused by different supramolecular synthons or they retain the same supramolecular synthons but exhibit different crystal packing. Conformational polymorphism is when molecules exists in more than one conformation in the solid state and is exemplified by 5-methyl-2-[(2-nitrophenyl)amino]-3-thiophenecarbonitrile, ROY where it crystallizes in eight polymorphic forms.

1.3.3 Salts

Salt formation has been the primary means to modify the physicochemical properties of an API. Indeed, approximately, 50% of marketed APIs are administered as salts.¹⁷ Salts are formed when a compound that is ionized in solution forms a strong

ionic interaction with an oppositely charged counterion. Its success and stability is dependent on the relative strength of the acid or base and the acidity and basicity constant of the components involved.¹⁸ The general rule of thumb for salt formation is that the acid ionization constant, pK_a , between the acid and the base should be different by at least two or three units. The limitation of this is that the pK_a values are only valid under the solution equilibrium conditions at which they were determined. Salt forms are advantageous because they enhance the physicochemical properties of the API and their preparation is relatively simple. However, its formation is limited to the presence of ionizable groups on the API and it compromises the intrinsic activity of the API. In addition, although hydrochloride salts are the most common anionic salt forming species, they may not necessarily enhance the solubility in a chloride containing solvent medium because of common ion effect. For example, the hydrochloride salt of the Prazosin, has an aqueous solubility of 1.4 mg/ml but 0.037 mg/ml solubility in 0.1M HCl solution.

1.3.4 Pharmaceutical Cocrystal

Pharmaceutical cocrystals,^{19,20} multi-component crystals in which at least one component is a neutral API and the cocrystal former is a pharmaceutically acceptable ion or molecule, have recently been added to the landscape of crystal forms of APIs. Early literature on pharmaceutical cocrystals focused primarily on the crystal structures of pharmaceutical cocrystals. Perhaps, the earliest reported pharmaceutical cocrystal is the 1934 French patent which disclosed cocrystals of barbiturates.²¹ Caira and others reported the potential of complexes of sulphonamide drugs in drug development²² and Whitesides reported the supramolecular assemblies of melamine and barbiturates

derivatives.²³ In 2002, Oswald and coworkers demonstrated the cocrystallization of the drug paracetamol²⁴ and shortly after, Zaworotko et al reported pharmaceutical cocrystals of the APIs ibuprofen, flurbiprofen and aspirin.²⁵ In recent years, pharmaceutical cocrystals have emerged as a new paradigm in pharmaceutical solid form development as they are an effective means of altering physicochemical properties such as solubility, bioavailability and stability of APIs.²⁶ Indeed, the significant impact of pharmaceutical cocrystals has resulted in the recent release of a FDA draft guidance concerning the regulatory classification of pharmaceutical cocrystals.²⁷ The draft proposed the definition and classification of pharmaceutical cocrystals.

Pharmaceutical cocrystals are advantageous in four-fold because: (1) they are susceptible to design since the directionality and selectivity of the hydrogen bond allows for the rational construction of new functional solid forms (2) enables a diverse number of crystal forms of a given API from a wide range of pharmaceutically acceptable cocrystal formers and the formation is not limited to the nature of the molecule e.g. presence of ionizable groups on the API (3) fine-tunes the structural and physicochemical properties of the solid and therefore creates intellectual property opportunities and (4) the intended intrinsic activity of the API is preserved.

1.4 Supramolecular Chemistry

Molecular chemistry, thus, has established its power over the covalent bond. The time has come to do the same over non-covalent intermolecular forces. Beyond molecular chemistry based on the covalent bond there lies the field of supramolecular chemistry, whose goal is to gain control over the intermolecular bond.

Jean Marie Lehn²⁸

Supramolecular chemistry, described as “chemistry beyond the molecule” expands over several science disciplines such as classical inorganic and organic chemistry, material science and physics. The beginning of supramolecular chemistry can be traced back to the late 19th century through the introduction of transition-metal coordination chemistry by Werner,²⁹ Emil Fischer’s lock and key mechanism in enzyme reactions and the discovery of cyclodextrins by Hebd. However, it was the pioneering works of Pederson,³⁰ Lehn and Cram in the discovery of crown ethers that ignited interest in supramolecular chemistry. Supramolecular chemistry extends beyond the realm of atomic and molecular chemistry to afford highly complex, well-defined supramolecular entities.³¹ It emphasizes the use of intermolecular interactions in the self-assembly of molecules governed by their chemical and geometrical factors.

Intermolecular Interaction	Strength (kJ/mol)
Ion-Ion	100-350
Ion-Dipole	50-200
Hydrogen Bond	4-120
Dipole-Dipole	5-50
π - π Stacking	<50
Van der Waals	<5

Table 1.1: Strength of Non-covalent Interactions.

These intermolecular interactions include hydrogen bonding, π - π stacking, coordinative bonds, dipolar interactions and van der Waals forces (Table 1.1).³² They play a critical role in the structure and function of biological systems such as protein folding and enzyme catalysis. The hydrogen bond is perhaps the most significant intermolecular interaction and is fundamental in the stability of the double helix structure in DNA, the best known self-assembling supramolecular entity in nature. The hydrogen bond is defined as, “an attractive interaction between a hydrogen atom from a molecule or a molecular fragment X–H in which X is more electronegative than H, and an atom or a group of atoms in the same or a different molecule, in which there is evidence of bond formation.”³³ The hydrogen bond has been extensively studied and is viewed as a synthetic vector in the structural assembly of molecules. Its strength, selectivity and directionality influence the crystal packing of molecules thereby determining its physical and chemical properties. Research in the understanding of the nature and role of these

intermolecular interactions in the context of crystal packing stealthily increased with the advancement of X-ray crystallography, giving rise to a new scientific genre, crystal engineering.

1.5 Crystal Engineering

“Crystallization of organic ions with metal-containing complex ions of suitable sizes, charges and solubilities results in structures with cells and symmetries determined chiefly by packing of complex ions. These cells and symmetries are to a good extent controllable: hence crystals with advantageous properties can be ‘engineered’ ...”

Pepinsky, 1955

Crystal engineering, synonymous to solid state supramolecular synthesis, focuses on the synthesis and design of functional crystalline materials. It stems from the premise that the crystal, described as the perfect supermolecule,³⁴ supermolecule par excellence,³⁵ is the de facto manifestation of self-assembly of molecules. Although the term was coined in 1955 by Pepinsky,³⁶ it is the pioneering work by Gerald Schmidt in 1971 that is generally considered to be the birth of crystal engineering.³⁷ Schmidt studied photodimerization reactions of olefins in the solid state and determined that the photoreactivity was governed by the stereochemical vicinity between olefins rather than intrinsic electronic properties. He postulated that photochemical reactions occurred only if the distance between the C=C double bonds of adjacent molecules was between 3.5 and

4.2 Å and the stereochemistry at the nearest neighbor double bonds were either antiparallel (related by a crystallographic center of symmetry) or parallel (related by a translation axis). Schmidt's work revealed that the physical and chemical properties of crystalline solids were dependent on the packing of the molecules within the crystal lattice. Soon after, the focus shifted from the engineering of structures to the engineering of properties and in 1989, Desiraju defined crystal engineering as, "*the understanding of intermolecular interactions in the context of crystal packing and the utilization of such understanding in the design of new solids with desired physical and chemical properties.*"³⁸ Subsequently, the field has matured into an interdisciplinary scientific discipline with a wide scope of applications in areas such as catalysis,³⁹ energy storage,⁴⁰ electronics⁴¹ and pharmaceuticals.⁴²

1.6 Graph Set Analysis and Supramolecular Synthons

Seminal works by Etter and Desiraju were pivotal in understanding the nature of intermolecular interaction in molecular crystals. Etter used mathematical graph theory to delineate the nature of hydrogen bonding patterns and classify them into simpler notations known as graph set analysis. Graph set analysis is written in the format, $G^a_d(n)$ where G is the hydrogen bond motif and can be denoted as one of the following: (1) D: dimer or finite (2) C: chain (3) S: intramolecular (4) R: ring. The number of acceptors, donors and atoms are denoted a, d and n respectively. Through extensive studies of hydrogen bonding patterns of organic crystals, she devised empirical rules to define the hierarchical nature of hydrogen bonds: (1) all good proton donors and acceptors are used (2) six membered ring intramolecular hydrogen bonds will form in preference to

intermolecular hydrogen bonds and (3) the best proton donors and acceptors remaining after intramolecular hydrogen bonding will form intermolecular hydrogen bonds with each other.⁴³ Desiraju coined the term “supramolecular synthon” and it is defined as, “structural units within supermolecules which can be formed and/or assembled by known or conceivable intermolecular interactions.”⁴⁴ The concept was extended by Zaworotko into two distinct classes: supramolecular homosynths and supramolecular heterosynths.⁴⁵ Supramolecular homosynthon is the result of intermolecular interactions between identical self-complementary functional groups such as carboxylic acid dimers and amide dimers (Figure 1.6), whereas supramolecular heterosynthon are intermolecular interactions between two or more different but complementary functional groups such as carboxylic acid-amide and carboxylic acid-aromatic nitrogen (Figure 1.7). The concepts of graph set analysis and supramolecular synths and the systematic analysis of existing crystal structures is essential in crystal engineering and can be used as a prototypal tool in the design of crystalline solids. This is facilitated through the technique of database mining using the Cambridge Structure Database.⁴⁶

1.7 Cambridge Structural Database

The Cambridge Structural Database (CSD) is an established primary repository for the experimentally determined 3D structures of organic and organometallic compounds. It is a structural visualization and analysis software developed by the Cambridge Crystallographic Data Centre (CCDC). The CCDC was founded by the University of Cambridge in 1965 with the primary objective: “advancement and promotion of the science of chemistry and crystallography for the public benefit.” The

CSD comprises of over half a million structures making it a comprehensive and highly curated scientific resource for crystal engineering. The CSD facilitates reliable and fast retrieval, visualization and analysis of experimentally measured crystallographic data to further understand the behavior of molecules and intermolecular forces within a crystal. This knowledge is fundamental to crystal engineering as it gives information concerning the type of intermolecular interaction, the geometrical preferences, the directional characteristics and the types of supramolecular synthons involved.

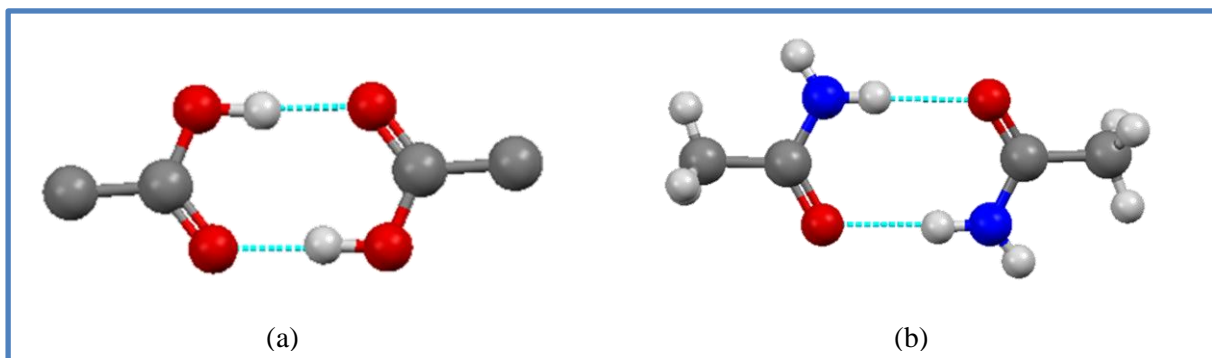


Figure 1.6: Illustration of (a) carboxylic acid supramolecular homosynthon and (b) amide supramolecular homosynthon.

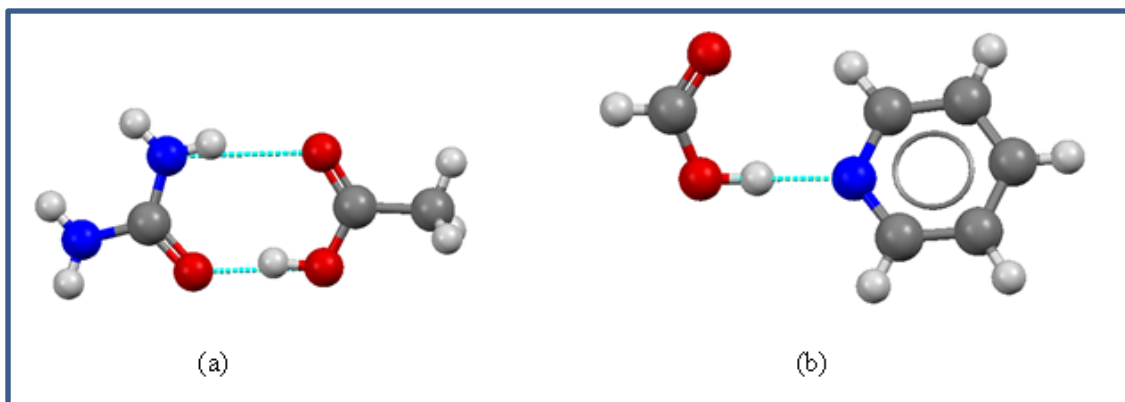


Figure 1.7: Illustration of (a) carboxylic acid-amide supramolecular heterosynthon and (b) carboxylic acid-aromatic nitrogen supramolecular heterosynthon.

1.8 Cocrystal

1.8.1 Definition

The definition of cocrystal is an active subject of debate. The debate started in 2003 when Desiraju expressed the unsuitability of the term co-crystal and suggested that the previously used terms such as molecular complexes should be adhered to.⁴⁷ Dunitz, however, stated that the term molecular complex is too vague and while the term “co-crystal” is not perfect, it has been irrevocably established.⁴⁸ He defined a co-crystal as “a crystal containing two or more components together.” Both Dunitz and Desiraju agreed that the term should be “co-crystal” in contrast to “cocrystal” to indicate togetherness of two components. Aakeroy offered a more restrictive definition in that the components of cocrystals must be neutral and exists as a solid at ambient conditions with a well-defined stoichiometry.⁴⁹ However, Bond found this definition unsatisfactory due to the restriction that all components must be solid.⁵⁰ Zaworotko proposed the definition, “a

stoichiometric multiple component crystal that is formed between two crystalline materials that are solids under ambient conditions. At least one of the components is molecular (target molecule) and forms a supramolecular synthon with the remaining component (cocrystal former).”

1.8.2 History

The earliest example of a cocrystal was quinhydrone, a complex formed between hydroquinone and quinone reported by Wohler in 1844.⁵¹ Subsequently, other examples of cocrystals were reported in the literature but were called organic molecular compounds⁵², heteromolecular crystals,⁵³ molecular complexes⁵⁴ and addition compounds.⁵⁵ The term ‘cocrystal’ was coined in 1967 to describe the hydrogen bonded complex formed 9-methyladenine and 1-methylthymine (Fig. 1.8)⁵⁶ and was later popularized through the works of Etter.⁵⁷ Cocrystals are of topical interest because they create an opportunity to address the hierarchy of intermolecular interactions and they have applications in pharmaceutical formulation, non-linear optics and green chemistry.

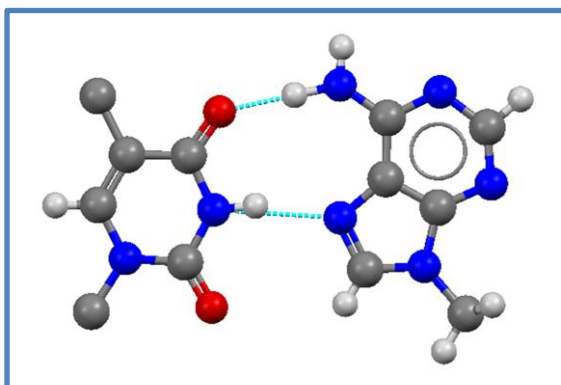


Figure 1.8: Interaction between 9-methyladenine and 1-methylthymine molecules.

1.8.3 *Designing Cocrystals*

The design of cocrystals utilizes the first principles of crystal engineering and self-assembly of molecules. It places emphasis on the hierarchy of supramolecular synthons by evaluating the reliability of intermolecular interactions between specific functional groups and analysis of the crystal packing. Design strategies, such as the supramolecular synthon approach comprises of examining the arrangement and frequency of occurrence of supramolecular synthons formed between functional groups. The supramolecular synthon approach consists of the following steps: (1) identifying the functional groups present on the target molecule (2) perform an empirical analysis of the supramolecular heterosynthons formed between complementary functional groups of experimental crystal structures using the CSD and (3) arrange in hierarchical order the robust or commonly occurring supramolecular synthons and select the cocrystal formers accordingly. This method is advantageous in delineating the hierarchy of supramolecular synthons between complementary functional groups.⁵⁸ Bis et al studied the preferential interaction between alcohols and aromatic nitrogen, N_{arom} in the presence of cyano functional groups.⁵⁹ Shattock and others focused on the ability of alcohols and carboxylic acids to form reliable supramolecular heterosynthons in the presence of competing functional moieties.⁶⁰ Kavuru and coworkers discussed the formation of charge assisted H bonds between carboxylates and weakly acidic hydroxyl moieties.⁶¹

1.8.4 *Cocrystal Synthesis*

Mechanochemistry, grinding of solids, has been used in the preparation of cocrystals since the 19th century. Also known as neat grinding or dry grinding,^{62,63} it is a

cost effective and environmentally-friendly technique and provides a cleaner alternative to conventional solution based approaches. Some of the early examples of cocrystals were produced by grinding which include the preparation of the quinhydrone cocrystal,²³ charge transfer complexes⁶⁴ and methyladenine and methylthymine cocrystal.⁶⁵ Shan and coworkers demonstrated a modified mechanochemistry technique known as solvent drop grinding (liquid assisted grinding) where the addition of minute amount of solvent increased kinetics of cocrystal formation.⁶⁶ Alternative methods for the preparation of cocrystals include melt crystallization, solution based methods such as slow evaporation, slurring and SonicSlurry,⁶⁷ supercritical fluid crystallization,⁶⁸ twin screw extrusion⁶⁹ and spray drying.⁷⁰ Systematic studies have been implemented to understand the thermodynamic factors in the formation of cocrystals. Nair pioneered reaction crystallization, where the formation of the cocrystal is driven by the non-stoichiometric concentration of the individual components.⁷¹ She suggested that the solubility of the cocrystal can be represented as the product of the component concentrations.

$$K_{sp} = [A]^a [B]^b \quad (1)$$

Where [A] and [B] are molar concentrations of individual components at equilibrium

Therefore, an increase in the concentration of the more soluble component in excess of their stoichiometric composition will lower the solubility of the stable cocrystal and hence it will crystallize out of solution. Chiarella and coworkers used ternary phase diagrams to deduce that cocrystal formation takes place in the region of the phase diagram where the cocrystal is the stable solid phase.⁷² They rationalized that screening of new cocrystal of a particular system should be determined by the relative solubilities of the two components rather than stoichiometry. ter Horst and coworkers determined

that cocrystal formation can be assessed by comparing the saturation temperature corresponding to where both components are saturated and the saturation temperature of the pure components.⁷³ Given that the saturation temperature of both components is higher than the saturation temperature of pure components indicates that a stable, less soluble cocrystal phase has been formed. Zhang et al reported a suspension/slurry technique known as solution mediated phase transformation.⁷⁴ This method is based on the principle that when crystals of both single components are present in excess, the cocrystal forms spontaneously.

1.9 Impact of Pharmaceutical Cocrystals

1.9.1 Solubility

One of the earliest examples of the solubility of a drug complex, digoxin-hydroquinone was reported by Higuchi and Ikeda in 1974.⁷⁵ Although it was not termed a cocrystal, the authors showed the improvement of solubility of the complex in comparison to the free drug digoxin. However, itraconazole is considered to be the first example of an API that addressed the use of pharmaceutical cocrystals to modify physicochemical properties of APIs. Almarrson et al reported the dissolution studies of the antifungal drug itraconazole with 1,4-dicarboxylic acids. All the cocrystals revealed an enhanced dissolution of 4-20 fold higher than the itraconazole free base and the dissolution rate of itraconazole-malic acid was comparative to the marketed amorphous form (Fig. 1.9).⁷⁶ In 2004, Childs and others demonstrated the use of pharmaceutical cocrystals to significantly modify the physicochemical properties of the API, fluoxetine

HCl.⁷⁷ Fluoxetine HCl was cocrystallized with benzoic acid, succinic acid and fumaric acid. The dissolution profiles of the cocrystals revealed that they had an aqueous solubility that was 50% less (benzoic acid), comparable (fumaric acid) or 2 fold higher (succinic acid) than the crystalline salt of the API (Fig. 1.10). An intriguing observation in the dissolution profile of the pharmaceutical cocrystal of fluoxetine HCl and succinic acid was its “spring and parachute.” The “spring” illustrates a high energy form of the API which enables it to solubilize rapidly and the “parachute” is the transition from high energy forms to more stable crystal energy forms.⁷⁸ Since 2003, the ability to increase the solubility of APIs via pharmaceutical cocrystals has been reiterated through several studies.

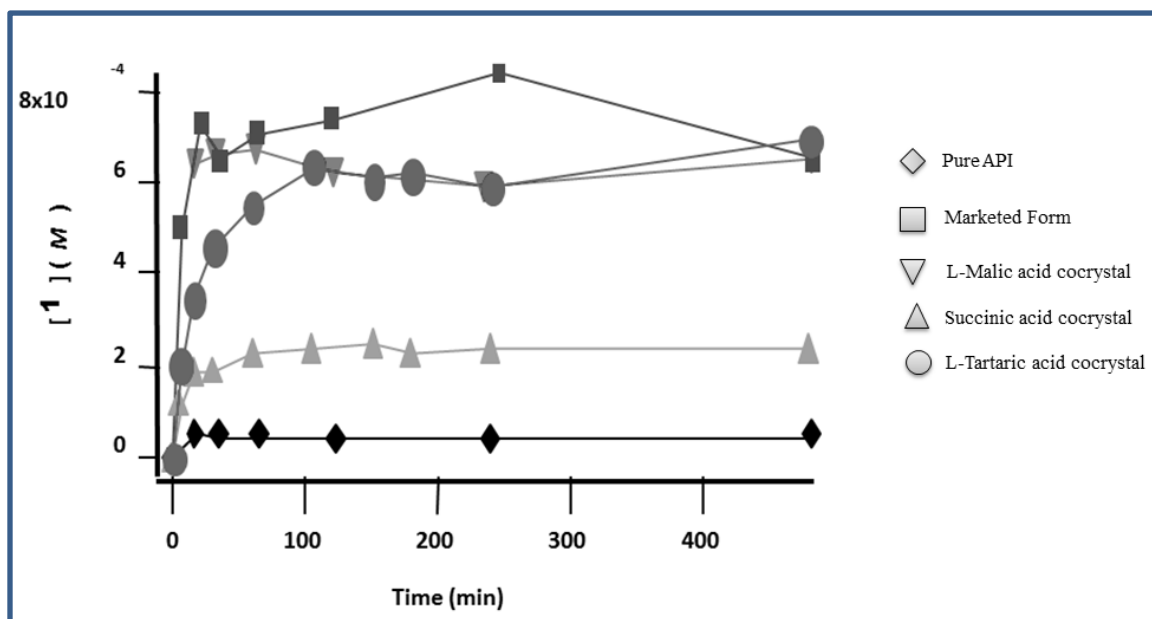


Fig. 1.9: Dissolution profile of pharmaceutical cocrystals of itraconazole.

1.9.2 Bioavailability

Seminal studies by Hickey and McNamara demonstrated that pharmaceutical cocrystals are a viable method to alter the pharmacokinetic profile of a drug. Hickey and coworkers reported higher exposure levels in dogs of the pharmaceutical cocrystal carbamazepine-saccharin in comparison to the marketed anhydrous form.⁷⁹ McNamara et al performed bioavailability studies in dogs on a 1:1 pharmaceutical cocrystal composing of a sodium channel blocker API and glutaric acid. The cocrystal exhibited a 3-fold increase in the plasma concentration in dose levels of 5 and 50mg/kg. In addition, the cocrystal exhibited an increase in the intrinsic dissolution rate of 18 times in contrast to the pure drug.⁸⁰ About the same time, In another study, L-883555, a phosphodiesterase IV inhibitor was cocrystallized with l-tartaric acid, and the cocrystal exhibited an area under the concentration– time curve (AUC) of 5.5 as compared to 0.24 exhibited by the free base.⁸¹ Bak et al described the pharmacokinetics of AMG517-sorbic acid cocrystal in Sprague-Dawley rats and at 500 mg/kg dose, the peak plasma concentration of AMG517 in the cocrystal was 7 times higher than the free base.⁸² Further pharmacokinetic studies of AMG517 with a series of carboxylic acids and amides showed improvement.^{83, 84} Investigation in the dissolution and bioavailability of lamotrigine revealed that the anhydrate and monohydrated cocrystal of lamotrigine-nicotinamide had lower serum concentration than the pure drug although the powder dissolution rates were higher.⁸⁵

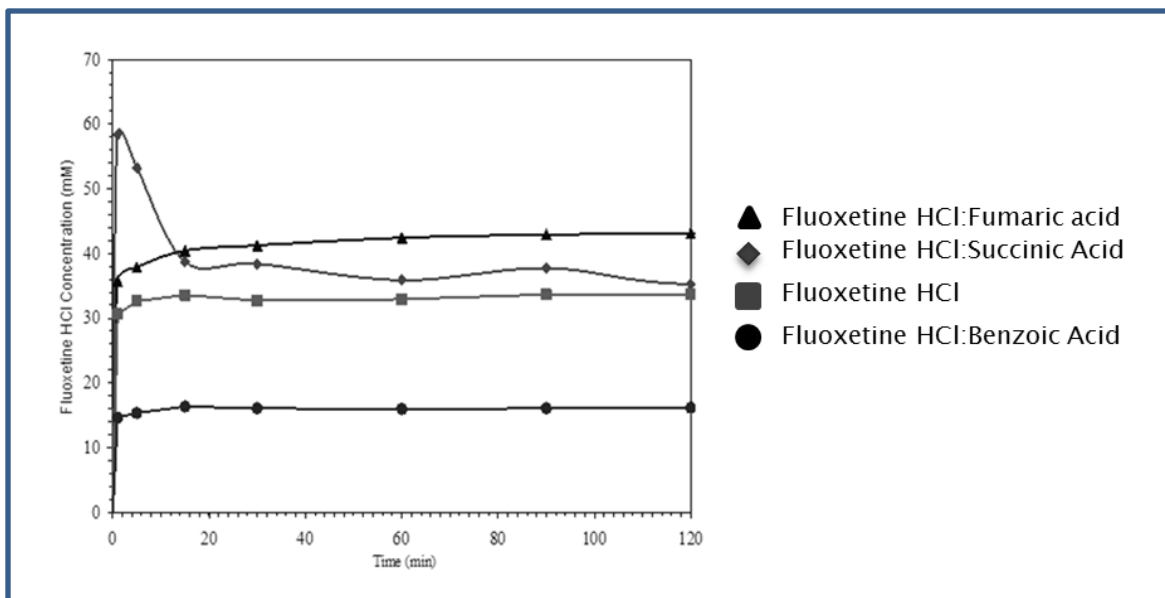


Fig. 1.10: Dissolution profile of pharmaceutical cocrystals of fluoxetine HCl.

1.9.3 Hydration Stability

Hydration stability is relevant in pharmaceutical science because the transformation of one crystal form to another jeopardizes the desired physicochemical properties of the API. A prominent example is illustrated by stability studies of six pharmaceutical cocrystals of caffeine. Caffeine, a central nervous system stimulant, converts to its hydrated form between relative humidity 75 and 98%. The study revealed that the 2:1 pharmaceutical cocrystal caffeine-oxalic acid was very stable upon exposure of 98% relative humidity over seven weeks.⁸⁶ Similar studies were done on four pharmaceutical cocrystals of theophylline with oxalic acid, glutaric acid, malonic acid and maleic acid. It was shown that only the pharmaceutical cocrystal theophylline-oxalic acid displayed an improvement in the physical stability, the remaining cocrystals had similar stability to theophylline.⁸⁷ Other studies demonstrate that carbamazepine-saccharin cocrystal was physically stable at 60% relative humidity and 75% relative

humidity for two weeks, despite the fact that carbamazepine readily forms the dihydrate under these conditions.⁷³

1.9.4 Mechanical properties

Pharmaceutical cocrystals can be used to alter the mechanical properties of APIs as exemplified by studies involving caffeine-methylgallate cocrystal. The cocrystals showed high tensile strength and improved tableting properties in comparison to the individual components.⁸⁸ The improvement in mechanical properties was presumed to be attributed to the layered structure of the cocrystal. Another example is illustrated in the study of tablet formation and mechanical properties on pharmaceutical cocrystals of paracetamol, form I with naphthalene, theophylline, oxalic acid and acridine.⁸⁹ Three-layered crystal structures of paracetamol were constructed using only planar cocrystal formers and as a result the weak shear planes promoted improved elasticity and tableability.

1.10 Overview of Dissertation

Pharmaceutical cocrystals have matured to be an integral part of pharmaceutical solid form development because they afford the discovery of novel, diverse crystal forms of APIs and therefore generate new intellectual property. In addition, pharmaceutical cocrystals have been demonstrated to be a viable approach to profoundly modify the physicochemical properties such as solubility/dissolution rate, stability and bioavailability. Consequently, several factors regarding their development and application becomes of interest which includes but not limited to: the selection of

potential cocrystal formers, development of cocrystals screening methods, scale-up techniques, optimal design, characterization and evaluation of the physicochemical properties of cocrystals in comparison to the target molecule. This dissertation seeks to understand design strategies in the supramolecular synthesis of cocrystals and address the opportunities and challenges that exist in crystal engineering.

Chapter 2 demonstrates the use of nutraceuticals as cocrystal formers. Typically, cocrystal formers are limited to pharmaceutically approved carboxylic acids and chemical included in the generally regarded as safe (GRAS)⁹⁰ and everything added to food in the United States (EAFUS) lists.⁹¹ However, the library of cocrystal formers can be expanded to include other classes of compounds that have an acceptable toxicity profile such as nutraceuticals. The nutraceuticals, gallic acid and ferulic acid were selected since they possess phenolic and carboxylic acid moieties that are capable of forming reliable supramolecular synthons with complementary functional moieties. The cocrystals were systematically designed by applying the supramolecular synthon approach.

Chapter 3 reveals a crystal engineering design strategy in the synthesis of isostructural pharmaceutical cocrystals of the anti-psychotic API olanzapine. This strategy involved a comprehensive analysis of the crystal packing and hydrogen bonding patterns of known crystal structures of olanzapine. This analysis was utilized to synthesize isostructural quaternary multi-component crystal forms of olanzapine. These crystal forms consist of olanzapine, the cocrystal former, a water molecule and a solvate. This strategy is particularly effective in the systematic and successful design of

pharmaceutical cocrystals of complex APIs that possess multiple functional groups and/or conformational flexibility.

Chapter 4 (Appendix 2) addresses the role of water molecules in crystal engineering by studying the relationship between crystal structures and thermal stabilities of a series of synthesized cocrystal hydrates. It was found that their stoichiometric compositions, crystal packing are unpredictable. In addition, there was no correlation found between the crystal packing and thermal stability even when composition and structure are similar. Database mining using the CSD of crystalline hydrates possessing the functional groups carboxylic acids and phenols revealed the unpredictability of supramolecular synthons exhibited by hydrates due to the versatility of the water molecule to engage in diverse hydrogen bonding interactions.

Chapter 5 (Appendix 3) reports forms III and IV polymorphic forms of gallic acid monohydrate. This is the first tetramorphic hydrate for which fractional coordinates have been determined. An analysis of the hydrogen bonding patterns in these and other polymorphic hydrates suggests that waters of hydration are in general a nemesis to crystal engineers.

1.11 References

- ¹ Gardner, C.R.; Walsh, C.T.; Almarrson, Ö. *Nature Review Drug Discovery*, **2004**, *3*, 926-934 (b) Lipinski, C. A.; Lombardo, F.; Dominy, B. W.; Feeney, P. J. *Advanced Drug Deivery. Review* **2001**, *46*, 3-26.
- ² Babu, N. J.; Nangia, A. *Crystal Growth & Design*, **2011**, *11*, 2662–2679
- ³ Serajuddin, A. T. M., *Advanced Drug Delivery Reviews* **2007**, *59*, 603.
- ⁴ Dublin, C. H., *Drug Delivery Technologies* **2006**, *6*, 34.
- ⁵ Van De Waterbeemd, H.; Smith, D. A.; Beaumont, K.; Walker D. K. *Journal of Medicinal Chemistry*.**2001**, *44*, 1313-1333.
- ⁶ Thayer, A. M. *Chemical Engineering News*, **2010**, *88* 13–18.
- ⁷ Noyes, A.; Whitney, W., *Journal of the American Chemical Society* **1897**, *19*, 930.
- ⁸ Nernst, N., *Zeitschrift Fur Physikalische Chemie--Stoichiometrie Und Verwandtschaftslehre* **1904**, *47*, 52
- ⁹ Amidon, G. L.; Lennernas, H.; Shah, V. P.; Crison, J. R., *Pharmaceutical Research* **1995**, *12*, 413.
- ¹⁰ Khankari, R. K.; Law, D.; Grant, D. J. W. *International Journal of Pharmaceutics* **1992**, *82*, 117–127.
- ¹¹ Infantes, L.; Fabian, L; Motherwell, W. D. S. *CrystEngComm* **2007**, *9*, 65–71.
- ¹² Henck, J. O.; Griesser, U. J.; Burger, A. *Pharmazeutische Industrie* **1997**, *59*, 165–169.
- ¹³ Desiraju, G. R. *Journal of Chemical Society Chemical Communication* **1991**, 426–428.

- ¹⁴ H.P. Stahl, *The problems of drug interactions with excipients*, in *Towards Better Safety of Drugs and Pharmaceutical Products*, D.D. Braimar Ed., Elsevier, North-Holland Biomedical Press, **1980**, 265–280.
- ¹⁵ Gardner, C. R., O. Almarsson, H. Chen, S. Morissette, M. Peterson, Z. Zhang, S. Wang, A. Lemmo, J. Gonzalez-Zugasti, J. Monagle, J. Marchionna, S. Ellis, C. McNulty, A. Johnson, D. Levinson, M. Cima, Application of high throughput technologies to drug substance and drug product development," in *Proc. "Foundation of Computer Aided Process Operations"*, FOCAP02003), Florida (2003).
- ¹⁶ Morissette, S. L.; Soukasene, S.; Levinson, D.; Cima, M. J. Almarsson, O. PNAS, 2003, 100, 2180.
- ¹⁷ Stahl, P.H.; Wermuth C.F, *Handbook of Pharmaceutical Salts: Properties, Selection, and Use.*, Hoboken, N. J: Wiley VCH **2002**
- ¹⁸ L.D. Bighley, S.M. Berge, and D.C. Monkhouse, "Salt Forms of Drugs and Absorption," in *Encyclopedia of Pharmaceutical Technology*, Swarbrick, J.; Boylan, J.C. Eds. Marcel Dekker, New York, **1996**, 453–499
- ¹⁹ Vishweshwar P, McMahon JA, Bis JA, Zaworotko MJ. *Journal of Pharmaceutical Sciences*, **2006**, 95, 499–516.
- ²⁰ Schultheiss N, Newman A. *Crystal Growth & Design*, **2009**, 9, 2950–2967.
- ²¹ French patent: F. von Heyden et al., 769 586, **1934**.
- ²² (a) Caira, M R. *Journal of Chemical Crystallography*, **1994**, 24, 695 (b) Caira, M. R. *Journal of Crystallographic and Spectroscopic Research*, **1992**, 22, 193. (c) Caira, M. R. *Journal of Crystallographic and Spectroscopic Research*, **1991**, 21, 641.

- ²³ (a) Zerkowski, J. A.; MacDonald, J. C.; Whitesides, G. M. *Chemistry of Materials* **1997**, *9*, 1933 (b) Zerkowski, J. A.; Mathias, J. P.; Whitesides, G. M. *Journal of American Chemical Society*. **1994**, *116*, 4305 (c) Zerkowski, J. A.; Whitesides, G. M. *Journal of American Chemical Society* **1994**, *116*, 4298 (d) Zerkowski, J. A.; Seto, C. T.; Whitesides, G. M. *Journal of American Chemical Society* **1992**, *114*, 5473.
- ²⁴ Oswald, I.D.H.; Allan, D.R.; McGregor, P.A.; Motherwell, W.D.S.; Parsons, S.; Pulham, C.R. *Acta Crystallography* **2002**, *B58*, 1057.
- ²⁵ Walsh, R.D.; Bradner, M.D.; Fleischman, S.; Morales, L.A.; Moulton, B.; Rodriguez-Hornedo, N.; Zaworotko, M.J. *Chemical Communication* **2003**, 186.
- ²⁶ Shan, N.; Zaworotko, M. J. *Drug Discovery Today* **2008**, *13*, 440.
- ²⁷<http://www.fda.gov/downloads/Drugs/GuidanceComplianceRegulatoryInformation/Guidances/UCM281764.pdf>
- ²⁸ Lehn, J.M. *Supramolecular Chemistry: Concepts and Perspectives*, Weinheim, **1995**.
- ²⁹ Bowman-James, K., *Accounts of Chemical Research*, **2005**, *38*, 671-678.
- ³⁰ Pedersen, C. J. *Journal of American Chemical Society*, **1967**, *89*, 2495-2496.
- ³¹ Lehn, J. M.; *Polymer International*, **2002**, *51*, 825-839
- ³² Steed, J. W.; Turner, D. R., *Core Concepts in Supramolecular Chemistry*. John Wiley and Sons: West Sussex, England, **2007**.
- ³³ Desiraju, G.R. *Angewandte Chemie International Edition*, **2011**, *50*, 52-59
- ³⁴ Desiraju, G. R.; *Perspectives in Supramolecular Chemistry: The Crystal as a Supramolecular Entity, Vol 2*, Wiley, Chichester, **1996**
- ³⁵ Dunitz, J. D., *Pure and Applied Chemistry* **1991**, *63*, 177.

- ³⁶ Pepinsky, R. *Physical Review* **1955**, *100*, 971.
- ³⁷ Schmidt, G. M. J., *Pure and Applied Chemistry*, **1971**, *27*, 647.
- ³⁸ Desiraju, G. R. *Crystal Engineering: The Design of Organic Solids*; Elsevier: Amsterdam, **1989**.
- ³⁹ Lee, J.Y.; *Chemical Society Reviews*, **2009**, *38*, 450–1459.
- ⁴⁰ Li, J.R.; Kuppler, R.J.; Zhou, H.C.; *Chemical Society Reviews*, **2009**, *38*, 1477–1504.
- ⁴¹ (a) Sokolov, A.N.; Frišćić, T.; MacGillivray, L.R.; *Journal of American Chemical Society*, **2006**, *128*, 2806–2807 (b) Gsaenger M, et al. *Angewandte Chemie International Edition* **2010**, *49*, 740–743.
- ⁴² (a) Frišćić, T.; Jones, W. *Journal of Pharmacy and Pharmacology* **2010**, *62*, 1547–1559 (b) Almarsson, O.; Zaworotko, M.J. *Chemical Communication*, **2004**, 1889–1896.
- ⁴³ Etter, M. C., *Journal of Physical Chemistry* **1991**, *95*, 4601
- ⁴⁴ Desiraju, G. R. *Angewandte Chemie International Edition*, **1995**, *34*, 2311
- ⁴⁵ Walsh, R. D. B.; Bradner, M. W.; Fleischman, S.; Morales, L. A.; Moulton, B.; Rodríguez-Hornedo, N.; Zaworotko, M. J., *Chemical Communications* **2003**, 186.
- ⁴⁶ (a) Allen, F. H.; Kennard, O. *Chemical Design Automation News.*, **1993**, *8*, 31. (b) Allen, F. H. *Acta Crystallography*, **2002**, *B58*, 380.
- ⁴⁷ Desiraju, G. R., *CrystEngComm* **2003**, *5*, 466.
- ⁴⁸ Dunitz, J. D., *CrystEngComm* **2003**, *5*, 506.
- ⁴⁹ Aakeröy, C. B.; Salmon, D. J., *CrystEngComm* **2005**, *7*, 439.
- ⁵⁰ Bond, A. D., *CrystEngComm* **2007**, *9*, 833.
- ⁵¹ Wöhler, F. *Justus Liebigs Ann. Chem.*, **1844**, *51*, 153.
- ⁵² Anderson, J.S. *Nature*, **1937** *140*, 583–584

- ⁵³ Pekker, S.; Kovats, E.; Oszlanyi, G.; Benyei, G.; Klupp, G.; Bortel, G.; Jalsovszky, I.; Jakab, E.; Borondics, F.; Kamaras, M.; Bokor, K.; Kriza, G.; Tompa, K.; Faigel, G. *Nature Materials*, **2005**, *4*, 764–767.
- ⁵⁴ Vanniekerk, J. N.; Saunder, D. H. *Acta Crystallography*, **1948**, *1*, 44
- ⁵⁵ Buck, J. S.; Ide, W. S. *Journal of American Chemical Society* **1931**, *53*, 2784.
- ⁵⁶ Schmidt, J.; Snipes, W. *International Journal of Radiation Biology*. **1967**, *13*, 101–109
- ⁵⁷ Etter, M.C. *Journal of Physical Chemistry* **1991**, *95*, 4601–4610
- ⁵⁸ Desiraju, G. R. *Science* **1997**, *278*, 404.
- ⁵⁹ Bis, J. A.; Vishweshwar, P.; Weyna, D.; Zaworotko, M. J., *Molecular Pharmaceutics* **2007**, *4*, 401.
- ⁶⁰ Shattock, T. R.; Arora, K. K.; Vishweshwar, P.; Zaworotko, M. J., *Crystal Growth & Design* **2008**, *8*, 4533.
- ⁶¹ Kavuru, P.; Aboarayas, D.; Arora, K. K.; Clarke, H. D.; Kennedy, A.; Marshall, L.; Ong, T. T.; Perman, J.; Pujari, T.; Wojtas, L.; Zaworotko, M. J., *Crystal Growth & Design* **2010**, *10*, 3568.
- ⁶² (a) Braga, D.; Giaffreda, S. L.; Grepioni, F.; Chierotti, M.R.; Gobetto, R.; Palladino, G.; Polito, M. *CrystEngComm*, **2007**, *9*, 879; (b) Trask, A.V.; Jones, W. *Topics in Current Chemistry*, **2005**, *254*, 41; (c) Cheung, E.Y.; Kitchin, S.J.; Harris, K.D.M.; Imai, Y.; Tajima, N.; Kuroda, R. *Journal of American Chemical Society*, **2003**, *125*, 14658
- ⁶³ (a) Frisćić, T.; Trask, A.V.; Jones, W.; Motherwell, W.D.S. *Angewandte Chemie International Edition*, **2006**, *35*, 3523 (b) Braga, D.; Giaffreda, S.L.; Grepioni, F.; Pettersen, A.; Maini, L.; Curzi, M.; Polito, M. *Dalton Transactions*, **2006**, 1249.
- ⁶⁴ Ling, A. R.; Baker, J. L. *Journal of Chemical Society* **1893**, *63*, 1314

- ⁶⁵ Etter, M.C.; Reutzel, S.M. Choo, C.G. *Journal of American Chemical Society*, **1993**, *115*, 4411.
- ⁶⁶ Shan, N.; Toda, F.; Jones, W. *Chemical Communication* **2002**, *20*, 2372.
- ⁶⁷ Childs, S.L.; Mougín, P.; Stahly, B.C US Patent Application, US2007/0287194 A1, **2007**.
- ⁶⁸ Luis Padrelaa, M. A. R.; Velagab, S. P.; Matosa, H. A.; de Azevedoa, E. G. *European Journal of Pharmaceutical Sciences*, **2009**, *38*, 9–17.
- ⁶⁹ Medina, C.; Daurio, D.; Nagapudi, K.; Alvarez-Nunez, F. *Journal of Pharmaceutical Sciences*, **2010**, *99*, 1693-1696.
- ⁷⁰ Amjad Alhalaweh and Sitaram P. Velaga *Crystal Growth & Design*, **2010**, *10*, 3302-3305
- ⁷¹ Rodriguez-Hornedo, N.; Nehm, S.; Seefeldt, K.; Pagan-Torres, Y.; Falkiewicz, C. *Molecular Pharmaceutics*, **2006**, *3*, 362–367.
- ⁷² Chiarella, R. A.; Davey, R. J.; Peterson, M. L. *Crystal Growth & Design*, **2007**, *7*, 1223–1226.
- ⁷³ ter Horst, J. H.; Deij, M. A.; Cains, P. W. *Crystal Growth & Design*, **2009**, *9*, 1531–1537.
- ⁷⁴ Zhang, G. G. Z.; Henry, R. F.; Borchardt, T. B.; Lou, X. *Journal of Pharmaceutical Sciences*, **2007**, *96*, 990–995.
- ⁷⁵ Higuchi, T.; Ikeda, M. *Journal of Pharmaceutical Sciences*, **1974**, *63*, 809–811.
- ⁷⁶ Remenar, J.F.; Morissette, S.L.; Peterson, M.L.; Moulton, B.; MacPhee, J.M.; Guzmán, H.M.; Almarsson, Ö *Journal of American Chemical Society*, **2003**, *125*, 8456.

- ⁷⁷ Childs, S.L.; Chyall, L.J.; Dunlap, J.T.; Smolenskaya, V.N.; Stahly, B.C.; Stahly, G.P. *Journal of American Chemical Society*, **2004**, *126*, 13335.
- ⁷⁸ Guzman, H. R.; Tawa, M.; Zhang, Z.; Ratanabanangkoon, P.; Shaw, P.; Gardner, C. L.; Chen, H.; Moreau, J.-P.; Almarsson, Ö.; Remenar, J. F. *Journal of Pharmaceutical Sciences*, **2007**, *96*, 2686–2702.
- ⁷⁹ Hickey, M.B.; Peterson, M.L.; Scopettuolo, L.A.; Morrisette, S.L.; Vetter, A.; Guzman, H.R.; Remenar, J.F.; Zhang, Z.; Tawa, M.D.; Haley, S.; Zaworotko, M.J.; Almarsson, Ö. *European Journal of Pharmaceutics and Biopharmaceutics*, **2007**, *67*, 112–119.
- ⁸⁰ McNamara, D.P.; Childs, S.L.; Giordano, J.; Iarriccio, A.; Cassidy, J.; Shet, M.S.; Mannion, R.; O'Donnell, E.; Park, A. *Pharmaceutical Research*, **2006**, *23*, 1888–1897.
- ⁸¹ Variankaval, N.; Wenslow, R.; Murry, J.; Hartman, R.; Helmy, R.; Kwong, E.; Clas, S.; Dalton, C.; Santos, I.; *Crystal Growth & Design*, **2006**, *6*, 690–700
- ⁸² Bak, A.; Gore, A.; Yanez, E.; Stanton, M.; Tufekcic, S.; Syed, R.; Akrami, A.; Rose, M.; Surapaneni, S.; Bostick, T.; King, T.; Neervannan, S.; Ostovic, D.; Koparkar, A. *Journal of Pharmaceutical Sciences*, **2008**, *97*, 3942-3956
- ⁸³ Stanton, M. K.; Kelly, R. C.; Colletti, A.; Kiang, Y. H.; Langley, M.; Munson, E. J.; Peterson, M. L.; Roberts, J.; Wells, M., *Journal of Pharmaceutical Sciences* **2010**, *99*, 3769.
- ⁸⁴ Stanton, M. K.; Kelly, R. C.; Colletti, A.; Kiang, Y. H.; Langley, M.; Munson, E. J.; Peterson, M. L.; Roberts, J.; Wells, M., *Journal of Pharmaceutical Sciences* **2011**, *100*, 2734.

- ⁸⁵ Cheney, M. L.; Weyna, D.R.; Shan, N.; Hanna, M.; Wojtas, L.; Zaworotko, M. J. *Journal of Pharmaceutical Sciences*, **2010**, *100*, 2172-2181
- ⁸⁶ Trask, A. V.; Motherwell, W. D. S.; Jones, W. *Crystal Growth & Design*, **2005**, *5*, 1013–1021.
- ⁸⁷ Trask, A. V.; Motherwell, W. D. S.; Jones, W. *International Journal of Pharmaceutics* **2006**, *320*, 114–123.
- ⁸⁸ Sun, C.C.; Hou, H. *Crystal Growth & Design*, **2008**; *8*, 1575–1579
- ⁸⁹ Karki, S.; Friscic, T.; Fabian, L.; Laity, P. R.; Day, G. M.; Jones, W., *Advanced Materials* **2009**, *21*, 3905-3909
- ⁹⁰ http://www.cfsan.fda.gov/_rdb/opagras.html.
- ⁹¹ http://vm.cfsan.fda.gov/_dms/eafus.html.

Chapter 2: A Crystal Engineering Study of Gallic Acid and Ferulic Acid as Cocrystal Formers

2.1 Introduction

Crystal engineering¹, the design of new molecular solids through invoking supramolecular chemistry, continues to invoke interest through the rapidly emerging fields of metal organic frameworks², solid-state synthesis³ and pharmaceutical cocrystals.⁴

The definition of a cocrystal is an active subject of discussion;⁵ we define it as “a stoichiometric multiple component crystal that is formed between two compounds that are solids under ambient conditions in which at least one cocrystal former is molecular and forms a supramolecular synthon with the remaining cocrystal former(s).” Cocrystals⁶ represent a long known but little studied class of compounds as they have been known since the 1840’s⁷ but even today they represent less than 0.5% of the structures that have been archived in the Cambridge Structural Database (CSD).⁸ Pharmaceutical cocrystals, cocrystals formed between active pharmaceutical ingredients (APIs) and a pharmaceutically acceptable cocrystal former have emerged into a new paradigm in pharmaceutical science as they afford new crystal forms of APIs without covalently modifying the API and they also create opportunities for intellectual property.⁹ Most importantly, they modify the physicochemical properties of the API such as stability,¹⁰

mechanical properties¹¹ and solubility.¹² As pharmaceutical cocrystals have become an inherent part of pharmaceutical solid form development, the selection of cocrystal former libraries remains a matter of debate. Conventional wisdom suggests that pharmaceutically approved carboxylic acids and chemicals included in the generally regarded as safe (GRAS)¹³ and everything added to food in the United States (EAFUS) lists¹⁴ are, in effect, the cocrystal former library. However, there are many other “safe” cocrystal formers that have the potential to serve as cocrystals formers as exemplified by nutraceuticals.¹⁵

Nutraceuticals are naturally occurring compounds defined as “food, or parts of food, that provide medical or health benefits, including the prevention and/or treatment of diseases.”¹⁶ They include dietary supplements, isolated natural substances and genetically-engineered designer foods, and are differentiated from pharmaceuticals by the claims, dosage and packaging of the product.¹⁷ Most nutraceuticals are derived from plants and exist as amino acids, carotenoids, vitamins and dietary polyphenols. Dietary polyphenols, secondary plant metabolites, represent a wide variety of compounds that occur in fruits, vegetables, wine, tea, and cocoa products. They are mostly derivatives and/or isomers of flavonoids, stilbenes, catechins, and phenolic acids. They exhibit many biologically significant functions, such as protection against oxidative stress and degenerative diseases, due to their antioxidant properties.¹⁸ Phenolic acids present in plants are hydroxylated derivatives of benzoic and cinnamic acids such as gallic acid and ferulic acid.¹⁹ They account for one third of the total intake of dietary polyphenols in the diet. Ferulic acid, a hydroxycinnamic acid, is concentrated in the bran of grains, peel of fruits and roots and peels of vegetables.²⁰ It is a bioactive agent that is found as the free

form or the conjugate form and has been approved as an additive antioxidant and food preservative in Japan.²¹ Gallic acid is found in the free form or esterified to catechins or proanthocyanidins. It is widely used as antioxidant in the pharmaceutical industry because in vivo and in vitro studies have shown that it is cytotoxic against cancer cells,²² possesses antibacterial and antifungal properties²³ and has been found to be active against the viruses HIV-1 and HSV-1.²⁴

Phenolic acids are strong candidates to serve as cocrystal formers, because they possess multiple hydrogen bond donors and acceptors that are capable of forming a stable and diverse range of supramolecular synthons. Furthermore, carboxylic acids and phenols are frequently encountered in APIs, pharmaceutical excipients and salt formers and can act as both hydrogen bond donors and hydrogen bond acceptors. They are therefore self-complementary and can also engage in robust and reliable supramolecular heterosynthons with complementary functional groups as seen in the examples of supramolecular synthons composed of carboxylic acid dimers,²⁵ amide dimers,²⁶ carboxylic acid-basic nitrogen,²⁷ carboxylic acid-amides,²⁸ phenol-basic nitrogen²⁹ and phenol-carboxylates.³⁰ An effective approach in the design of cocrystals is applying the supramolecular synthon approach, in particular exploiting reliable supramolecular synthons. This approach involves an empirical analysis of the arrangement and frequency of occurrence of supramolecular synthons of a large number of crystal structures using the Cambridge Structural Database (CSD).⁸ A high probability of occurrence of a particular supramolecular synthon suggests a robust and reliable supramolecular synthon.

This paper addresses the use of gallic acid and ferulic acid, both of which are phenolic acids as cocrystal formers. Eleven cocrystals of gallic acid and ferulic acid with cocrystal formers (Figure 2.1): isoniazid (**INZ**), adenine (**ADN**), 3,5-dimethylpyrazole (**DMP**), theobromine (**TBR**), urea (**URE**) and glycine anhydride (**GAH**) were isolated and structurally characterized.

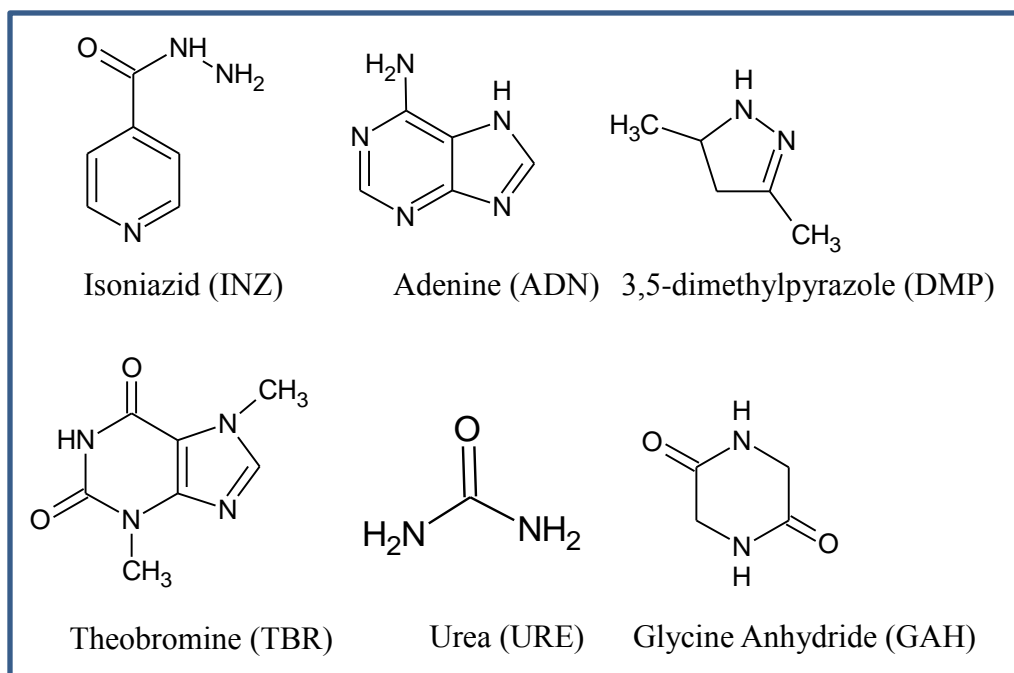


Figure 2.1. Cocrystal formers used herein, abbreviated as follows: INZ, ADN, DMP, TBR, URE, GAH.

2.2 Materials and Methods

2.2.1 Materials

All reagents and solvents were purchased from commercial vendors and used without further purification.

2.2.2 Preparation of Cocrystals

Gallic Acid.Isoniazid, GALINZ: Gallic acid (17.0 mg, 0.100 mmol) and *iso*-nicotinic acid hydrazide (13.8 mg, 0.100 mmol) were dissolved in 2ml of methanol until a clear solution was obtained. The solution was left for slow evaporation at room temperature. Light brown prisms of GALINZ were obtained after 5 days.

Gallic Acid.Dimethylpyrazole, GALDMP: Gallic acid (59.2 mg, 0.348 mmol) and 3,5-dimethylpyrazole (35.4 mg, 0.368 mmol) were dissolved in 5ml of methanol until a clear solution was obtained. The solution was left for slow evaporation at 5°C. Colorless prisms of **GALDMP** were obtained after 14 days.

Gallic Acid.Adenine, GALADN: Gallic acid (17.0 mg, 0.100 mmol) and adenine (13.7 mg, 0.100 mmol) were dissolved in a 4 ml water/ethanol (1:3 ratio) and allowed to slowly evaporate at room temperature in a fume hood. Colorless needles of **GALADN** were harvested after 3 days.

Gallic Acid.Urea, GALURE: Gallic acid (17.1 mg, 0.100 mmol) was dissolved in 1 ml of ethanol. The solution was added to 1 ml saturated solution of urea and allowed to slowly evaporate at room temperature in a fume hood. Colorless needles of **GALURE** were harvested after 8 days.

Gallic Acid.Glycine Anhydride, GALGAH: Gallic acid (17.0 mg, 0.100 mmol) and glycine anhydride (12.0 mg, 0.105 mmol) were dissolved in 2ml of 50% aqueous acetone solution. The solution was left for slow evaporation at 5°C. Colorless needles of **GALGAH** were obtained after a 7 days.

Ferulic Acid.Adenine, FERADN: Ferulic Acid (19.4 mg, 0.100 mmol) and adenine (13.7 mg, 0.100 mmol) were dissolved in a 4 ml water/ethanol (1:3 ratio) and allowed to slowly evaporate at room temperature in a fume hood. Colorless needles of **FERADN** were obtained after 9 days.

Ferulic Acid.Isoniazid, FERINZ: Ferulic acid (19.0 mg, 0.100 mmol) and isoniazid (13.7 mg, 0.100 mmol) were dissolved in 2ml of ethanol. The solution was left for slow evaporation at 5°C. Colorless needles of **FERINZ** were obtained after a 3 days.

Ferulic Acid.Dimethypyrazole, FERDMP: Ferulic acid (19.4 mg, 0.100 mmol) and 3,5-dimethylpyrazole 9.6 mg, 0.100 mmol) were dissolved in 5ml of methanol until a clear solution was obtained. The solution was left for slow evaporation at 5°C. Yellow plates of **FERDMP** were obtained after 14 days.

Ferulic Acid.Urea, FERURE: Ferulic acid (19.2 mg, 0.100 mmol) was dissolved in 2 ml of ethanol. The solution was added to 1 ml saturated solution of urea and allowed to slowly evaporate at room temperature in a fume hood. Colorless needles of **FERURE** were harvested after 8 days.

Ferulic Acid.Glycine Anhydride, FERGAH: Ferulic acid (19.0 mg, 0.1 mmol) and glycine anhydride (79.0 mg, 0.693 mmol) were dissolved in 2ml of 50% aqueous acetone solution. The solution was left for slow evaporation at 5°C. Colorless needles of **FERGAH** were obtained after a 10 days.

Ferulic Acid.Theobromine, FERTBR: Ferulic acid (19.0 mg, 0.100 mmol) and theobromine (19.0 mg, 0.693 mmol) were dissolved in 4ml of 50% aqueous ethanol

solution. The solution was left for slow evaporation at room temperature. Colorless needles of **FERTBR** were obtained after a 14 days.

2.2.3 *Methods*

Differential scanning calorimetry (DSC): Thermal analysis of the cocrystals was performed using a TA instrument DSC 2920 Differential Scanning Calorimeter. Hermetic aluminum pans were used for all samples and temperature calibrations were made using indium as a standard. The samples (1-3 mg) were scanned at a heating rate of 10 °C/min from 30°C-350°C under a dry nitrogen atmosphere (flow rate 70ml/min).

Thermogravimetric analysis (TGA): Thermogravimetric analysis was performed with a Perkin Elmer STA 6000 Simultaneous Thermal Analyzer. Open alumina crucibles were used for analysis in the temperature range 30°C to the appropriate temperature at 2-10 °C/min scanning rate under nitrogen stream.

Infrared spectroscopy (FT-IR): All crystalline samples were characterized by infrared spectroscopy using a Nicolet Avatar 320 FT-IR instrument. 2-3mg of material was used for all samples. Spectra were measured over the range of 4000 – 400cm⁻¹ and data were analyzed using EZ Omnic software.

Laboratory powder x-ray diffraction (PXRD): Bulk samples were analyzed by x-ray powder diffraction with a Bruker AXS D8 powder diffractometer using Cu K α radiation ($\lambda = 1.54056 \text{ \AA}$) and 40 kV; 30 mA. Scanning interval of data was in the range of 3–40° 2 θ ; time per step 0.5s. The experimental PXRD patterns and calculated PXRD patterns from single crystal structures were compared to confirm the composition of materials.

Single-crystal x-ray data collection and structure determinations: Suitable single crystals of **GALURE**, **GALGAH**, **GALINZ**, **GALDMP**, **FERADN**, **FERURE**, **FERGAH** and **FERINZ** were selected for single crystal x-ray crystallography. Quality single crystals of **FERDMP** and **GALADN** could not be obtained but the crystal structure of **GALADN** was solved from the synchrotron powder X-ray diffraction pattern as described below. The validity of structure solution of cocrystals from powder x-ray diffraction pattern has been well established, although structures from powder data generally have less precision in atomic positions than those from single crystal data.³¹ The diffraction data for single crystals of **GALDMP** was collected on a Bruker-AXS SMART APEX CCD diffractometer with monochromatized Mo K α radiation ($\lambda = 0.71073 \text{ \AA}$), whereas data for single crystals of the hydrates of **GALURE**, **GALGAH**, **GALINZ**, **FERADN**, **FERURE**, **FERGAH** and **FERINZ** were collected on a Bruker-AXS SMART APEX 2 CCD diffractometer with monochromatized Cu K α radiation ($\lambda = 1.54178 \text{ \AA}$). Diffractometers were equipped with KRYO-FLEX low temperature device and diffraction experiments were carried out at 100K. Indexing was performed using SMART v5.625³² or using APEX 2008v1-0.³³ Frames were integrated with SaintPlus 7.51³⁴ software package. Structures were solved by direct methods and refined by full matrix least-squares based on F2 using the SHELXTL package.³⁵ Absorption correction was performed by a multiscan method implemented in SADABS.³⁶ All non-hydrogen atoms were refined anisotropically. Hydrogen bonds were solved as follows:

GALINZ: Hydrogen atoms of NH₂ groups were located from difference Fourier map and freely refined except H7 for which $U_{iso}(H) = 1.2U_{eq}(-NH)$. All the other hydrogen atoms were placed geometrically and refined using riding model

with isotropic thermal parameters $U_{\text{iso}}(\text{H}) = 1.5U_{\text{eq}}(-\text{OH}, -\text{CH}_3)$, $U_{\text{iso}}(\text{H}) = 1.2U_{\text{eq}}(-\text{CH}, -\text{NH})$.

GALDMP: Hydrogen atoms of -OH and =NH groups were located from the difference Fourier map and refined freely or freely with thermal parameters: $U_{\text{iso}}(\text{H}) = 1.5U_{\text{eq}}(-\text{OH})$ for H231 and H271. Hydrogen H271 was refined using distance restraints (free refinement resulted in 1.055 Å O-H distance). All the other hydrogen atoms were placed geometrically and refined using riding model with isotropic thermal parameters $U_{\text{iso}}(\text{H}) = 1.2U_{\text{eq}}(-\text{CH})$, $U_{\text{iso}}(\text{H}) = 1.5U_{\text{eq}}(-\text{CH}_3)$.

GALURE: Hydrogen atoms of NH₂ groups were located from difference Fourier map and freely refined with isotropic thermal parameters. All the other hydrogen atoms were placed geometrically and refined using riding model with isotropic thermal parameters $U_{\text{iso}}(\text{H}) = 1.5U_{\text{eq}}(-\text{OH})$, $U_{\text{iso}}(\text{H}) = 1.2U_{\text{eq}}(-\text{CH})$.

GALGAH: Hydrogen atoms of NH groups were located from difference Fourier map and freely refined with isotropic thermal parameters. All the other hydrogen atoms were placed geometrically and refined using riding model with isotropic thermal parameters $U_{\text{iso}}(\text{H}) = 1.5U_{\text{eq}}(-\text{OH})$, $U_{\text{iso}}(\text{H}) = 1.2U_{\text{eq}}(-\text{CH}_2, -\text{CH})$.

FERADN: Hydrogen atoms of NH₂ group were located from difference Fourier map and refined using distance restraints with isotropic thermal parameters ($U_{\text{iso}}(\text{H}) = 1.5U_{\text{eq}}(-\text{NH}_2)$).

All the other hydrogen atoms were placed geometrically and refined using riding model with isotropic thermal parameters $U_{\text{iso}}(\text{H}) = 1.5U_{\text{eq}}(-\text{OH}, -\text{CH}_3)$, $U_{\text{iso}}(\text{H}) = 1.2U_{\text{eq}}(-\text{CH}, -\text{NH})$.

FERINZ: Hydrogen atoms of NH₂ group were located from difference Fourier map and refined using distance restraints with isotropic thermal parameters ($U_{iso}(H) = 1.5U_{eq}(-NH_2)$). All the other hydrogen atoms were placed geometrically and refined using riding model with isotropic thermal parameters $U_{iso}(H) = 1.5U_{eq}(-OH, -CH_3)$, $U_{iso}(H) = 1.2U_{eq}(-CH, -NH)$.

FERURE: Hydrogen atoms of -OH groups were located from the difference Fourier map and freely refined. All the other hydrogen atoms were placed geometrically and refined using riding model with isotropic thermal parameters $U_{iso}(H) = 1.2U_{eq}(-CH, -CH_2, -NH)$, $U_{iso}(H) = 1.5U_{eq}(-CH_3, -OH)$.

FERGAH: All hydrogen atoms were placed geometrically and refined using riding model with isotropic thermal parameters $U_{iso}(H) = 1.2U_{eq}(-CH, -NH_2)$, $U_{iso}(H) = 1.5U_{eq}(-CH_3, -OH)$.

Crystallographic data are presented in **Table 2.1**. Hydrogen bond parameters are given in **Table 2.2**.

Synchrotron powder x-ray data collection and structure determinations: A high resolution synchrotron X-ray powder diffraction pattern was collected at the X16C beamline at the National Synchrotron Light Source at Brookhaven National Laboratory. X-rays of wavelength 0.700154 Å were selected using a Si(111) channel cut monochromator. After the sample, the diffracted beam was analyzed with a Ge(111) crystal and detected by a NaI scintillation counter. Wavelength and diffractometer zero were calibrated using a sample of NIST Standard Reference Material 1976, a sintered plate of Al₂O₃. Samples were flame-sealed in thin walled glass capillaries of nominal

diameter 1.5 mm and spun during data collection for improved powder averaging. This measurement was performed at ambient temperature, nominally 295 K.

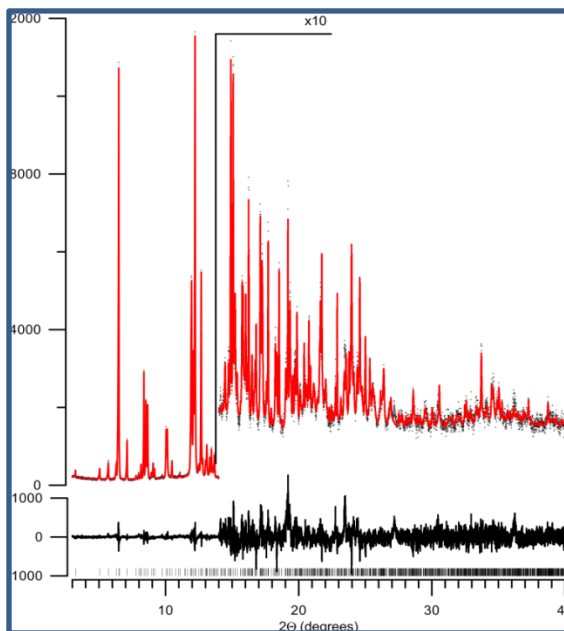


Figure 2.2: High-resolution synchrotron powder diffraction data (dots) and Rietveld fit of the data for **GALADN**. The lower trace is the difference, measured minus calculated, plotted to the same vertical scale

TOPAS-Academic^{37,38,39} was used to index, solve, and refine the crystal structure of **GALADN**. From systematic absences in the pattern, a space group of $P2_1/c$ was hypothesized. Structure solution was performed by simulated annealing, with each molecule being defined as a rigid body on a general position. From this preliminary solution, Rietveld refinement was successfully performed (Figure 2.2). Both of the molecules were defined as rigid bodies, with similar bonds and angles (aromatic bonds, C-C single bonds, e.g.) refined jointly to a single value. The powder diffraction data set does not contain sufficient information to give reliable hydrogen atom positions.

	GALINZ	GALDMP	GALADN	GALURE	GALGAH
Formula	$C_{13}H_{13}N_3O_6$	$C_{17}H_{22}N_4O_5$	$C_{12}H_{11}N_5O_5$	$C_8H_{10}N_2O_6$	$C_{11}H_{12}N_2O_7$
MW	307.26	362.39	305.25	230.18	284.23
Crystal system	Triclinic	Triclinic	Monoclinic	Monoclinic	Triclinic
Space group	<i>P</i> -1	<i>P</i> -1	<i>P</i> ₂ ₁ / <i>c</i>	<i>P</i> ₂ ₁ / <i>c</i>	<i>P</i> -1
a (Å)	8.6337(3)	8.074(2)	7.96634(14)	9.7502(3)	6.0418(2)
b (Å)	11.9056(5)	8.149(2)	6.33221(23)	9.8774(3)	7.9997(2)
c (Å)	13.3621(5)	15.091(4)	24.8483(4)	10.2927(3)	13.0244(3)
α (deg)	94.353(2)	95.811(5)	90	90	103.309(2)
β (deg)	99.401(2)	93.004(5)	96.2093(16)	109.204(2)	91.082(2)
γ (deg)	108.929(2)	117.408(4)	90	90	109.7880(10)
V / Å ³	1269.47(8)	871.4(4)	1246.11(4)	936.09(5)	573.19(3)
Dc/g cm ⁻³	1.608	1.381	1.589	1.633	1.647
Z	4	2	4	4	2
2θ range	3.38 to 65.97	2.73 to 25.03	3 to 40	4.80 to 67.95	3.51 to 66.04
Nref./Npara	4165/420	3031/265	-	1677/166	1914/196
T /K	100(2)	100(2)	300	100(2)	100(2)
R ₁ [I>2σ (I)]	0.0444	0.0406	-	0.0323	0.0369
wR ₂	0.1130	0.1060	-	0.0853	0.0925
R _{wp} ^a	-	-	0.0725	-	-
R _{exp} ^b	-	-	0.0476	-	-
GOF	0.999	1.039	1.523	1.084	1.095
Abs coef	1.109	0.103	0.123	1.237	1.211
	FERINZ	FERADN	FERURE	FERGAH	FERTBR
Formula	$C_{16}H_{17}N_3O_5$	$C_{15}H_{15}N_5O_4$	$C_{14}H_{18}N_4O_6$	$C_{14}H_{16}N_2O_6$	$C_{17}H_{20}N_4O_7$
MW	331.33	329.32	314.30	308.29	392.37
Crystal system	Monoclinic	Orthorhombic	Monoclinic	Monoclinic	Monoclinic
Space group	<i>P</i> ₂ ₁ / <i>c</i>	<i>Pca</i> ₂ ₁	<i>P</i> ₂ ₁ / <i>c</i>	<i>Pc</i>	<i>C</i> ₂ / <i>c</i>
a (Å)	13.681(4)	13.2739(4)	19.950(1)	10.9682(3)	30.546(4)

b (Å)	3.798(12)	16.2621(5)	10.2970(5)	12.7359(3)	6.8895(9)
c (Å)	29.843(10)	6.9427(3)	7.2349(4)	10.2315(3)	17.209(2)
α (deg)	90	90	90	90	90
β (deg)	101.914(5)	90	94.914(3)	97.599(2)	93.725(6)
γ (deg)	90	90	90	90	90
V / Å ³	1517(5)	1498.66(9)	1480.77(13)	1416.69(7)	3619.9(8)
Dc/g cm ⁻³	1.451	1.460	1.410	1.445	1.442
Z	4	4	4	4	8
2 θ range	3.30 to 44.48	2.72 to 67.07	2.22 to 65.82	3.47 to 65.98	2.90 to 52.63
Nref./Npara	1206/229	2421/226	2497/208	4124/403	2042/259
T /K	293(2)	100(2)	100(2)	225(2)	298(2)
R ₁ [I>2 σ (I)]	0.0762	0.0354	0.0445	0.0537	0.0742
wR ₂	0.1734	0.0827	0.1062	0.1413	0.1965
R _{wp} ^a	-	-	-	-	-
R _{exp} ^b	-	-	-	-	-
GOF	0.994	1.065	1.081	1.004	1.016
Abs coef	0.920	0.918	0.974	0.971	0.965

Table 2.1: Crystallographic data and structure refinement parameters for the cocrystals presented herein.

$${}^a R_{wp} = \sqrt{\frac{\sum_i \hat{a}_i w_i (y_i^{calc} - y_i^{obs})^2}{\sum_i \hat{a}_i w_i (y_i^{obs})^2}}, \quad {}^b R_{exp} = \sqrt{\frac{N}{\sum_i \hat{a}_i w_i (y_i^{obs})^2}}$$

where y_i^{calc} and y_i^{obs} are the calculated and observed intensities at the i^{th} point in the profile, normalized to monitor intensity. The weight w_i is $1/\sigma^2$ from the counting statistics, with the same normalization factor. N is the number of points in the measured profile minus number of parameters.

	Hydrogen bond	$d(\text{H} \cdots \text{A})$ /Å	$D(\text{D} \cdots \text{A})/\text{Å}$	<(DHA)
GALINZ	N-H \cdots O	2.20	2.942(2)	142.2
	N-H \cdots O	2.56(3)	3.427(3)	169(2)
	N-H \cdots O	2.24	2.913(2)	132.8
	N-H \cdots O	2.18(3)	3.044(3)	162(2)
	O-H \cdots O	2.07	2.802(2)	145.3
	O-H \cdots O	2.04	2.755(2)	142.8
	O-H \cdots N	1.80	2.636(2)	174.8
	O-H \cdots N	1.89	2.717(2)	167.6
	O-H \cdots N	1.84	2.675(2)	173.9
	O-H \cdots N	1.87	2.699(2)	167.6
GALDMP	N-H \cdots O	2.14(2)	2.9314(19)	151.7(17)
	N-H \cdots O	1.95(2)	2.8092(19)	162(2)
	O-H \cdots N	1.67(3)	2.6190(18)	167(2)
	O-H \cdots N	2.51(2)	3.3135(19)	140.6(18)
	O-H \cdots O	1.97(2)	2.7410(16)	144.9(19)
	O-H \cdots O	2.27(2)	2.7283(16)	112.0(17)
	O-H \cdots O	1.84(3)	2.6800(17)	160(2)
	O-H \cdots N	1.658(18)	2.5891(17)	169(3)
GALURE	O-H \cdots O	1.73	2.5282(14)	158.5
	O-H \cdots O	1.89	2.7012(14)	162.4
	O-H \cdots O	2.04	2.8346(14)	156.5
	O-H \cdots O	2.10	2.8263(14)	144.7
	N-H \cdots O	2.37(2)	3.2347(17)	159.9(16)
	N-H \cdots O	2.542(19)	3.0048(17)	112.2(15)
	N-H \cdots O	2.31(2)	2.8264(17)	120.0(16)
	N-H \cdots O	2.12(2)	2.9961(18)	168.5(18)
GALGAH	O-H \cdots O	1.80	2.6382(14)	178.6
	O-H \cdots O	2.06	2.7229(15)	135.2
	O-H \cdots O	1.91	2.7480(15)	175.7
	O-H \cdots O	1.78	2.6102(15)	169.1
	N-H \cdots O	1.94(2)	2.8537(17)	165.7(18)
	N-H \cdots O	2.08(2)	2.9349(17)	166.7(19)
FERINZ	O-H \cdots O	2.19	2.647(8)	115.8
	O-H \cdots O	2.37	3.000(8)	134.4
	O-H \cdots N	1.82	2.634(9)	174.6
	N-H \cdots O	2.06(2)	2.91(1)	176(8)
	N-H \cdots O	2.32(4)	3.17(1)	159(8)
	N-H \cdots O	2.25(7)	2.96(1)	137(8)

FERADN	O-H...N	1.98	2.715(2)	146
	N-H...N	2.00	2.826(2)	155
	N-H...O	2.09(2)	2.964(3)	164(2)
FERURE	O-H...O	1.75(3)	2.639(2)	168(3)
	N-H...O	2.14	2.983(3)	160.7
	N-H...O	2.32	3.023(2)	136.4
	N-H...O	2.41	3.108(2)	137.0
	N-H...O	2.08	2.951(3)	168.5
	N-H...O	2.25	2.986(2)	141.2
	N-H...O	2.06	2.936(2)	172.1
	N-H...O	2.07	2.945(2)	174.2
	N-H...O	2.29	3.079(2)	150.0
	O-H...O	1.72(4)	2.616(2)	
FERGAH	O-H...O	2.02	2.677(5)	135.1
	O-H...O	2.01	2.646(4)	132.5
	N-H...O	2.58	3.157(5)	124.5
	N-H...O	2.25	3.097(5)	164.1
FERTBR.H₂O	O-H...O	1.79	2.600(7)	167.4
	O-H...O	1.89	2.710(7)	175.5
	N-H...O	2.00	2.858(7)	172.5
	O-H(W)...O	2.09(5)	2.865(7)	150(7)
	O-H(W)...O	1.90(3)	2.764(7)	169(9)

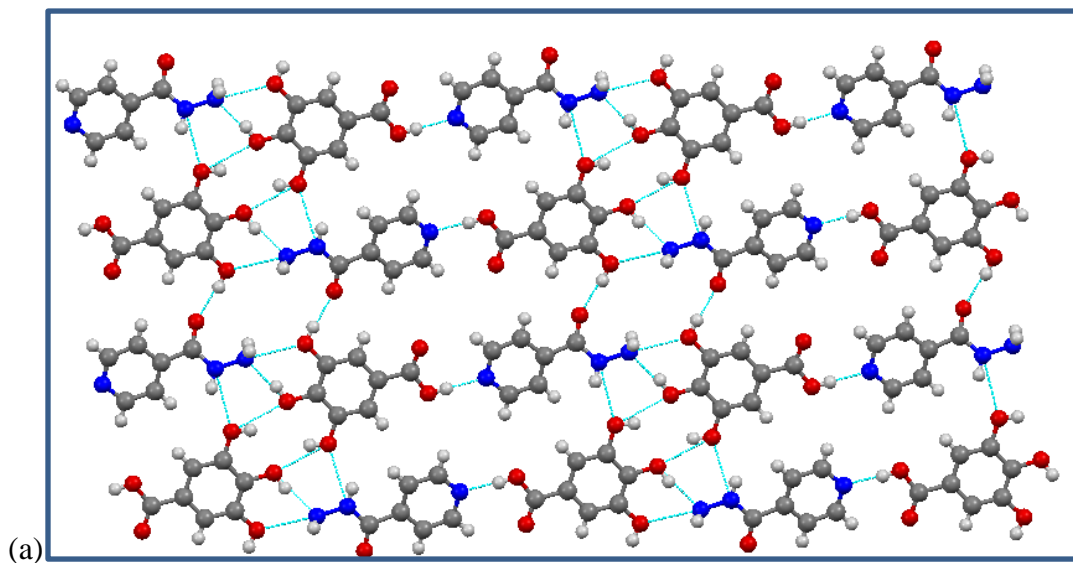
Table 2.2: Selected hydrogen bond distances and parameters of cocrystals

Supramolecular Synthons	Carboxylic acids and Primary Amides		Carboxylic acids and Secondary amides	
	Raw (254 entries)	Refined (38 entries)	Raw (1141 entries)	Refined (184 entries)
COOH...CONH	124 (48.8%)	32 (84.2%)	78 (6.8%)	7 (3.8%)
COOH...COOH	15 (5.9%)	3 (7.9%)	123 (10.8%)	40 (21.7%)
CONH...CONH	87 (34.3%)	4 (10.5%)	117 (10.3%)	36 (19.6%)

Table 2.3: Comparison of Supramolecular Homosynthon versus Supramolecular Heterosynthon of Carboxylic acids with Primary and Secondary Amides

2.3 Results

GALINZ: **GAL** and **INZ** form a cocrystal that crystallizes in the space group $P-1$ with two independent molecules of **GAL** and two independent molecules of **INZ** in the asymmetric unit. The crystal structure reveals the existence of hydrogen bonded interactions between the two symmetrically independent **GAL** molecules via phenolic supramolecular homosynthons ($O\cdots O$: 2.757(1), $O\cdots O$: 2.805 (1)Å). The phenolic homodimers of **GAL** act as H-bond donors and acceptors to the hydrazone moieties of the two symmetrically independent molecules of **INZ** via $R^3_3(7)$ ring motifs so as to form four component supramolecular assemblies of **GAL** and **INZ** molecules. This four component supramolecular assembly in turn forms H-bonded tapes that are sustained by $COOH\cdots N_{basic}$ supramolecular heterosynthons ($O\cdots N$: 2.636(3) Å), thereby forming a two dimensional network (Fig. 2.3a). The carbonyl moiety of one symmetrically independent **GAL** molecule hydrogen bonds with the amine moiety of **INZ** ($N\cdots O$: 3.044(1) Å) to form bilayers that are connected by π interactions (Fig. 2.3b).



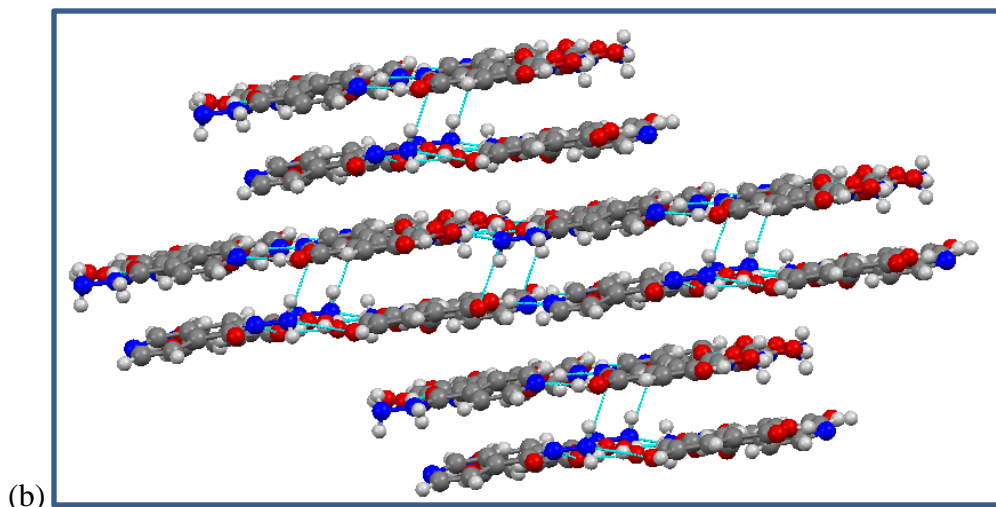


Fig 2.3: (a) Crystal packing in **GALINZ** reveals form H-bonded tapes that are sustained by $\text{COOH} \cdots \text{N}_{\text{basic}}$ supramolecular heterosynthons (b) Illustration of bilayers of **GALINZ** sheets.

GALDMP: **GALDMP** is a 1:2 cocrystal that crystallizes in space group $P-1$ with one molecule of **GAL** and two molecules of **DMP** in the asymmetric unit. The crystal structure of **GALDMP** reveals that **GAL** molecules form phenolic supramolecular homosynthons ($\text{O} \cdots \text{O}$: 2.741(7) Å) that self-assemble to form tapes along the b axis. The homodimers further hydrogen bond to crystallographically independent **DMP** molecules via an $R^3_3(7)$ ring motif (Fig. 2.4a). The third hydroxyl moiety of the gallic acid molecule interacts with the basic nitrogen of the second crystallographically independent **DMP** molecule and the phenolic moiety of a **GAL** molecule to generate a trimeric ring motif, $R^3_3(9)$ (Fig. 2.4b). The crystal packing is a two dimensional network (Fig. 2.4c).

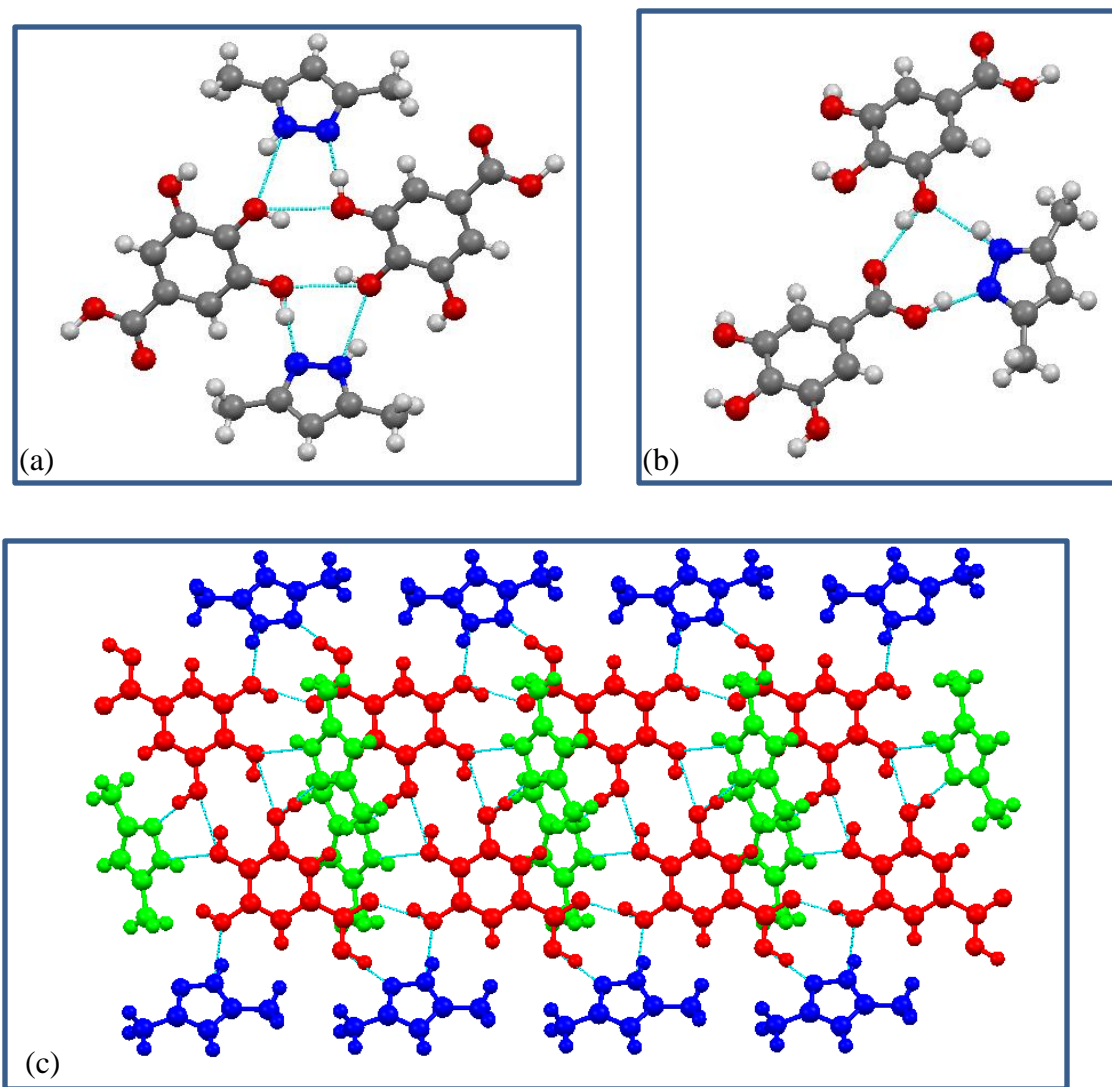


Fig. 2.4: (a) Phenolic homodimers of **GAL** molecules acts as a donor and an acceptor to **DMP** molecules (b) $R^3_3(9)$ trimeric motif involving two **GAL** molecules and a **DMP** molecule (c) Crystal packing in **GALDMP** reveals a 2D network of **GAL** and **DMP** molecules.

GALADN: The crystal structure of **GALADN** reveals the self-assembly of **GAL** and **ADN** molecules in the monoclinic space group $P2_1/c$. The carboxylic acid moieties of **GAL** molecules and the aminopyridine moieties of **ADN** molecules form $R^2_2(8)$

supramolecular heterosynthons ($N\cdots O$: 2.880(17) Å; $O\cdots O$: 2.644(78) Å) to generate chains. These chains are interconnected through the formation of phenolic homodimers of **GAL** molecules ($O\cdots O$: 2.701(11) Å, Fig. 2.5). In addition, the exterior H-bond donor and acceptor sites of the phenolic homodimers are exploited by **ADN** molecules of adjacent chains to generate a 3D network.

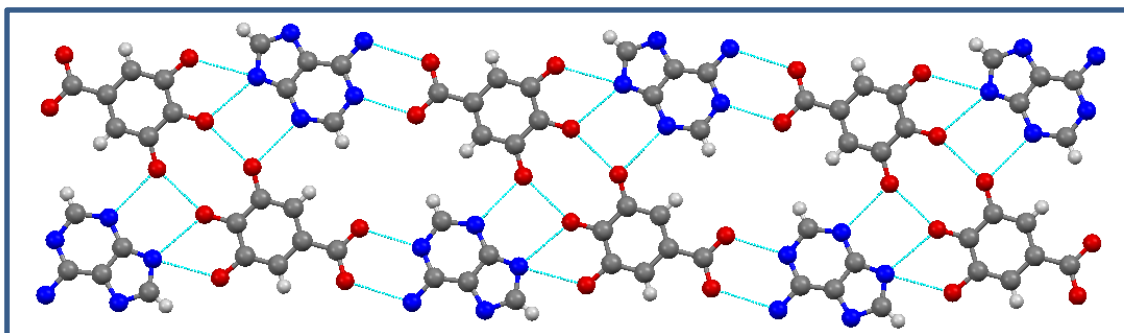


Fig 2.5: Crystal packing in **GALADN** reveals form H-bonded interactions between the carboxylic acid moiety of **GAL** molecules and the aminopyridine moiety of **ADN** molecules.

GALURE: **GAL** and **URE** molecules crystallize in the monoclinic space group $P2_1/c$ with one molecule of each in the asymmetric unit. The crystal structure reveals that **GAL** and **URE** molecules form carboxylic acid-amide supramolecular heterosynthons ($O\cdots O$ 2.528(1)Å, $N\cdots O$: 2.996(1) Å). These heterodimers are cross linked by $NH\cdots OH$ hydrogen bonds ($N\cdots O$: 3.005(1) Å) to form tapes. The heterodimers are linked perpendicularly to adjacent tapes by accepting a hydrogen bond from the amine and phenolic moieties ($O\cdots O$: 2.701(1) Å; $N\cdots O$: 2.826(1) Å). Additionally, the phenolic moiety of the **GAL** molecule from the adjacent tape accepts a bifurcated hydrogen bond

from the phenolic moiety of the **GAL** molecule and the amine moiety of the **URE** molecule ($O\cdots O$: 2.835(1) Å; $N\cdots O$: 2.984(1) Å, Fig. 2.6).

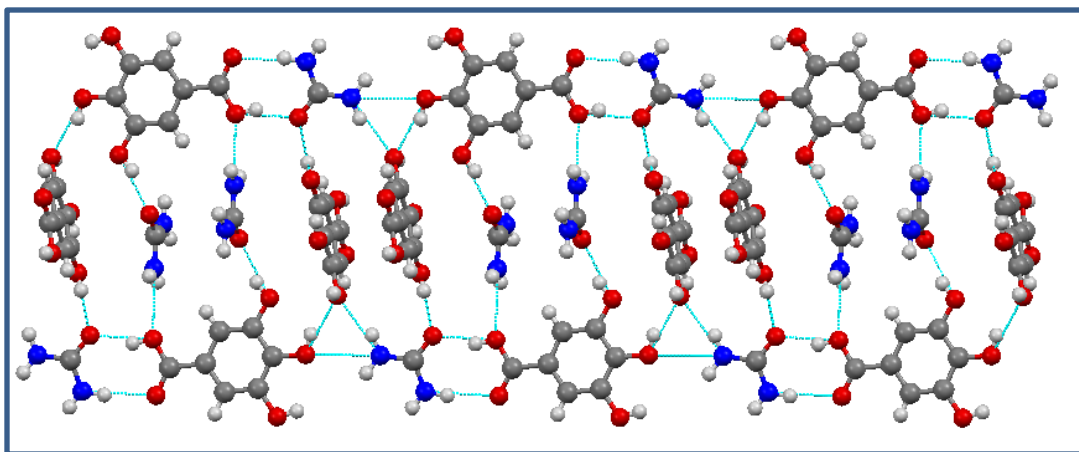


Fig. 2.6: Crystal packing in **GALURE** reveals molecular tapes of heterodimers of **GAL** and **URE** molecules.

GALGAH: The crystal structure of **GALGAH** contains two independent molecules of **GAH** molecules and one independent molecule of **GAL** in the unit cell. The **GAL** molecules form undulating chains sustained by carboxylic acid supramolecular homosynthons ($O\cdots O$: 2.610(1) Å) and phenolic supramolecular homosynthons ($O\cdots O$: 2.723(1) Å). This undulating chain of homodimers is absent in both the anhydrous and hydrated forms of **GAL**. An independent **GAH** molecule acts as both a hydrogen bond donor and acceptor towards the phenolic homodimers by forming a tetrameric motif ($NH\cdots OH$: 2.935(1) Å, $OH\cdots O$: 2.635(1) Å) to connect each chain, thereby forming a sheet (Fig. 2.7a). The other **GAH** molecule interacts with the **GAL** chains via $OH\cdots O$ hydrogen bonds ($O\cdots O$: 2.748(1) Å) and further connect the sheets above and below through amide-amide supramolecular homosynthons ($N\cdots O$: 2.854(1) Å, Fig. 2.7b).

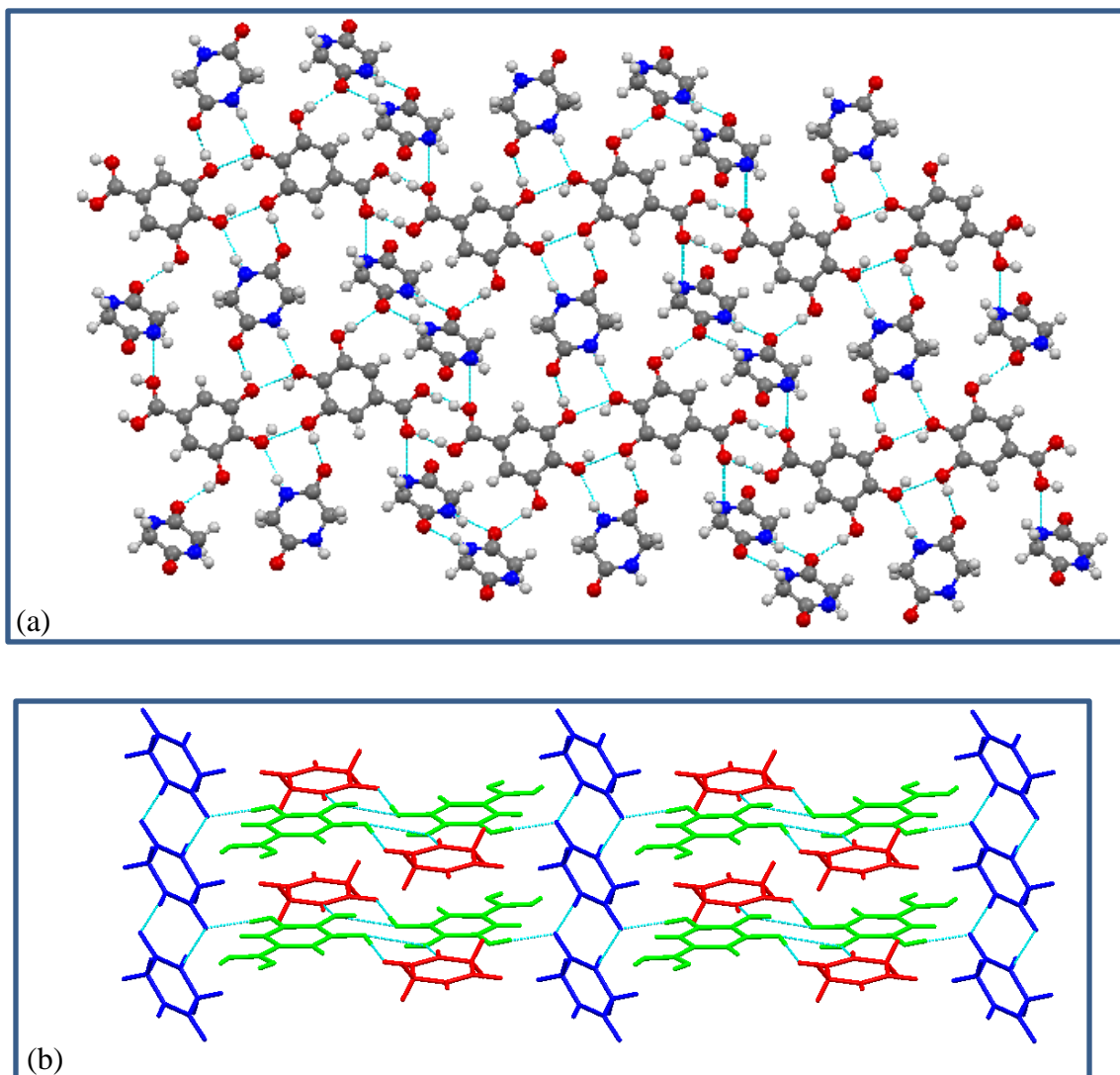


Fig. 2.7: (a) Crystal packing in **GALGAH** reveals undulating tapes sustained by dimers of **GAL** molecules linked by **GAH** molecules to form sheets (b) Illustration of sheets interconnected by homodimers of **GAH** molecules.

FERADN: The crystal structure of **FERADN** reveals that **FER** and **ADN** molecules in the unit cell. **FER** and **ADN** molecules form two point supramolecular heterosynthons between the acid moiety of **FER** and the amine and basic nitrogen of the **ADN** molecule

to form 1-D chains ($\text{NH}\cdots\text{O}$: 2.839 (1)Å; $\text{OH}\cdots\text{O}$: 2.692(1) Å, Fig. 2.8a). Adjacent chains are cross linked by hydrogen bonding interactions between one **FER** molecule and two **ADN** molecules via $\text{R}^3_3(10)$ motifs to result in an interpenetrated three dimensional network (Fig. 2.8b).

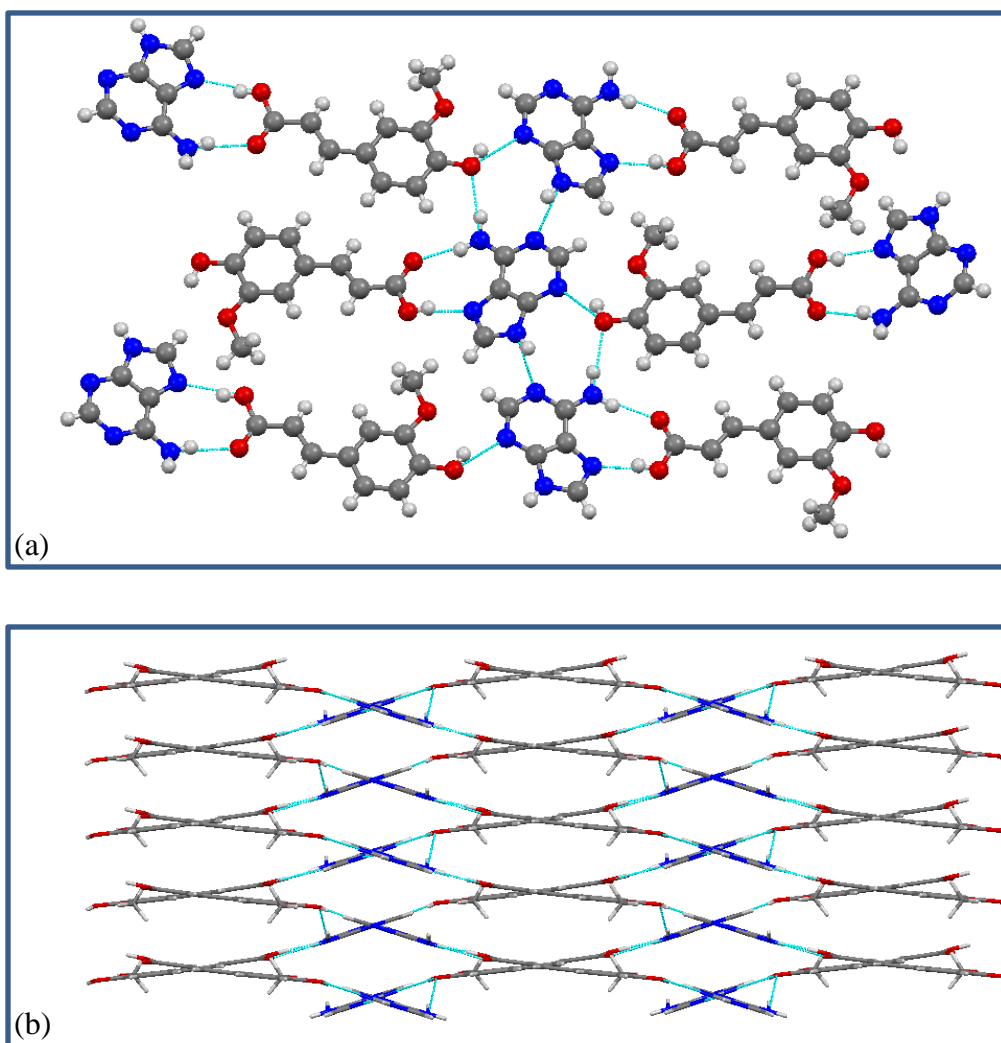


Fig. 2.8: (a) Crystal packing in **FERADN** reveals two point recognition supramolecular heterosynthons between the acid moiety of **FER** molecule and the amine and the basic nitrogen moiety of the **ADN** molecule (b) Crystal packing of **FERADN** is that of a 3D interpenetrated network.

FERINZ: **FER** and **INZ** crystallize in space group $P-1$ with two molecules of each component in the asymmetric unit. The crystal structure of **FERINZ** is sustained by the robust $\text{COOH} \cdots \text{N}_{\text{basic}}$ supramolecular heterosynthons ($\text{O} \cdots \text{N}$: 2.636(5) Å, Fig. 7a). The **INZ** molecules interact via $\text{NH} \cdots \text{O}$ ($\text{N} \cdots \text{O}$: 2.968(7) Å) supramolecular homosynthons to form $\text{R}^2_2(10)$ dimers (Fig. 2.9a). The intermolecular H-bonding generates a herring bone pattern as presented in Fig. 2.9b.

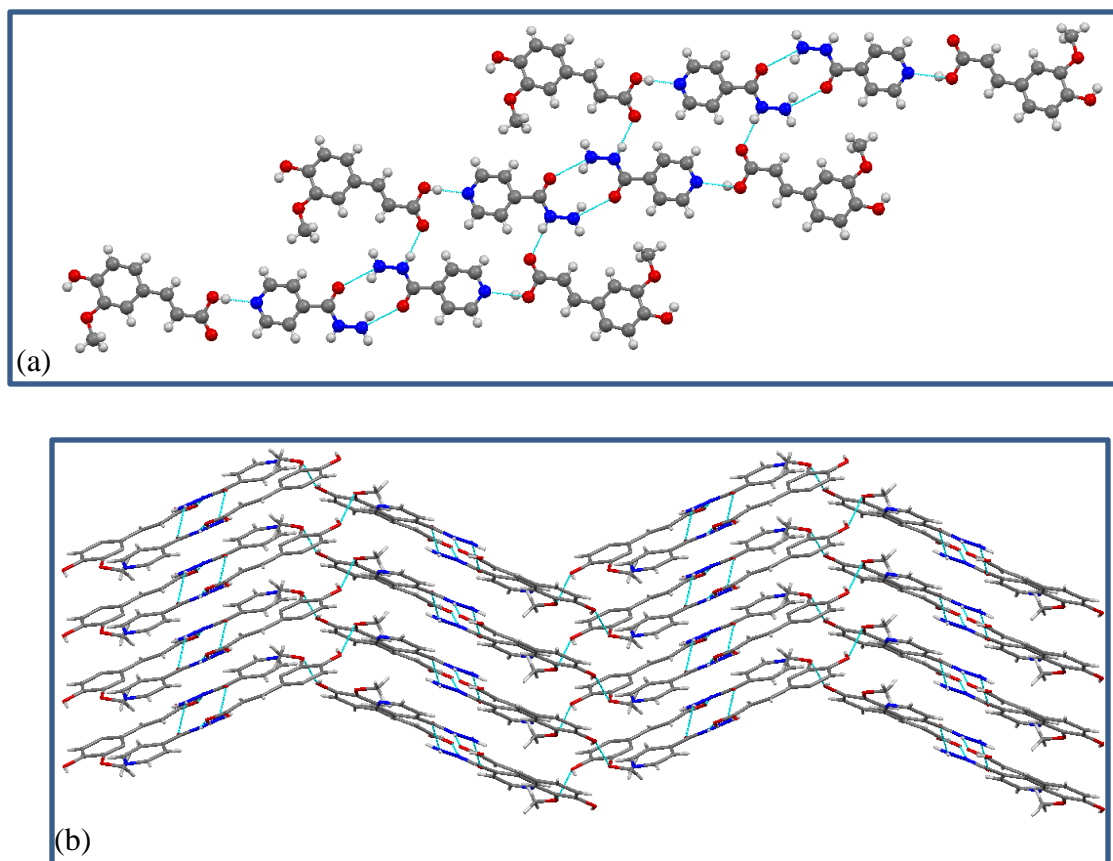


Fig. 2.9: (a) Crystal packing in **FERINZ** sustained by $\text{COOH} \cdots \text{N}_{\text{basic}}$ supramolecular heterosynthons (b) Herring bone pattern of **FERINZ**.

FERURE: **FER** and **URE** molecules form a 1:2 adduct that crystallizes in the monoclinic space group $P2_1/c$. Both independent **URE** molecules form amide-amide supramolecular homosynthons that generate tapes along the b axis. The $\text{NH}\cdots\text{O}$ bond distances are 2.945(3)Å and 2.936(3)Å for the first independent **URE** molecule and 2.982(3)Å and 2.951(3)Å for the second independent **URE** molecule. The homodimers are further interconnected through a two point hydrogen bond between the amine moieties of **URE** and the hydroxyl and methoxyl moieties of **FER** ($\text{N}\cdots\text{O}$: 2.986(2)Å, $\text{N}\cdots\text{O}$: 3.023(2)Å, Fig. 4a) at a dihedral angle of 77.33°. In addition, the carbonyl moiety of the **URE** molecule accepts a hydrogen bond from the carboxylic acid moiety of **FER** (Fig. 2.10).

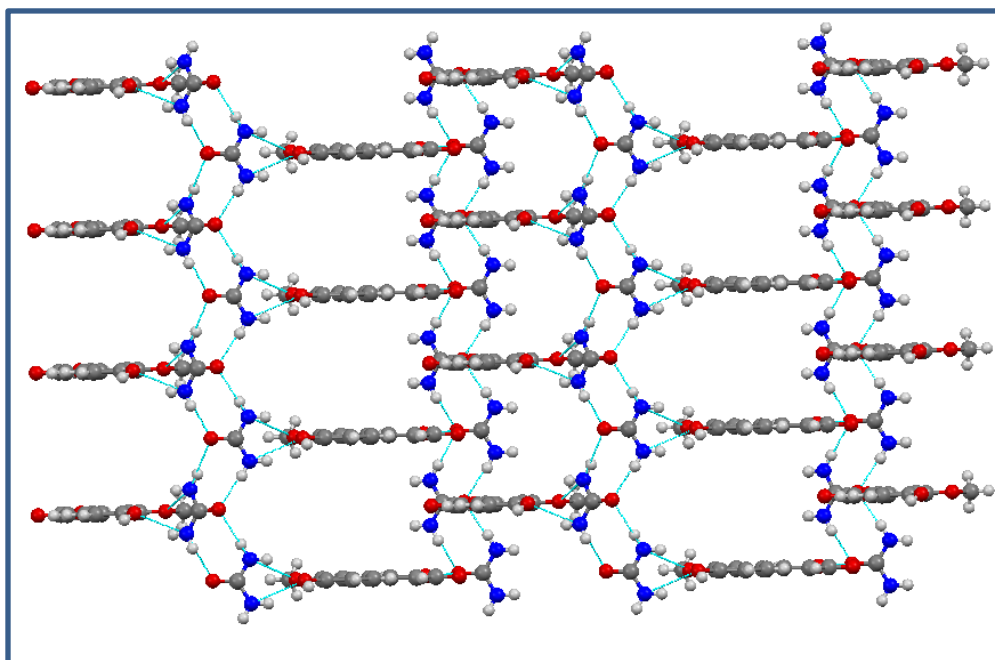


Fig. 2.10: Crystal packing in **FERURE** reveals amide-amide supramolecular homosynthons between **URE** molecules to generate tapes that are interconnected by **FER** molecules.

FERGAH: The 2:2 cocrystal of **FER** and **GAH** is sustained by chains of **GAH** molecules via amide-amide supramolecular homosynthons ($N\cdots O$: 2.987(1) Å; $N\cdots O$: 2.225(1) Å). The chains of **GAH** molecules are interconnected by **FER** molecules through $OH\cdots O$ hydrogen bonding ($O\cdots O$: 2.615(1)Å) resulting in the formation of a sheet as illustrated in Fig. 2.11.

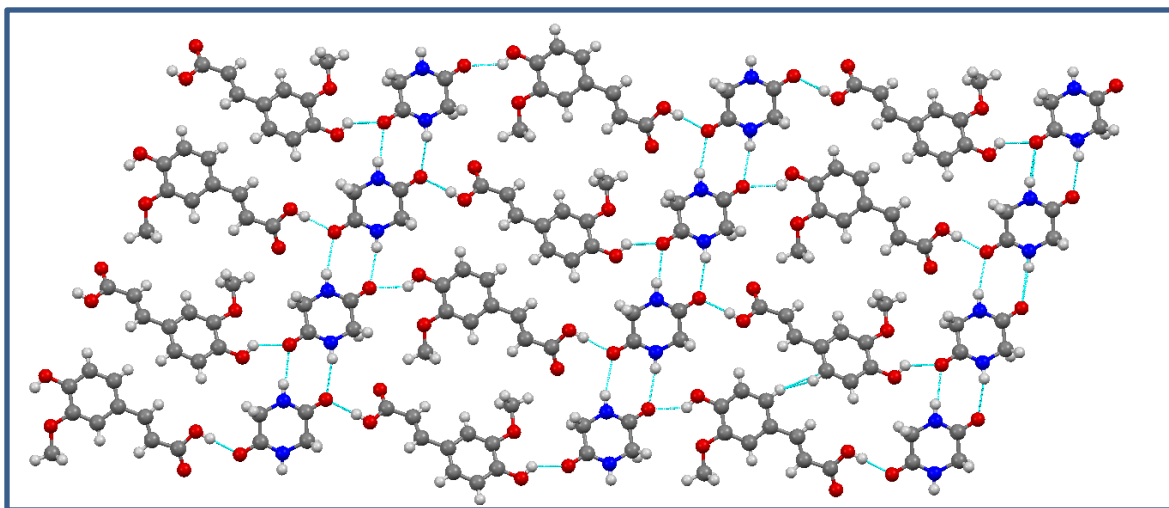


Fig. 2.11: Crystal packing in **FERGAH** reveals molecular tapes of amide-amide supramolecular homosynthons between **GAH** molecules interconnected by **FER** molecules.

FERTBR: The crystal structure of **FERTBR** · **H₂O** reveals a 1:1 cocrystal monohydrate which crystallizes in the monoclinic space group *C2/c*. The crystal structure consists of **FER** and **TBR** molecules that form acid-imide supramolecular heterosynthons ($N\cdots O$: 2.858(3) Å, $O\cdots O$: 2.602(3) Å) interconnected by water molecules to form discrete 6-component supramolecular assemblies (Fig 2.12).

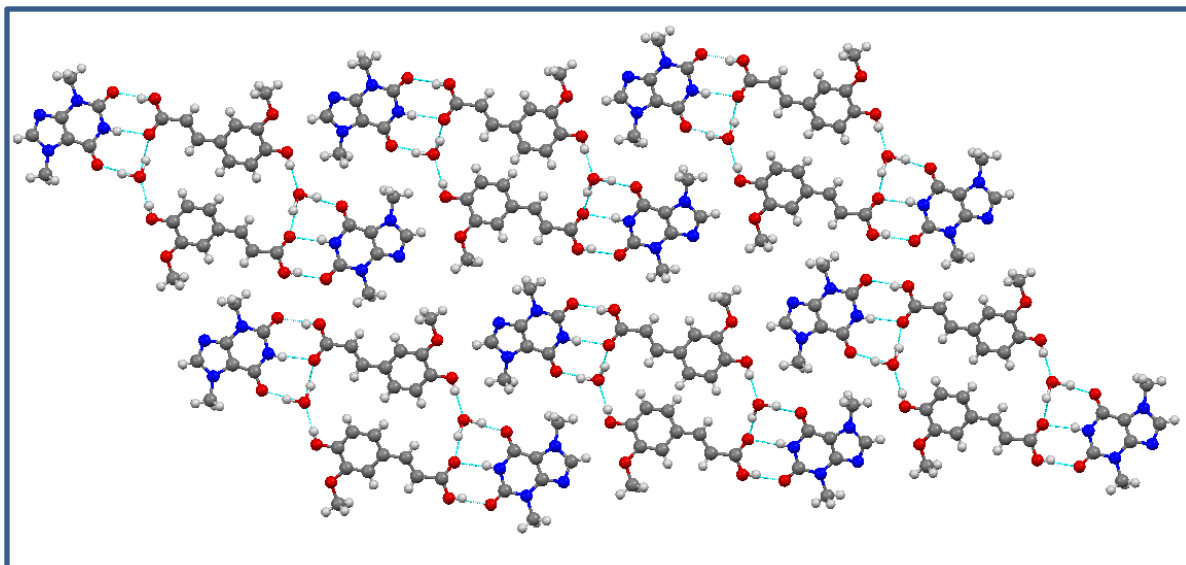


Fig 2.12: Crystal packing of **FERTBR · H₂O** reveals that **FERTBR** heterodimers are connected by water molecules.

2.4 Discussion

Six cocrystal formers were studied herein and they afforded five pairs of cocrystals of gallic acid and ferulic acid (**INZ**, **ADN**, **DMP**, **URE** and **GAH**). The eleventh **FERTBR.H₂O** can also be paired since the crystal structure of gallic acid and theobromine dihydrate has been reported elsewhere.⁴⁰ The data presented herein shows that phenolic acids can generally be considered as reliable cocrystal formers with molecules that contain a basic nitrogen/amide moiety. A CSD survey of phenolic acids (i.e. hydroxylated derivatives of benzoic acids and cinnamic acids) resulted in 324 entries, of which 159 are cocrystals. However, the number of entries of gallic acid and ferulic acid cocrystals are 8 and 5 entries respectively.

The reliability of the supramolecular synthon approach as a design tool for the preparation of cocrystals has been systematically explored in several studies.^{25,27,41} Carboxylic acids are known to form persistent supramolecular heterosynthons with

weakly basic nitrogen or amide moieties. Studies have also focused upon weakly acidic OH groups and their ability to form supramolecular heterosynthons with basic nitrogen and carboxylate moieties have been established. For example, it has been reported that the probability of occurrence of $\text{COOH}\cdots\text{N}_{\text{basic}}$ in the presence and absence of competing functional moieties are 77% and 97%, respectively.²⁵ The cocrystals reported herein focus upon the hierarchy of supramolecular synthons when phenolic and carboxylic acid moieties are present in the same molecule. **GALADN**, **GALDMP**, **GALINZ**, **FERINZ** and **FERADN** all exhibit the carboxylic acid-basic nitrogen supramolecular heterosynthon. The $\text{COOH}\cdots\text{N}_{\text{basic}}$ bond distance range is 2.588(4) to 2.692(1) Å and reveals the robustness of the $\text{COOH}\cdots\text{N}_{\text{basic}}$ supramolecular heterosynthon. The bond distance range of carboxylic acid aromatic nitrogen supramolecular heterosynthon ranges from 2.5 to 3.0 with a mean distance of 2.652(2). However, in **FERTBR.H₂O**, the $\text{COOH}\cdots\text{N}_{\text{basic}}$ supramolecular heterosynthon is absent and is replaced by the acid-imide supramolecular heterosynthon. This anomaly may be attributed to the presence of the water molecule. Indeed, a CSD survey of **TBR** cocrystals with carboxylic acids reveals five entries: **CSATBR**, **HIJYAB**, **HIJYEF**, **NURYUV** and **MUPPET**. **HIJYAB** and **NURYUV** formed the $\text{COOH}\cdots\text{N}_{\text{basic}}$ supramolecular heterosynthon and the **TBR** molecules formed the imide homodimers. Similarly, crystal structures of **CSATBR** and **HIJYEF** are sustained by the $\text{COOH}\cdots\text{N}_{\text{basic}}$ supramolecular heterosynthon and also form the acid-imide supramolecular heterosynthon due to the presence of a second carboxylic acid moiety. In contrast, **MUPPET**, a cocrystal consisting of gallic acid, theobromine and two water molecules, did not form the $\text{COOH}\cdots\text{N}_{\text{basic}}$ supramolecular heterosynthon, instead water molecules are hydrogen bonded to the imidazolyl moiety and the acid-imide

supramolecular heterosynthon is formed. In both **FERTBR.H₂O** and **GALTBR.2H₂O**, a six component supramolecular assembly between two **FER** or **GAL** molecules, two **TBR** molecules and water molecule(s) is observed. Indeed, it has been asserted that, although carboxylic acids and phenols form supramolecular synthons with aromatic nitrogen even in the presence of competing functional groups, the supramolecular synthons exhibited between carboxylic acids, phenols and water molecules are rather diverse.³⁴ Furthermore, the promiscuity of waters of hydration in terms of the supramolecular heterosynthons they exhibit is exemplified by the four polymorphs of gallic acid monohydrate.⁴²

GALURE exhibits the acid-amide supramolecular heterosynthon but it is absent in **FERURE**, **FERGAH** and **GALGAH**. **FERGAH** and **FERURE** both exhibit infinite chains of self-complementary amide-amide supramolecular homosynthons. **GALGAH** consists of two independent **GAH** molecules, one of which retained the amide-amide supramolecular homosynthons whereas the other hydrogen bonds to the phenolic homosynthons. Infantes et al, studied the probability of hydrogen bonding interactions of various functional groups and it was demonstrated that the relative strength of supramolecular homosynthons is in the order of: amides > acids > alcohols functional groups.⁴³ However, several studies show that in the presence of carboxylic acids, there is 84% probability of the occurrence of the acid-primary amide supramolecular heterosynthon.^{24,25} Indeed, a recent study concerning the hydrogen bonding binding energy between primary amides vs that between acid and primary amides indicated that the acid-amide interaction is stronger than the amide-amide interaction.⁴⁴ These studies concentrated on primary amides and the question arises if this also holds true for

secondary amides. A CSD analysis of the occurrence of the acid-secondary amide supramolecular heterosynthon indicates 3.8% occurrence in the absence of competing functional groups (Table 3). Further analysis reveals that the acid supramolecular homosynthon and the amide supramolecular homosynthon occur 21.7% and 19.6%, respectively.

The phenolic supramolecular homosynthon is observed in cocrystals of **GALADN**, **GALINZ**, **GALDMP** and **GALGAH**. A CSD survey reveals that out of 466 entries of organic molecules with a catechol functional moiety, 94 (20.1%) form phenolic homodimers. Elimination of competing functional moieties resulted in 13 entries, and 8 (61.5%) formed phenolic homodimers. The rule of thumb in hydrogen bonding according to Etter is that hydrogen bonds form in a hierarchical fashion whereby the best hydrogen bond donor and acceptor preferentially interact with each other, followed by the second best hydrogen bond donor and acceptor, etc.⁴⁵ Indeed, the crystal structures of **GALADN**, **GALDMP** and **GALINZ** are consistent with Etter's rule since the phenolic homodimers are presumably a consequence of the formation of the robust $\text{COOH} \cdots \text{N}_{\text{basic}}$ supramolecular heterosynthon.

2.5 Conclusion

In summary, this work has demonstrated the use of gallic acid and ferulic acid as reliable cocrystal formers with molecules containing a basic nitrogen/amide moiety. Of the six cocrystal formers studied; five pairs of cocrystals of gallic acid and ferulic acid with **INZ**, **ADN**, **DMP**, **URE** and **GAH** were afforded. **FERTBR.H₂O** can also be paired since **GALTBR.2H₂O** was previously reported. The crystal structures of the

anhydrous cocrystals reveal the hierarchy of the COOH⁺N_{basic} supramolecular heterosynthon in the presence of phenolic moieties. However, **FERTBR.H₂O** illustrates the challenges that may arise when a water molecule is incorporated in the crystal lattice since crystalline hydrates are capricious in terms of the supramolecular heterosynthon they exhibit.

2.6 References

- ¹ (a) Desiraju, G. R. *Crystal Engineering: The Design of Organic Solids*; Elsevier: Amsterdam, **1989**. (b) Moulton, B.; Zaworotko, M. J. *Chem. Rev.* **2001**, *101*, 1629.
- ² Long, J.R.; Yaghi, O.M. *Chem. Soc. Rev.* **2009**, *38*, 1213.
- ³ MacGillivray, L.R. *J. Org. Chem.* **2008**, *73*, 3311.
- ⁴ (a) Zaworotko, M.; Arora, K. Pharmaceutical co-crystals: A new opportunity in pharmaceutical science for a long-known but little studied class of compounds. In *Polymorphism in Pharmaceutical Solids*, 2nd ed.; Brittain, H. G., Ed.; Informa Healthcare: London, **2009**. (b) Shan, N.; Zaworotko, M.J. *Drug Discov. Today*, **2008**, *13*, 440-446. (c) Almarsson, Ö.; Zaworotko, M. J. *Chem. Commun.* **2004**, 1889. (d) Vishweshwar, P.; McMahon, J.A.; Bis, J.A.; Zaworotko, M.J. *J. Pharma. Sci.*, **2006**, *95*, 499.
- ⁵ (a) Desiraju, G.R. *CrystEngComm*, **2003**, *5*, 466 (b) Dunitz, J.D. *CrystEngComm*, **2003**, *4*, 506 (c) Bond, A.D. *CrystEngComm*, **2007**, *9*, 833-834 (d) Aakeröy, C.B.; Fasulo, M.E. Desper, J. *Mol. Pharm.*, **2007**, *4*, 317-322 (e) Stahly, G.P. *Cryst. Growth Des.* **2007**, *7*, 1007-1026 (f) Zukerman-Schpector, J.; Tiekink, E.R.T. *Zeit. Fur Kristallogr.*, **2008**, *223*,

233-234 (g) Parkin, A.; Gilmore, C.J.; Wilson, C.C. *Zeit. Fur Kristallogr.* **2008**, *223*, 430.

⁶ (a) Childs, S.L.; Zaworotko, M. J. *Cryst. Growth Des.* **2009**, *9*, 4208-4211. (b) Stahly, G. P. *Cryst. Growth Des.* **2007**, *7*, 1007.

⁷ Wöhler, F.; *Justus Lieb. Ann. Chem.* **1844**, *51*, 153.

⁸ (a) Allen, F. H.; Kennard, O. *Chem. Des. Automat. News.*, **1993**, *8*, 31. (b) Allen, F. H. *Acta Crystallogr.*, **2002**, *B58*, 380.

⁹ Trask, A.V. *Mol. Pharmacol.*, **2007**, *3*, 301.

¹⁰ (a) Friščić, T.; Jones, W. J. *Pharm. Pharmacol.* **2010**, *62*, 1547–1559 (b) Trask, A.V.; Samuel Motherwell, W.D.; Jones, W. *Cryst. Growth Des.*, **2005**, *5*, 1013.

¹¹ Karki, S.; Friščić, T.; Fabian, L.; Laity, P. R.; Day, G. M.; Jones, W. *Adv. Mater.* **2009**, *21*, 3905.

¹² (a) Jagadeesh Babu, N.; Nangia, A. *Cryst. Growth Des.* **2011**, *11*, 2662. (b) Cheney, M. L.; Shan, N.; Healey, E. R.; Hanna, M.; Wojtas, L.; Zaworotko, M. J.; Sava, V.; Song, S.; Sanchez-Ramos, J. R. *Cryst. Growth Des.* **2010**, *10*, 394. (c) Good, D.; Rodriguez-Hornedo, N. *Cryst. Growth Des.*, **2009**, *9*, 2252. (d) Stanton, M. K.; Bak, A. *Cryst. Growth Des.* **2008**, *8*, 3856. (e) Bak, A.; Gore, A.; Yanez, E.; Stanton, M.; Tufekcic, S.; Syed, R.; Akrami, A.; Rose, M.; Surapaneni, S.; Bostick, T.; King, A.; Neervannan, S.; Ostovic, D.; Koparkar, A. *J. Pharm. Sci.* **2008**, *97*, 3942. (f) Childs, S. L.; Chyall, L. J.; Dunlap, J. T.; Smolenskaya, V. N.; Stahly, B. C.; Stahly, G. P. *J. Am. Chem. Soc.* **2004**, *126*, 13335.

¹³ http://www.cfsan.fda.gov/_rdb/opagras.html.

¹⁴ http://vm.cfsan.fda.gov/_dms/eafus.html.

- ¹⁵ (a) Sanphui, P.; Goud, N.R.; Khandavilli, U.B.R.; Nangia, A. *Cryst. Growth Des.* **2011**, *11*, 4135-4145 (b) Bethune, S.J.; Schultheiss, N.; Henck, J. *Cryst. Growth Des.*, **2011**, *11*, 2817-2823 (c) Schultheiss, N.; Bethune, S.; Henck, J.; *CrystEngComm*, 2010, *12*, 2436-2442
- ⁽¹⁶⁾ Mannion, M.; *Am J Nat Med*; **1998**; *5*, 30.
- ⁽¹⁷⁾ Lockwood, B.; *Nutraceuticals*, Pharmaceutical Press: London, UK, **2007**.
- ¹⁸ Han, X.; Shen, T.; Lou, H. *Int. J. Mol. Sci.* **2007**, *8*, 950.
- ¹⁹ Shahidi, F.; Naczki, M. *Food Phenolics: Sources, Chemistry, Effects and Applications*, Technomic Publishing Company Inc., Lancaster, PA, **1995**.
- ²⁰ (a) Mattila, P.; Hellstrom, J.; Torronen, R. *J. Agric Food Chem*, **2006**, *54*, 7193. (b) Mattila, P., Hellstrom, J. *J. Food Comp. Anal.*, **2007**, *20*, 152. (c) Kroon, P. A.; Williamson, G. *J. Sci. Food Agric.*, **1999**, *79*, 355.
- ²¹ Graf, E. *Rad. Biol. Med.*; **1992**, *13*, 435.
- ²² Elvira, G. M.; Chandra, S.; MarcoVinicio, R. M.; Wenyi, W. *Food Chem. Toxicol.* **2006**, *44*, 1191.
- ²³ Misao, U.; Hisashi, Y.; Yukiko, K.; Masanori, H.; Tomihiko, H.; Koyama, A. *AntiViral Res.* **2007**, *73*, 85.
- ²⁴ Müller Kratz, J.; Andrighetti-Fröhner, C. R.; Kolling, D. J.; Leal, P. C.; Cirne-Santos, C. C.; Yunes, R. A.; Nunes, R. J.; Trybala, E.; Bergström, T.; Frugulhetti, I.; Barardi, C. R. M.; Simões, C. M. O.; *Mem Inst Oswaldo Cruz*, **2008**, *103*, 437.
- ²⁵ Cate, A. T. T.; Kooijman, H.; Spek, A. L.; Sijbesma, R. P.; Meijer, E. W. *J. Am. Chem. Soc.* **2004**, *126*, 3801.

- ²⁶ McMahon, J. A.; Bis, J. A.; Vishweshwar, P.; Shattock, T. R.; McLaughlin, O. L.; Zaworotko, M. J. *Zeit. Kristallogr.* **2005**, *220*, 340.
- ²⁷ (a) Shattock, T. R.; Arora, K. K.; Vishweshwar, P.; Zaworotko, M. J. *Cryst. Growth Des.* **2008**, *8*, 4533 (b) Aakeröy, C. B.; Beatty, A. M.; Helfrich, B. A. *J. Am. Chem. Soc.* **2002**, *124*, 14425–14432. (h) Bhogala, B. R.; Vishweshwar, P.; Nangia, A. *Cryst. Growth Des.* **2002**, *2*, 325–328.
- ²⁸ Aakeröy, C. B.; Beatty, A. M.; Helfrich, B. A.; Nieuwenhuyzen, M. *Cryst. Growth Des.* **2003**, *3*, 159. (b) Aakeröy, C. B.; Beatty, A. M.; Helfrich, B. A. *Angew. Chem. Int. Ed.* **2001**, *40*, 3240.
- ²⁹ (a) Bis, J.A.; Vishweshwar, P.; Weyna, D.; Zaworotko, M.J. *Mol. Pharm.*, **2007**, *4*, 401-416 (b) Papaefstathiou, G.S.; MacGillivray, L.R. *Org. Lett.*, **2001**, *3*, 3835–3838001). (c) Vishweshwar, P.; Nangia, A.; Lynch, V.M. *CrystEngComm*, **2003**, *5*, 164-168.
- ³⁰ Kavuru, P.; Aboarayas, D.; Arora, K. K.; Clarke, H. D.; Kennedy, A.; Marshall, L.; Ong, T.; Perman, J.; Pujari, T.; Wojtas, y.; Zaworotko, M. J. *Cryst. Growth Des.* **2010**, *10*, 3568.
- ³¹ Lapidus, S.L.; Stephens, P.W.; Arora, K.K.; Shattock, T.R.; Zaworotko, M.J. *Cryst. Growth. Des.* **2010**, *10*, 4630.
- ³² Bruker-AXS, SMART-V5.625. Data Collection Software. Madison, Wisconsin, USA, **2001**.
- ³³ Bruker, APEX2 (Version 2008.1-0). Madison, Wisconsin, USA, **2008**.
- ³⁴ SAINT-V7.51A, Bruker-AXS, Data Reduction Software. Madison, Wisconsin, USA, **2008**.
- ³⁵ Sheldrick, G. M. SHELXTL, University of Göttingen: Göttingen, Germany, **1997**.

- ³⁶ Sheldrick, G. M. SADABS. Program for Empirical Absorption Correction; University of Gottingen: Germany, 2008.
- ³⁷ Bruker AXS: *TOPAS V4: General profile and structure analysis software for powder diffraction data*. - User's Manual, Bruker AXS, Karlsruhe, Germany.
- ³⁸ Coelho, A.A. *J. Appl. Cryst.* **2000**, *33*, 899.
- ³⁹ TOPAS-Academic is available at <http://www.topas-academic.net>.
- ⁴⁰ Clarke, H. D.; Arora, K. K.; Bass, H.; Kavuru, P.; Ong, T.; Pujari, T.; Wojtas, y.; Zaworotko, M. J. *Cryst. Growth Des.* **2010**, *10*, 2152.
- ⁴¹ (a) Cheney, M.; Weyna, D.R.; Shan, N.; Hanna, M.; Wojtas, L.; Zaworotko, M.J. *Cryst. Growth Des.* **2010**, *10*, 4401. (b) Bis, J. A.; Vishweshwar, P.; Weyna, D.; Zaworotko, M. J. *Mol. Pharmaceutics* **2007**, *4*, 401.
- ⁴² Clarke, H. D.; Arora, K. K.; Wojtas, L.; Zaworotko, M. J. *Cryst. Growth Des.* **2011**, *11*, 964.
- ⁴³ Infantes, L.; Motherwell, W. D. S. *Chem. Commun.* **2004**, 1166.
- ⁴⁴ Seaton, C.C.; Parkin, A. *Cryst. Growth Des.* **2011**, *11*, 1502.
- ⁴⁵ Etter, M. C. *Acc. Chem. Res.* **1990**, *23*, 120.

Chapter 3: Crystal Engineering of Isostructural Quaternary Multi-Component Crystal Forms of Olanzapine.

3.1 Introduction

Crystal engineering,^{1,2} has matured into a well-recognized aspect of solid-state chemistry research and is focused on the design of novel crystalline solids with tunable physicochemical properties. The selection of a suitable crystal form of an active pharmaceutical ingredient (API) is particularly relevant to oral drug delivery,³ and it profoundly influences the development and performance of the API. Crystal forms of APIs have spanned polymorphs,⁴ solvates,⁵ hydrates⁶ and more recently, pharmaceutical cocrystals.^{7,8}

Pharmaceutical cocrystals can be defined as multiple component crystals in which at least one component is molecular and a solid at room temperature (the cocrystal former) and forms a supramolecular synthon with a molecular or ionic API. Pharmaceutical cocrystals have emerged as a new paradigm in pharmaceutical solid form development to diversify the range of crystal forms exhibited by APIs, allowing opportunities for improved performance characteristics and extend the product life and patent coverage of the API.^{9,10} Most importantly, pharmaceutical cocrystals can enhance physicochemical properties of APIs such as solubility,¹¹ stability¹² and mechanical properties¹³ while preserving the intended intrinsic activity of the API. In addition,

pharmaceutical cocrystals have been incorporated with other techniques used to modulate physicochemical properties as noted in the examples of nanocrystalline cocrystals¹⁴ and cocrystals of salts.¹⁵

Pharmaceutical cocrystals are amenable to design due to the ubiquitous nature of APIs, in that, they possess exterior functional groups that readily engage in supramolecular synthons with a wide variety of pharmaceutically acceptable cocrystal formers. However, this semi-empirical approach becomes challenging for APIs that exhibit conformational flexibility and/or possess multiple functional groups.¹⁶ In addition, the design or engineering of compositions with more than two unique components becomes challenging due to the functional diversity introduced by each component.

Olanzapine (2-methyl-4-(4-methyl-1-piperazinyl)-10H-thieno-[2,3b][1,5]benzodiazepine), a BCS¹⁷ class II (low solubility, high permeability) API was selected as a crystal engineering candidate. Olanzapine is a widely prescribed atypical antipsychotic drug marketed under the trademark name Zyprexa[®] by Eli Lilly and Company. The drug is therapeutically effective in treating psychiatric disorders such as schizophrenia and manic episodes associated with bipolar disorder.¹⁸ Olanzapine has been shown to be effective in the reduction of not only positive symptoms (hallucinations and delusions), but also negative and cognitive symptoms (social and emotional withdrawal) in acute and relapsing schizophrenics.¹⁹ Crystal forms of olanzapine are well-documented and include six anhydrous polymorphs,^{20,21,22,23} three polymorphic dihydrates,²⁴ two polymorphic sesquihydrates, several solvated forms,²⁵ mixed solvates and hydrates,²⁶ salts and an amorphous form.²⁷ Much research has been done to develop novel crystal forms of

olanzapine. Reutzel-Edens et al discussed the polymorphism of olanzapine dihydrate and the structural relationship between the anhydrates and hydrates.²⁸ Nangia et al showed that the solubility of olanzapinium monomaleate and dimaleate salts was 225-550 times greater than that of free base olanzapine.²⁹

Isostructural cocrystals, i.e. crystal forms that exhibit the same or similar crystal structure,³⁰ have been reported in the literature.³¹ These crystal forms, primarily binary cocrystals, are generally designed by interchanging structurally equivalent functional groups such as chloride/methyl exchange, Br/I or CH/N.³² The design and successful synthesis of isostructural olanzapine cocrystals is remarkable in the context that it contains four distinct molecular entities. Indeed, it has been shown recently that the subtle changes in the chemical composition of the API, i.e. swapping the sodium for the potassium cation, can result in significant and unpredictable changes in both the packing arrangement³⁰ and physicochemical properties of the salt of the API.³³ The design of isostructural cocrystals based on the analysis of the existing crystal forms offers unique opportunities to systematically fine-tune the physicochemical properties of the API by controlling the molecular arrangement in the solid state. This article illustrates a design strategy to construct multi-component crystal forms of olanzapine *a priori* from the systematic analysis of existing crystal structures, culminating in the formation of multi-component compositions with four unique molecules.

3.2 Materials and Methods

3.2.1 Materials

Olanzapine was obtained from Alkermes Inc. and used without further purification.

Cocrystal formers were purchased from commercial vendors and used without further purification (Figure 3.1). Solvents purchased from commercial vendors were distilled before use. All cocrystals were analyzed by powder X-ray diffraction (PXRD), and single crystal X-ray analysis where applicable.

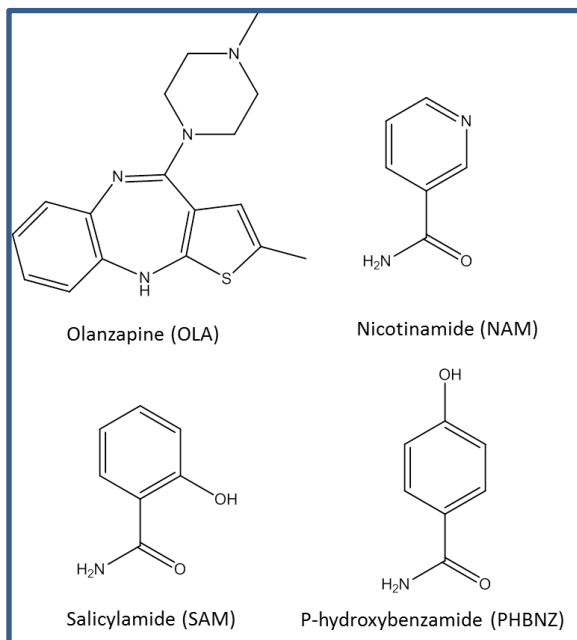


Figure 3.1: Chemical structures of olanzapine and cocrystal formers used herein.

3.2.2 Preparation of Cocrystals

Olanzapine ·Nicotinamide Isopropyl acetate Tetrahydrate, OLANAM.IPA.4H₂O:

Olanzapine (40 μ L of a 25mg/ml stock solution) and nicotinamide (37.6 μ L of a 20 mg/mL stock solution) were added to a glass vial and the solvent was dried under nitrogen flow. Isopropyl acetate was added to the mixture and the sealed vial was heated at 70 °C for two hours. The solution was then cooled at 5 °C for 24 hours. The solution was concentrated to 50 μ L total volume, recapped and left at 5 °C for an additional 24

hours. Large yellow plates of the **OLANAM.IPA.H₂O** were collected and allowed to dry at ambient conditions.

Olanzapine ·Salicylamide Isopropyl acetate Tetrahydrate OLASAM.IPA.H₂O:

Olanzapine (7.5 mg, 0.024 mmol) and salicylamide (5.1 mg, 0.037 mmol) were dissolved in 1 mL isopropyl acetate and heated at 90 °C until all the solid material was dissolved. The vial was sealed and the solution was allowed to slowly evaporate at 5 °C. After three days, large yellow plates of the **OLASAM.IPA.H₂O** were collected by gravimetric filtration and dried at room temperature.

Olanzapine ·p-Hydroxybenzamide Isopropyl acetate Tetrahydrate,

OLAPHBNZ.IPA.4H₂O: Olanzapine (7.5 mg, 0.024 mmol) and p hydroxybenzamide (7.0 mg, 0.051 mmol) were dissolved 1 mL isopropyl acetate and heated at 90 °C until all the solid material was dissolved. The sealed vial was sealed was allowed to slowly evaporate at 5 °C. After eleven days, yellow plates of the **OLAPHBNZ.IPA.H₂O** were collected by gravimetric filtration and dried at room temperature.

3.2.3 *Methods*

Powder X-ray diffraction (PXRD): Bulk samples were analyzed by powder X-ray diffraction with a Bruker AXS D8 powder diffractometer. Experimental conditions: Cu K α radiation ($\lambda = 1.54056 \text{ \AA}$); 40 kV; 30 mA; scanning interval 3–40° 2 θ ; time per step 0.5s. The experimental PXRD patterns and calculated PXRD patterns from single crystal structures were compared to confirm that the composition of the bulk materials was consistent with that of the single crystal used for X-ray crystallography.

Single Crystal X-ray Diffraction Analysis: Single crystal X-ray data were collected using Bruker-AXS SMART-APEXII CCD diffractometer using CuK α radiation, $\lambda = 1.54178 \text{ \AA}$ for **OLASAM.IPOAc.H₂O** and Mo K α radiation ($\lambda = 0.71073 \text{ \AA}$) for **OLANAM.IPOAc.H₂O**. Indexing was performed using APEX2³⁴ (Difference Vectors method). Data integration and reduction were performed using SaintPlus 6.01.³⁵ Absorption correction was performed by multi-scan method implemented in SADABS.³⁶ Space groups were determined using XPREP implemented in APEX2. The structure was solved using SHELXS-97 (direct methods) and refined using SHELXL-97 (full-matrix least-squares on F²) contained in APEX2 and WinGX v1.70.01^{37,38,39,40} [4,5,6,7] programs packages. All non-hydrogen atoms were refined anisotropically. Hydrogen atoms of water molecules and –NH groups for **OLANAM.IPOAc.H₂O** were found in the Fourier difference map and included in the refinement process using distance restraints (DFIX) with isotropic thermal parameters: Uiso(H) = 1.5Ueq(-NH,-OH). All remaining hydrogen atoms were placed in geometrically calculated positions and included in the refinement process using riding model with isotropic thermal parameters: Uiso(H) = 1.2Ueq(-CH, -CH₂), Uiso(H) = 1.5Ueq(-OH, -CH₃).

Hydrogen atoms of water molecules and –NH groups for **OLASAM.IPOAc.H₂O** were found in the Fourier difference map and included in the refinement process using distance restraints (DFIX, SADI) with isotropic thermal parameters: Uiso(H) = 1.5Ueq(-NH,-OH). All remaining hydrogen atoms were placed in geometrically calculated positions and included in the refinement process using riding model with isotropic thermal parameters: Uiso(H) = 1.2Ueq(-CH, -CH₂), Uiso(H) = 1.5Ueq(-OH, -CH₃). Crystallographic data and hydrogen bond parameters are presented in the appendix 4.

3.3 Results

Crystal Structures of **OLANAM.IPA.4H₂O** and **OLASAM.IPA.4H₂O**:

OLANAM.IPA.4H₂O and **OLASAM.IPA.4H₂O** crystallize in the monoclinic space group $P2_1/c$ where each cocrystal contains two **OLA** molecules, four water molecules, an isopropyl acetate molecule and one molecule of the cocrystal former (**NAM** or **SAM**). The crystal structures of **OLANAM.IPA.4H₂O** and **OLASAM.IPA.4H₂O** reveal a two-dimensional hydrogen-bonded network where four water molecules hydrogen bond to each other to form a tetrameric catemer. This tetrameric catemer interacts with four **OLA** molecules by donating four hydrogen bonds and accepting two hydrogen bonds (Figs. 3.2a and 3.2b). The isopropyl acetate molecules and the **NAM/ SAM** terminate the tetrameric catemer of water molecules via $\text{OH}\cdots\text{O}$ and $\text{NH}\cdots\text{O}$ hydrogen bond interactions. **NAM/ SAM** molecules form amide homodimers along the c axis (Figs. 3.3a and 3.3b). Olanzapine molecules are aligned in a herring bone pattern and are stacked in an eclipsed fashion (Figs. 3.4a and 3.4b). Single crystals suitable for X-ray structure determination were not obtained for **OLAPHBNZ.IPA.4H₂O**. However, **OLAPHBNZ.IPOAc.4H₂O** is presumably isostructural to **OLANAM.IPA.4H₂O** and **OLASAM.IPA.4H₂O** since the powder pattern obtained was found to be similar to the powder patterns of **OLANAM.IPA.4H₂O** and **OLASAM.IPA.4H₂O** (appendix 4).

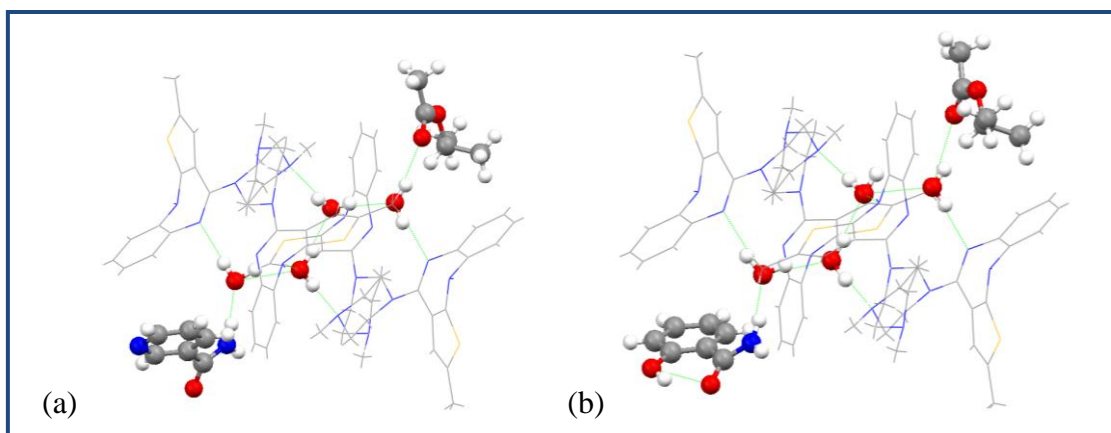


Figure 3.2: Crystal packing view along *a* axis of (a) **OLANAM.IPA.4H₂O** and (b) **OLASAM.IPA.4H₂O** exhibiting a tetrameric catemer of water molecules that is hydrogen bonded to four **OLA** molecules. The tetrameric catemer of water molecules offers 4 hydrogen bond donors and 2 hydrogen bond acceptors to complement a pair of olanzapine molecules. The isopropyl acetate and the cococrystal former (**NAM** or **SAM**) hydrogen bond to each side of the tetrameric catemer of water molecules.

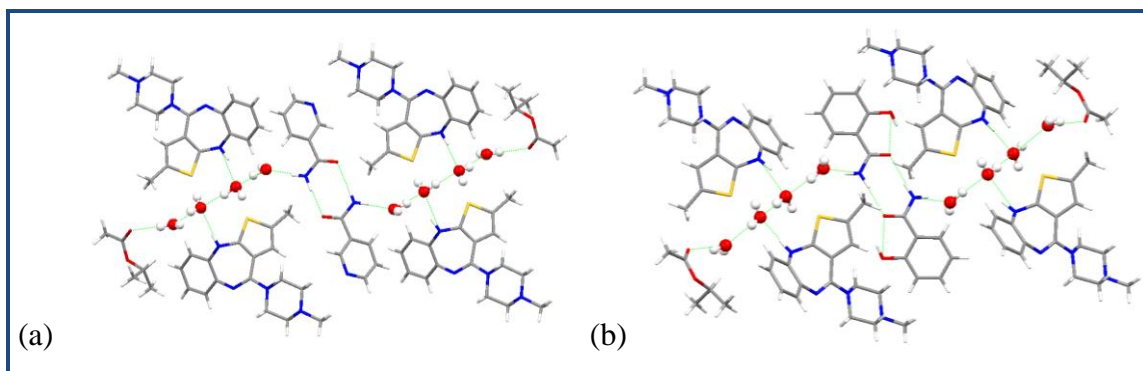


Figure 3.3: Crystal packing view along *c* axis of **OLANAM.IPA.4H₂O** and (b) **OLASAM.IPA.4H₂O** showing how the tetrameric catemers of water molecules are terminated by the cococrystal former (**NAM** or **SAM**). The **NAM** and **SAM** molecules form dimers to extend the structure. In each case, two olanzapine molecules are omitted for clarity.

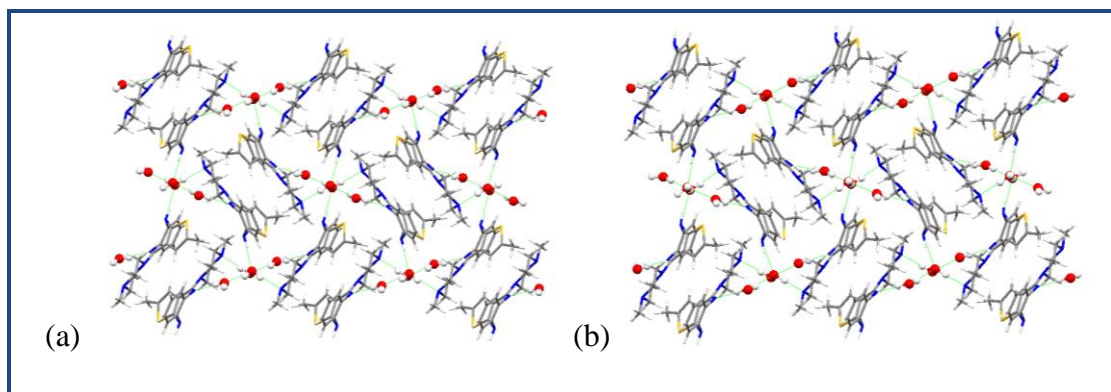


Figure 3.4: Crystal packing of **OLANAM.IPA.4H₂O** and (b) **OLASAM.IPA.4H₂O** showing a herring bone pattern of pairs of olanzapine enantiomers hydrogen bonded to four water molecules. **NAM, SAM** and isopropyl acetate molecules omitted for clarity.

<u>Anhydrate</u>	<u>Dihydrate</u>	<u>Sesquihydrate</u>
UNOGIN UNOGIN01	AQOMAU AQOMAU01 AQOMAU02	AQOMEY AQOMEY01
<u>Solvates</u>	<u>Mixed hydrates and solvates</u>	<u>Salts</u>
UNOGOT (methanol)	CAYTUS (DMSO monohydrate)	JIXROY (olanzapinium benzoate)
WEXQAS (dichloromethane)	ELEVOG (methanol monohydrate)	TAQNUV (olanzapinium nicotinate)
	WEXPUL (butan-2-ol monohydrate)	AMIYUR (olanzapinium maleate (1:1))
	WEXQEW (ethanol dihydrate)	AMIZAY (olanzapinium maleate (1:2))

Table 3.1: Refcodes for crystal structures of olanzapine deposited in the CSD.

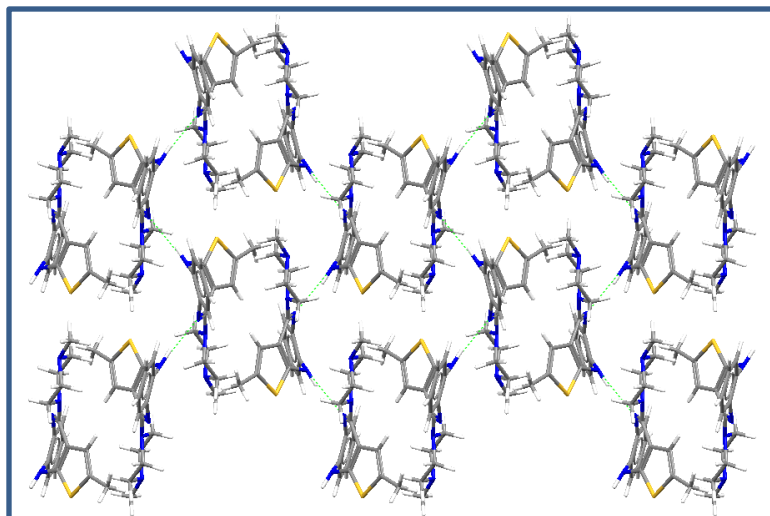


Figure 3.5: Crystal packing of olanzapine anhydrate form I showing olanzapine enantiomers sustained by NH...N hydrogen bond interactions along the *c* axis.

3.4 Discussion

A critical step in the design of cocrystals is the study of crystal packing and hydrogen bonding patterns exhibited within the crystal structure of the target molecule. Analysis of the crystal structures of olanzapine deposited in the CSD reveals an anhydrate; three polymorphs of olanzapine dihydrate; two polymorphs of olanzapine sesquihydrate; methanol and dichloromethane solvates; four mixed solvates and hydrates; and salts with benzoate, nicotinate and maleate anions (Table 3.1). Observation of the crystal packing in the crystal forms of olanzapine reveals pairs of olanzapine molecules where olanzapine adopts mirror-related conformations.⁴¹ In olanzapine anhydrate, these pairs of olanzapine molecules are connected by NH...N hydrogen bond interactions (Fig. 3.5). However in the solvated and salt forms of olanzapine, the NH...N interaction is disrupted by solvent molecules or anions occupying sites between the pairs of olanzapine molecules.

Many of these crystal forms are isostructural and can be categorized according to their crystal packing arrangement and crystallographic unit cell parameters are denoted packing A, packing B, packing C and packing D (Tables 4-7).

Packing A is exhibited in the crystal structure of olanzapine dihydrate form D (AQOMAU, Fig. 3.7). In packing A, supramolecular heterosynthon 1 (Fig. 3.6a) is observed where the water molecules are arranged as a cyclic tetramer between the pairs of olanzapine molecules such that it offers four hydrogen bond donors and two hydrogen bond acceptors. The number of hydrogen bond donors and acceptors is complementary to a pair of olanzapine molecules since olanzapine possesses one hydrogen bond donor and two hydrogen bond acceptors. The pairs of olanzapine molecules form a herring bone pattern and the sheets are eclipsed to each other (Fig. 3.7b).

Packing B is exhibited in three isostructural crystal forms of olanzapine: AQOMAU01 (dihydrate form B), AQOMEY01 (sesquihydrate form II) and UNOGOT (methanol solvate). Packing B exhibits a three dimensional network where the solvent molecules lie between pairs of olanzapine molecules and hydrogen bonds to four olanzapine molecules (Figure 3.8). In all three crystal forms, the pairs of olanzapine molecules are aligned along the crystallographic *a* axis in a herring bone pattern to form sheets that are stacked in an eclipsed manner. Supramolecular heterosynthon 2 (Fig. 3.6b) is observed in the hydrated crystal forms AQOMAU01 and AQOMEY01 where the water molecules are arranged as a catamer and offers the same number of hydrogen bond donors and acceptors similar to supramolecular synthon 1 to match a pair of olanzapine molecules. In the methanol solvate (UNOGOT), a pair of methanol molecules lies between the pairs

of olanzapine molecules and hydrogen bonds to four olanzapine molecules via NH...O and OH...O interactions.

Packing C is exhibited in various crystal forms: AQOMEY (sesquihydrate form I), AQOMAU02 (dihydrate form E), CAYTUS (DMSO solvate) and ELEVOG (methanol monohydrate). Similar to packing A and B, the solvent molecules occupy sites between the pairs of olanzapine molecules to form bridges that hydrogen bonds to four olanzapine molecules. Supramolecular heterosynthon 2 is also observed in the hydrated crystal forms. The difference between packing B and packing C is the orientation of adjacent sheets where they are stacked in a staggered fashion (Figure 3.9).

Packing D is exhibited in salts of olanzapine with benzoate (JIXROY) and nicotinate (TAQNUV) anions. Analysis of the crystal structures reveals the alignment of the pairs of olanzapine molecules along the *c* axis (Figure 3.10). The pairs of olanzapine molecules are connected via charge assisted interactions formed between the carboxylate of the benzoate and nicotinate anion and the ammonium of the olanzapine cation.

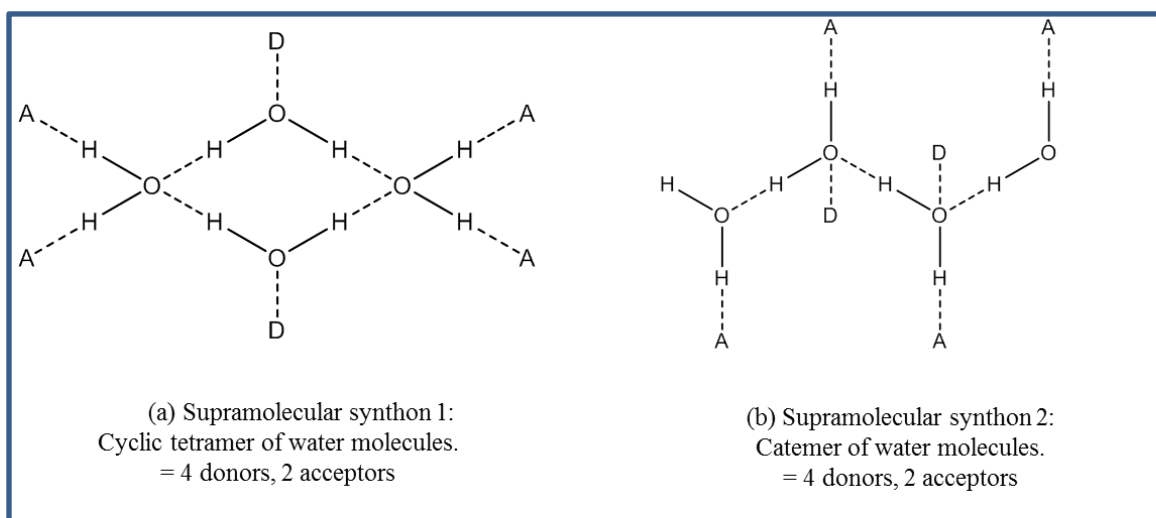


Figure 3.6: Two types of supramolecular heterosynthon exhibited in crystal structures of olanzapine dihydrate.

REF CODE	Compound	<i>a</i> (Å)	<i>b</i> (Å)	<i>c</i> (Å)	α (°)	β (°)	γ (°)	Volume	Space Group
AQOM AU	Dihydrate	9.927 (5)	10.095 (5)	10.514 (6)	84.71 (1)	62.66 (<1)	71.18 (<1)	884.00 1	P-1

Table 3.2: Crystal forms of olanzapine that exhibits packing A.

REF CODE	Compound	<i>a</i> (Å)	<i>b</i> (Å)	<i>c</i> (Å)	α (°)	β (°)	γ (°)	Volume	Space Group
AQOM EY01	Sesquihydrate	10.040 (2)	12.900 (3)	14.510 (3)	90	92.97 (<1)	90	1802.8 10	P2 ₁ /c
AQOM AU01	Dihydrate	9.869 (1)	12.716 (1)	14.385 (1)	90	92.97 (<1)	90	1802.8 10	P2 ₁ /c
UNOG OT	Methanol solvate	10.207 (3)	12.440 (4)	14.278 (5)	90	92.60 (3)	90	1811.0 84	P2 ₁ /c

Table 3.3: Crystal forms of olanzapine that exhibits packing B.

REF CODE	Compound	<i>a</i> (Å)	<i>b</i> (Å)	<i>c</i> (Å)	α (°)	β (°)	γ (°)	Volume	Space Group
AQOME Y	Sesquihydrate	25.130 9 (2)	12.238 (1)	14.912 (1)	90	124.98 (<1)	90	3757.2 14	C ₂ /c
AQOMA U02	Dihydrate	24.520	12.350	15.218	90	125.82	90	3736.2 81	C ₂ /c
CAYTUS	DMSO solvate	24.584 (4)	12.534 (1)	15.153 (3)	90	125.45 (1)	90	3803.4 30	C ₂ /c
ELEVO G	Methanol monohydrate	25.359 (<1)	11.973 (<1)	15.609 (<1)	90	127.58 (<1)	90	3753.7 71	C ₂ /c

Table 3.4: Crystal forms of olanzapine that exhibits packing C.

REF CODE	Compound	a (Å)	b (Å)	c (Å)	α (°)	β (°)	γ (°)	Volume	Space Group
TAQNU V	Olanzapine nicotinate	9.296 (1)	11.242 (1)	12.000 (1)	63.16 (<1)	87.48 (<1)	83.73 (<1)	1111.442	P-1
JIXROY	Olanzapine benzoate	9.257	11.222	12.063	64.59 (<1)	87.57 (<1)	83.25 (<1)	1124.753	P-1

Table 3.5: Crystal forms of olanzapine that exhibits packing D.

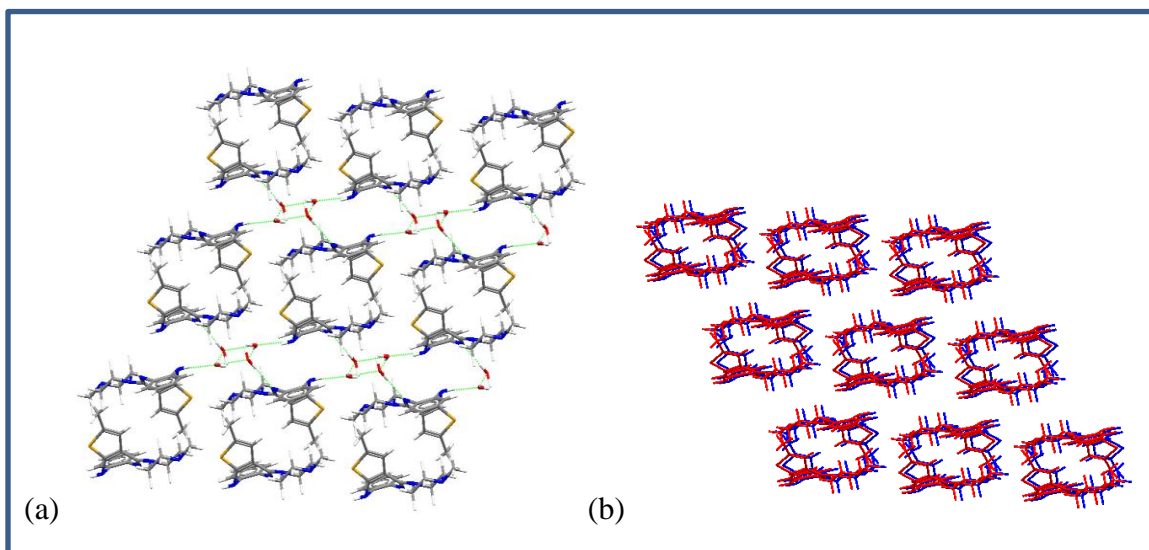


Figure 3.7: (a) Crystal structure of olanzapine dihydrate form D exhibiting packing A where a cyclic tetramer of water molecules hydrogen bonds to four olanzapine molecules along the b axis. (b) Sheets of olanzapine molecules eclipse one another; water molecules deleted for clarity.

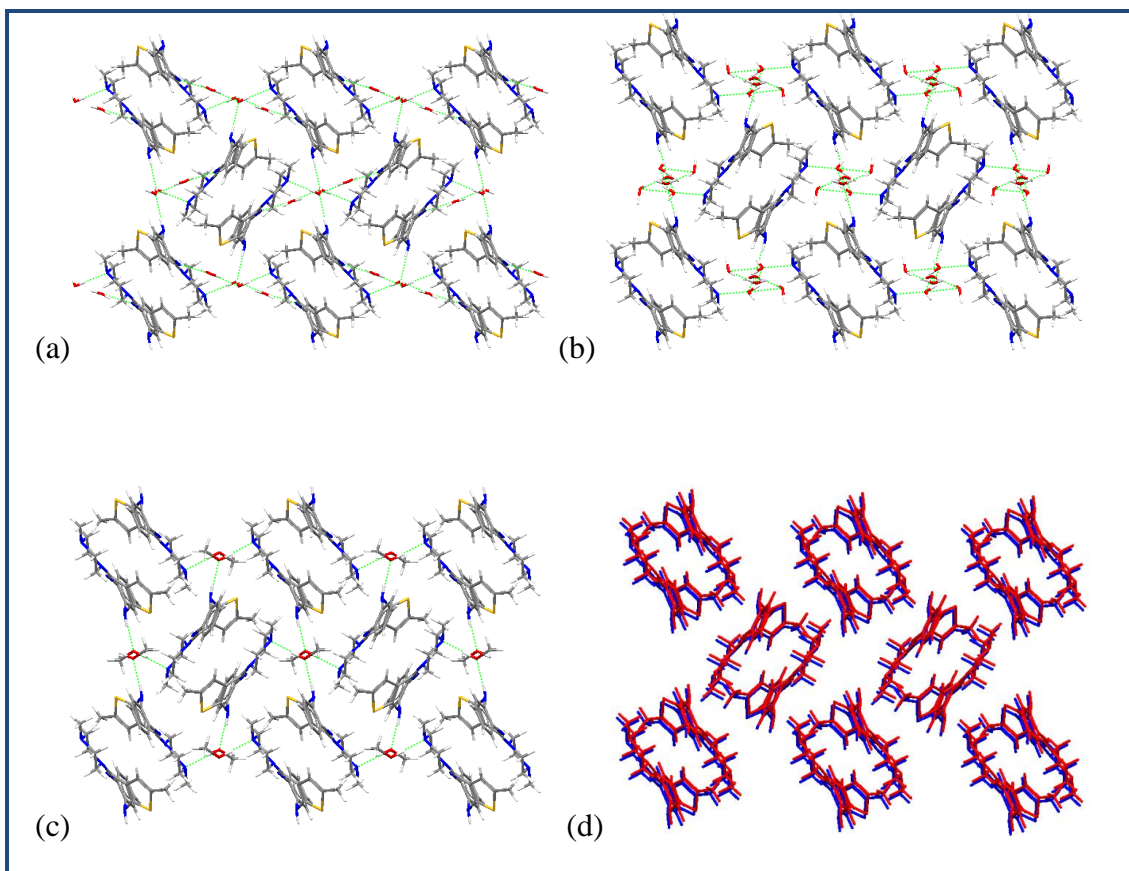


Figure 3.8: Crystal packing of (a) olanzapine dihydrate form B (b) olanzapine sesquihydrate form II and (c) olanzapine methanol solvate exhibiting packing B, wherein the solvent molecules are arranged such that they hydrogen bond to four olanzapine molecules. (d) Illustrates sheets that are arranged in a herring bone pattern and stack in an eclipsed manner; solvent molecules deleted for clarity.

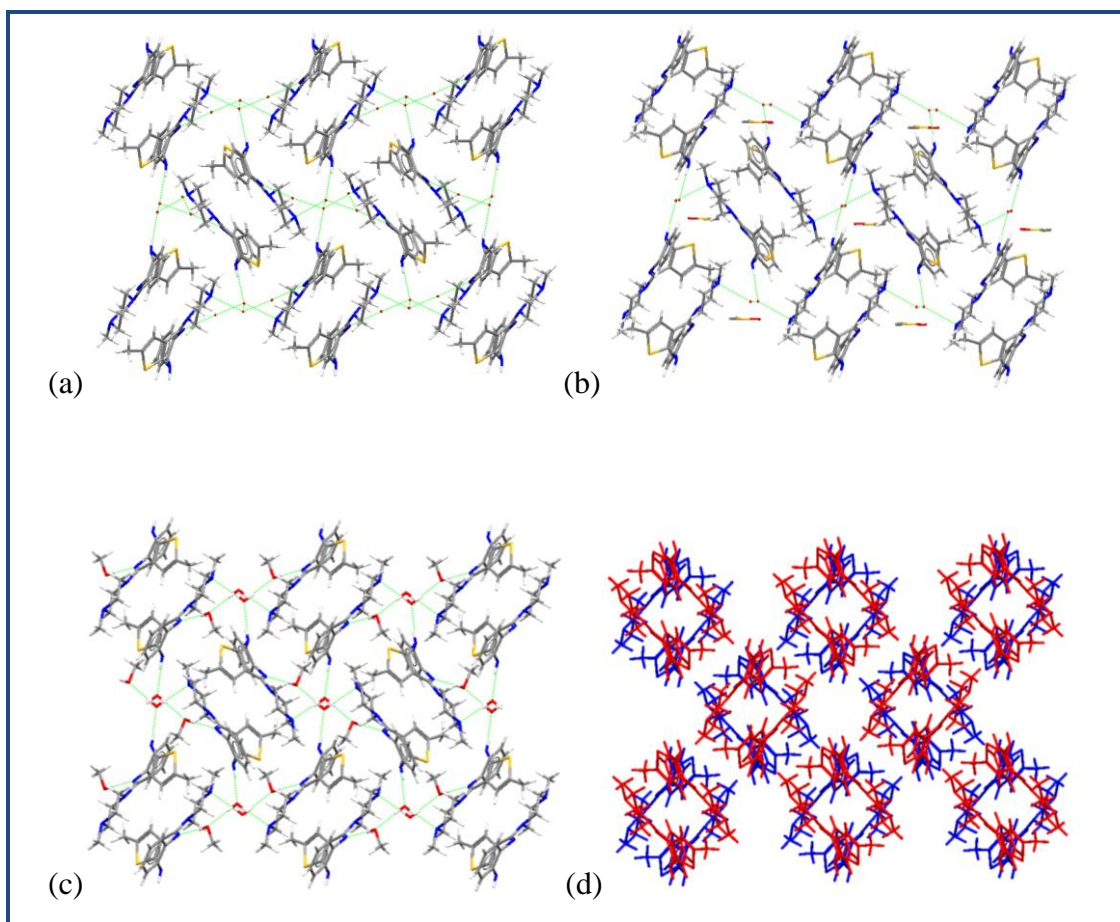


Figure 3.9: Crystal forms of (a) olanzapine sesquihydrate form I (b) olanzapine DMSO solvate and (c) olanzapine methanol monohydrate exhibiting packing C where the solvent molecules form bridges to hydrogen bond to four olanzapine molecules. (d) Illustrates adjacent sheets that stack in a staggered manner; solvent molecules deleted for clarity.

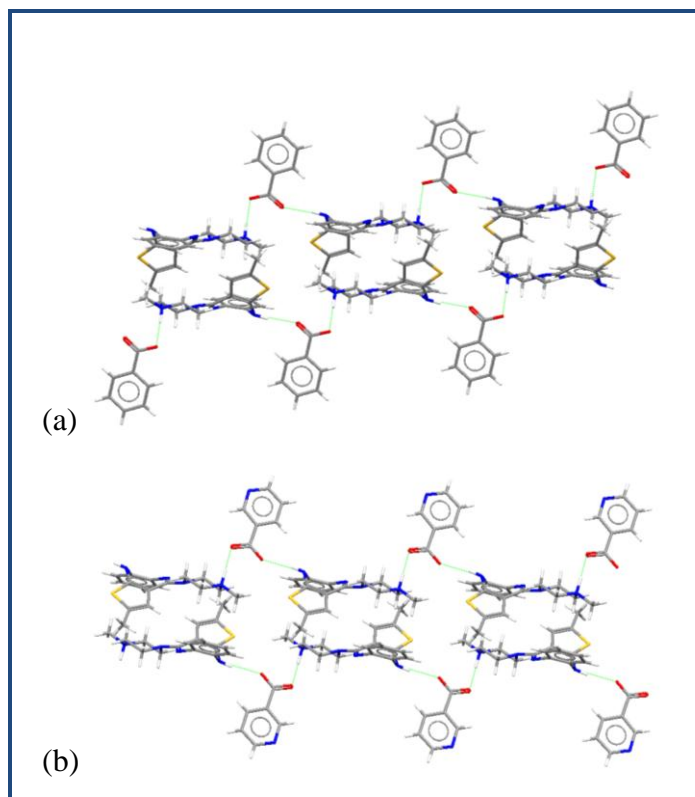


Figure 3.10: Packing D exhibiting olanzapine cation interacts with nicotinate and benzoate anions via charge assisted $\text{NH}\cdots\text{COO}^-$ hydrogen bonds along the a axis.

Crystal Engineering of Isostructural Cocrystals of Olanzapine: The formation of centrosymmetric pairs of olanzapine molecules is observed in crystal forms that exhibit packing A, B, C and D. Analysis of these crystal forms reveals the solvent molecules always arrange themselves between pairs of olanzapine molecules and hydrogen bonds to four olanzapine molecules irrespective of the solvent molecule. It has been asserted that water molecules are promiscuous in terms of the supramolecular synthons they exhibit, as well as resulting structural stability and stoichiometry.⁴² Indeed, the water molecule has been described as chameleon-like due to its small size and versatile hydrogen bonding capabilities. For example, gallic acid monohydrate, the first tetramorphic hydrate for which fractional coordinates have been determined, exhibits different

supramolecular synthons and crystal packing in each polymorph. In contrast, analysis of the polymorphic forms of olanzapine dihydrate for which coordinates have been determined reveals that the water molecules arrange to offer four hydrogen bond donors and two acceptors to complement a pair of olanzapine molecules (Figure 5). Therefore, it can be presumed that the pairs of olanzapine molecules are the supramolecular building blocks of the crystal structure and therefore dictate the supramolecular assembly of the other components within the crystal. This supramolecular building block was therefore exploited to yield isostructural cocrystals of olanzapine consisting of four chemical entities: olanzapine, the cocrystal former, an iso-propyl acetate solvent molecule and four water molecules.

Crystal structures of **OLANAM.IPA.4H₂O** and **OLASAM.IPA.4H₂O** reveal the presence of a tetrameric catemer of water molecules as exhibited in the solvated crystal forms of olanzapine. The presence of this tetrameric catemer of water molecules within the crystal lattice results in an imbalance of the number of hydrogen bond donors and acceptors such that there is an excess of a single hydrogen bond donor and a hydrogen bond acceptor. The excess hydrogen bond donor and acceptor become satisfied by the incorporation of the solvent molecule and the cocrystal former to afford four hydrogen bond donors and two hydrogen bond acceptors to match a pair of olanzapine molecules. The underlying principle in the synthesis of isostructural cocrystals of olanzapine is that the persistence of the pairs of olanzapine molecules and the tetrameric catemer of water molecules allows for the substitution of cocrystal formers that are structurally consistent without altering the crystal packing.

	No. of entries	% of structures
Total number of entries	152	100
Entries where one chemical entity is a solid at ambient temperature	45	29.6
Entries with two chemical entities that are solids at ambient temperature	85	55.9
Entries with three chemical entities that are solids at ambient temperature	17	11.1
Entries with four chemical entities that are solids at ambient temperature	5	3.8

* Conquest 1.13, Nov 2011 update, only organics, 3D coordinates known, $R \leq 7.5$, No ions.

Table 3.6: CSD statistics of crystal forms containing four distinct molecular chemical entities.

CSD statistics of crystal structures that contain four distinct molecular chemical entities

A CSD analysis was conducted to evaluate the number of crystal forms that contains four distinct chemical entities to reveal a total of 152 hits. These structures were further divided into four categories where at least 1 component was solid, at least two components were solid, at least three components were solid and at least four components were solid (Table 3.6).

There are 45 entries where one chemical entity was solid at ambient temperature whereas 85 of the 152 entries fall into the category where at least two chemical entities are solid at ambient temperature. Analysis of the categories where all three and four chemical entities are solid reveals 17 and 5 entries respectively. Cocrystals of olanzapine

reported herein fall into the category where two chemical entities are solid at ambient temperature. Of the 152 entries, only three crystal forms, MESRUX, OHUXAQ and POHXUG contain a molecule that exhibits biological activity. OHUXAG contains only one molecule that is solid at room temperature and MESRUX and POHXUG contains two and three molecules that are solid at room temperature respectively. Analysis of crystal forms containing four chemical entities reported in the CSD reveal that few exhibit isostructurality, notably CIKWAV, CIKWEZ, CIKWED (where two chemical entities are solid), ROBHAS, ROBHEW, ROBHA (where three chemical entities are solid), QUFZIB and QUFZOH (where four chemical entities are solid). Most of these structures are host-guest inclusion compounds where isostructurality is achieved through the exchange of guest molecules that are loosely held in the crystal structure. A literature survey of isostructural cocrystals reveals mainly two component crystal forms sustained by hydrogen and halogen bonding networks.^{32, 43} Indeed it has been reported that isostructural structures rarely include more than two members due to the close packing of molecules in crystalline solids.⁴⁴ However to the best of our knowledge, this is the first reported isostructural four component crystal forms that contain water and solvent molecules.

3.5 Conclusion

In summary, this study has shown how the systematic analysis and understanding of existing crystal structures of olanzapine facilitates the synthesis of four component isostructural cocrystals of olanzapine. These cocrystals are relevant as they illustrate that

in general crystal structures of APIs can be deliberately designed and their physicochemical properties can be systematically customized.

3.6 References

¹ Desiraju, G. R. *Crystal Engineering: The Design of Organic Solids*; Elsevier: Amsterdam, **1989**.

² Moulton, B.; Zaworotko, M. J. *Chem. Rev.* **2001**, *101*, 1629–1658.

³ (a) Allen, L. V.; Popovich, N. G.; Ansel, H. C., *Ansel's pharmaceutical dosage forms and drug delivery systems*; Lippincott Williams and Wilkins: Baltimore, MD, **2005** (b) Almarsson, Ö.; Zaworotko, M. J. *Chem. Commun.*, **2004**, 1889-1896.

⁴ (a) Bernstein, J. *Polymorphism in Molecular Crystals*; Clarendon Press: Oxford, **2002**. (b) Hilfiker, R. *Polymorphism: in the Pharmaceutical Industry*; Wiley VCH: New York, **2006**.

⁵ (a) Morris, K. In *Structural aspects of hydrates and solvates*; Brittain, H. G., Ed.; *Polymorphism in Pharmaceutical Solids, Vol. I*; Marcel Dekker: **1999**; pp 125_226. (b) Vippagunta, S. R.; Brittain, H. G.; Grant, D. J. W. *Adv. Drug Delivery Rev.* **2001**, *48*, 3.

⁶ Khankari, R. K.; Grant, D. J. *Thermochim. Acta* **1995**, *248*, 61–79.

- ⁷ Vishweshwar P, McMahon JA, Bis JA, Zaworotko MJ. *J Pharm Sci*, **2006**, *95*, 499–516.
- ⁸ Schultheiss N, Newman A. *Cryst Growth Des*, **2009**, *9*, 2950–2967.
- ⁹ Shan, N.; Zaworotko, M. J. *Drug Discovery Today* **2008**, *13*, 440.
- ¹⁰ Peterson, M.L.; Collier, E.A.; Hickey, M.B.; Guzman, H.; Almarsson, Ö, *Multi-Component Pharmaceutical Crystalline Phases: Engineering for Performance*; in *Organic Crystal Engineering: Frontiers in Crystal Engineering*; Tiekink, E. R.T.; Vittal, J. J.; Zaworotko, M. J., Eds.; John Wiley Publishers: New York, **2010**.
- ¹¹ (a) Jagadeesh Babu, N.; Nangia, A. *Cryst. Growth Des.* **2011**, *11*, 2662. (b) Cheney, M. L.; Shan, N.; Healey, E. R.; Hanna, M.; Wojtas, L.; Zaworotko, M. J.; Sava, V.; Song, S.; Sanchez-Ramos, J. R. *Cryst. Growth Des.* **2010**, *10*, 394. (c) Good, D.; Rodriguez-Hornedo, N. *Cryst. Growth Des.*, **2009**, *9*, 2252. (d) Childs, S. L.; Chyall, L. J.; Dunlap, J.T.; Smolenskaya, V.N.; Stahly, B. C.; Stahly, G. P. *J. Am. Chem. Soc.* **2004**, *126*, 13335–13342 (e) Remenar, J.F.; Morissette, S.L.; Peterson, M.L.; Moulton, B.; MacPhee, J.M.; Guzman, H.R.; Almarsson, Ö. *J. Am. Chem. Soc.*, **2003**, *125*, 8456–8457. (f) Stanton, M. K.; Bak, A. *Cryst. Growth Des.* **2008**, *8*, 3856.
- ¹² Trask, A. V.; Motherwell, W. D. S.; Jones, W. *Cryst. Growth Des.*, **2005**, *3*, 1013–1021.
- ¹³ Friščić, T.; Jones, W. J. *Pharm. Pharmacol.* **2010**, *62*, 1547–1559

- ¹⁴ (a) Buc̣ar, D., MacGillivray, L.R. *J. Am. Chem. Soc.* **2007**, *129*, 32-33 (b) Sander, J.R.G.; Buc̣ar, D.; Henry, R.F.; Zhang, G.G.Z.; MacGillivray, L.R. *Angew. Chem. Int. Ed.* **2010**, *49*, 7284–7288
- ¹⁵ Chen, A.M.; Ellison, M.E.; Peresykin, A.; Wenslow, R.M.; Variankaval, N.; Savarin, C.G.; Natishan, T.K.; Mathre, D.J.; Dormer, P.G.; Euler, D.H.; Ball, R.G.; Ye, Z.; Wang, Y.; Santos, I. *Chem. Commun.*, **2007**, 419–421
- ¹⁶ (a) Lipinski, C. A.; Lombardo, F.; Dominy, B. W.; Feeney, P. J. *Adv. Drug Del. Rev.* **2001**, *46*, 3-26. (b) Chessari, G.; Woodhead, A. J. *Drug Discov. Today* **2009**
- ¹⁷ Amidon, G. L.; Lennernas, H.; Shah, V. P.; Crison, J. R. *Pharm. Res.* **1995**, *12*, 413-420.
- ¹⁸ (a) *Neuropsychopharmacol* **1996**,*14*, 87-96. (b) Tollefson, G. D.; Beasley, C. M., Jr.; Tran, P. V.; Street, J. S.; Krueger, J. A.; Tamura, R. N.; Graffeo, K. A.; Thieme, M. E. *Am. J. Psychiatry* **1997**, *154*(4), 457-465.
- ¹⁹ Smith, R. C.; Infante, M.; Singh, A.; Khandat, A. *Int. J. Neuropsychopharmacol.* **2001**, *4*, 239–50.
- ²⁰ Chakrabarti, J.K.; Hotten, T.M. ; Tupper, D.E. US Patent No. 5,229,382, Lilly Industries Ltd, England, 1993.
- ²¹ Bunnell, C.A.; Hendriksen, B.A.; Larsen, S.D. US Patent No. 5,736,541, Eli Lilly and Co., USA, 1998

- ²² Hamied, Y.K.; Kankan, R.N.; Rao, D.R. US Patent No. 6,348,458, U and I Pharmaceuticals Ltd, USA, **2002**.
- ²³ Reddy, R.B.; Ramesh, C. Patent WO 03/091260, DR. Reddy's Laboratories Ltd., India, **2003**.
- ²⁴ Bunnell, C.A.; Larsen, S.D.; Nichols, J.R.; Reutzel, S.M.; Stephenson, G.A. Patent EP 0831098, Eli Lilly and Co., USA, **1997**.
- ²⁵ (a) Bunnell, C.A.; Hotten, T.M.; Larsen, S.D.; Tupper, D.E. Patent US 5,631,250, Eli Lilly and Co., USA, **1995**. (b) Hickey, M.B.; Remenar, J. Patent US2006/0223794, Transform Pharmaceuticals Inc., USA, **2006**
- ²⁶ Wawrzycka-Gorczyca, I.; Borowski, P.; Osypiuk-Tomasik, J.; Mazur, L.; Koziol, A.E. *J. Mol. Struct.*, **2007**, *830*, 188–197
- ²⁷ Gray, J.; Ellend, S.A. Patent WO2004/113346, Generics Ltd., UK, **2004**
- ²⁸ Reutzel-Edens, S.M.; Bush, J.K.; Magee, P.A.; Stephenson, G.A.; Byrn, S.R. *Cryst. Growth Des.*, **2003**, *3*, 897-907
- ²⁹ Thakuria, R.; Nangia, A. *CrystEngComm*, **2011**, *13*, 1759–1764
- ³⁰ http://reference.iucr.org/dictionary/Isostructural_crystals
- ³¹ (a) Ebenezer, S.; Thomas Muthiah, P.; Butcher, R.J. *Cryst. Growth Des.* **2011**, *11*, 3579–3592 (b) Cinc'ic', D.; Frišćic', T.; Jones, W. *Chem. Eur. J.* **2008**, *14*, 747 – 753 (c) Cinc'ic', D.; Frišćic', T.; Jones *New J. Chem.*, **2008**, *32*, 1776–1781 (d) Cinc'ic', D.; Frišćic', T.; Jones, W. *Chem. Mater.* 2008, *20*, 6623–6626. (e) Dabros, M.; Emery, P.R.; Thalladi, V.R. *Angew. Chem., Int. Ed.*, **2007**, *46*, 4132. (f) Smolka, T.; Boese, R.;

- Sustmann, R. *Struct. Chem.*, **1999**, *10*,429. (g) Babu, N.J.; Nangia, A. *Cryst. Growth Des.*, **2006**, *6*, 1753.
- ³² (a) Edwards, M. R.; Jones, W.; Motherwell, W. D. S. *Cryst. Eng. Comm.* **2006**, *8*, 545.
(b) Edwards, M. R.; Jones, W.; Motherwell, W. D. S.; Shields, G. P. *Mol. Cryst. Liq. Cryst.* **2001**, *356*, 337–353.
- ³³ (a) Wood, P.A.; Oliveira, M.A.; Zinkb, A.; Hickey, M.B. *Cryst. Eng. Comm*, **2012**, DOI: 10.1039/C2CE06588F (b) Ong, W.; Cheung, E.Y.; Schultz, K.A.; Smith, C.; Bourassa, J.; Hickey, M.B. *Cryst. Eng. Comm*, **2012**, 10.1039/C2CE06631A.
- ³⁴ Bruker (APEX2). Bruker AXS Inc., Madison, Wisconsin, USA, **2010**.
- ³⁵ Bruker SAINT, Data Reduction Software, Bruker AXS Inc., Madison, Wisconsin, USA, **2009**.
- ³⁶ Sheldrick, G. M. SADABS. Program for Empirical Absorption Correction, University of Gottingen, Germany, **2008**.
- ³⁷ Farrugia, L. *Journal of Applied Crystallography*, **1999**, *32*, 837-838
- ³⁸ Sheldrick, G.M. SHELXL-97. Program for the Refinement of Crystal, **1997**
- ³⁹ Sheldrick, G.M. *Acta Crystallographica*. **1990**, *A46*, 467-473
- ⁴⁰ Sheldrick, G. M. *Acta Crystallographica* **2008**, *A64*, 112-122
- ⁴¹ Petcher, T. J.; Weber, H.-P. *J. Chem. Soc., Perkin Trans. 2* **1976**, 1415-1420
- ⁴² Clarke, H. D.; Arora, K. K.; Bass, H.; Kavuru, P.; Ong, T.; Pujari, T.; Wojtas, y.; Zaworotko, M. J. *Cryst. Growth Des.* **2010**, *10*, 2152.
- ⁴³ Saha, B.K.; Nangia, A. *Heteroat. Chem.*, **2007**, *18*, 185

⁴⁴ (a) G. R. Desiraju, *Science*, **1997**, 278, 404; (b) G. R. Desiraju, *Nat. Mater.*, **2002**, 1,

77.

Summary

The increasing number of poorly soluble new drug candidates has challenged the pharmaceutical industry to develop new drug delivery technologies. Pharmaceutical cocrystals have become an inherent part of drug development as it is one means to improve the physicochemical and biopharmaceutical properties of the API. As pharmaceutical cocrystals play an active role in drug development strategies, several issues such as their design i.e. the selection of cocrystals former libraries, the challenges that arise in their design and scale up become of interest.

The research herein focuses on the design of cocrystals in the context of the selection of the cocrystals former libraries. Typically, cocrystals former libraries include pharmaceutically acceptable carboxylic acids however this can be expanded to include compounds such as nutraceuticals, zwitterions and inorganic salts. The phenolic acids, gallic acid and ferulic acid (a subclass of nutraceuticals) were used as model compounds since they possess the functional moieties carboxylic acid and phenols. These functional moieties readily engage in molecular recognition events with complementary functional groups basic nitrogen, amides and carbonyls. Therefore, based on the statistical success rate of supramolecular heterosynthons formed between these complementary functional moieties and using the concepts of self-assembly, cocrystals formers were selected. The six cocrystals formers selected yielded 6 pairs of cocrystals with the compounds gallic acid and ferulic acid respectively. Studies of the crystal packing and supramolecular

synthons of these cocrystals revealed the hierarchical nature of the $\text{COOH} \cdots \text{N}_{\text{basic}}$ supramolecular heterosynthon. This study has shown that cocrystals can be designed by first principles of crystal engineering using the concepts of supramolecular chemistry and self-assembly. It reiterates the fact that a detailed understanding of the supramolecular synthons formed between functional groups is pivotal in the design of cocrystals. However, this strategy falls short when a molecule possesses multiple functional groups and exhibits conformational flexibility.

A crystal engineering strategy was developed to address such compounds using the model compound, olanzapine. This design strategy included a comprehensive analysis of the crystal packing of existing crystal forms of olanzapine. Analysis of the crystal forms of olanzapine deposited in the Cambridge Structural Database (CSD) revealed four types of crystal packing. In addition, analysis of the hydrated crystal forms of olanzapine revealed that the water molecules are arranged such that the number of hydrogen bond donors and acceptors is complementary to a pair of olanzapine molecules. This understanding was advantageous to afford four quaternary isostructural multi-component crystal forms of olanzapine. These crystal forms consist of olanzapine, the cocrystal former, an *iso*-propyl acetate solvent molecule and a water molecule. These cocrystals are relevant as they illustrate that in general crystal structures of APIs can be deliberately designed and their physicochemical properties can be systematically customized.

The role of water molecules in crystal engineering was investigated in terms of the nemesis it presents in the design of crystal forms. Although hydrates represent 10% of the crystal structures archived in the CSD and numerous hydrates are known for a

given compound, the question is asked, “In general, can a hydrate be synthesized or designed intentionally?” In other words, is there anything predictable about hydrates, that is, their preparation, thermal stability or the supramolecular synthons they exhibit. A series of cocrystals hydrates were investigated and were categorized according to the thermal property they exhibit. In addition, a Cambridge Structural Database (CSD) analysis was conducted in order to address the supramolecular heterosynthons that water molecules exhibit with two of the most relevant functional groups in the context of active pharmaceutical ingredients, carboxylic acids, and alcohols. It was concluded that there was no correlation between the crystal structure and the thermal stability exist in any of the other categories of hydrate. The CSD analysis suggests that, unlike cocrystals, there is great diversity in the supramolecular heterosynthons exhibited by water molecules when they form hydrogen bonds with carboxylic acids or alcohols.

That hydrates can be regarded as the nemesis in crystal engineering can be reiterated by the isolation of two polymorphic forms of gallic acid monohydrate to give the first tetramorphic hydrate for which fractional coordinates have been determined. Analysis of the crystal packing in each form revealed significantly different hydrogen bonding patterns. Moreover, a CSD survey of polymorphic hydrates exhibited different supramolecular synthons with respect to the water molecule. Therefore, the promiscuity of hydrates in terms of the supramolecular synthons they exhibit or their thermal stability reveals the challenges in crystal engineering.

Future direction should focus on the advancement of the understanding of cocrystal formation. In addition to the expansion of cocrystal formers, incorporating phase solubility diagrams is relevant since it defines the thermodynamically stable region

of the cocrystal in relation to its pure components. Emphasis must be placed on the physical stability of cocrystals in order to develop scale-up procedures in the manufacture of cocrystals. Focus should be placed on the low cost scale-up of the cocrystal without changing its optimized properties and reproducibility.

Appendix 1: Copyright Approval

Appendix 1 continued

Crystal growth & design

ISSN: 1528-7483

Publication year(s): 2001 - present

Author/Editor: American Chemical Society

Publication type: Journal

Publisher: AMERICAN CHEMICAL SOCIETY

Language: English

Country of publication: United States of America

Rightsholder: AMERICAN CHEMICAL SOCIETY

Permission type selected:

Republish or display content

Type of use selected:

reuse in a Thesis/Dissertation

Article title: Structure–Stability Relationships in Cocrystal Hydrates: Does the Promiscuity of Water Make Crystalline Hydrates the Nemesis of Crystal Engineering?

Author(s): Clarke, Heather D. ; et al

DOI: 10.1021/CG901345U

Date: May 5, 2010

Volume: 10

Issue: 5

PERMISSION/LICENSE IS GRANTED FOR YOUR ORDER AT NO CHARGE

This type of permission/license, instead of the standard Terms & Conditions, is sent to you because no fee is being charged for your order. Please note the following:

- Permission is granted for your request in both print and electronic formats.
- If figures and/or tables were requested, they may be adapted or used in part.
- Please print this page for your records and send a copy of it to your publisher/graduate school.
- Appropriate credit for the requested material should be given as follows: "Reprinted (adapted) with permission from (COMPLETE REFERENCE CITATION). Copyright (YEAR) American Chemical Society." Insert appropriate information in place of the capitalized words.
- One-time permission is granted only for the use specified in your request. No additional uses are granted (such as derivative works or other editions). For any other uses, please submit a new request.

Copyright 2012 Copyright Clearance Center

Appendix 1 continued

Crystal growth & design

ISSN: 1528-7483

Publication year(s): 2001 - present

Author/Editor: American Chemical Society

Publication type: Journal

Publisher: AMERICAN CHEMICAL SOCIETY

Language: English

Country of publication: United States of America

Rightsholder: AMERICAN CHEMICAL SOCIETY

Permission type selected:

Republish or display content

Type of use selected:

reuse in a Thesis/Dissertation

Article title: Polymorphism in Multiple Component Crystals: Forms III and IV of Gallic Acid Monohydrate

Author(s): Clarke, Heather D. ; et al

DOI: 10.1021/CG2001865

Date: Apr 6, 2011

Volume: 11

Issue: 4

PERMISSION/LICENSE IS GRANTED FOR YOUR ORDER AT NO CHARGE

This type of permission/license, instead of the standard Terms & Conditions, is sent to you because no fee is being charged for your order. Please note the following:

- Permission is granted for your request in both print and electronic formats.
- If figures and/or tables were requested, they may be adapted or used in part.
- Please print this page for your records and send a copy of it to your publisher/graduate school.
- Appropriate credit for the requested material should be given as follows: "Reprinted (adapted) with permission from (COMPLETE REFERENCE CITATION). Copyright (YEAR) American Chemical Society." Insert appropriate information in place of the capitalized words.
- One-time permission is granted only for the use specified in your request. No additional uses are granted (such as derivative works or other editions). For any other uses, please submit a new request.

Copyright 2012 Copyright Clearance Center

Appendix 2: Publication 1: Structure–Stability Relationships in Cocrystal Hydrates: Does the Promiscuity of Water Make Crystalline Hydrates the Nemesis of Crystal Engineering?

Note to Reader

Reprinted with permission from *Cryst. Growth Des.*, 2010, 10 (5), pp 2152–2167.
Copyright 2010, American Chemical Society.

Structure–Stability Relationships in Cocrystal Hydrates: Does the Promiscuity of Water Make Crystalline Hydrates the Nemesis of Crystal Engineering?

Heather D. Clarke, Kapildev K. Arora, Heather Bass, Padmini Kavuru, Tien Teng Ong, Twarita Pujari, Lukasz Wojtas, and Michael J. Zaworotko*

*Department of Chemistry, University of South Florida, CHE205, 4202 East Fowler Avenue, Tampa, Florida 33620**Received October 28, 2009; Revised Manuscript Received March 4, 2010*

ABSTRACT: This contribution addresses the role of water molecules in crystal engineering by studying the crystal structures and thermal stabilities of 11 new cocrystal hydrates, all of which were characterized by single crystal X-ray crystallography, powder X-ray diffraction (PXRD), infrared spectroscopy (IR), thermogravimetric analysis (TGA), and differential scanning calorimetry (DSC). The cocrystal hydrates can be grouped into four categories based upon thermal stability: (1) water is lost at < 100 °C; (2) water is lost between 100 and 120 °C; (3) water is lost at > 120 °C; (4) dehydration occurs concurrently with the melt of the cocrystal. In order to address if there is any correlation between structure and stability, the following factors were considered: type of hydrate (tunnel hydrate or isolated hydrate); number of hydrogen bond donors and acceptors; hydrogen bond distances; packing efficiency. Category 1 hydrates exhibit water molecules in tunnels. However, no structure/stability correlations exist in any of the other categories of hydrate. To complement the cocrystal hydrates reported herein, a Cambridge Structural Database (CSD) analysis was conducted in order to address the supramolecular heterosynthons that water molecules exhibit with two of the most relevant functional groups in the context of active pharmaceutical ingredients, carboxylic acids, and alcohols. The CSD analysis suggests that, unlike cocrystals, there is great diversity in the supramolecular heterosynthons exhibited by water molecules when they form hydrogen bonds with carboxylic acids or alcohols. It can therefore be concluded that the promiscuity of water molecules in terms of their supramolecular synthons and their unpredictable thermal stability makes them a special challenge in the context of crystal engineering.

Crystal engineering,^{1,2} the understanding of intermolecular interactions in crystalline solids and their exploitation for the rational design of new crystal forms with controlled properties, continues to be a vibrant and growing topic in solid state chemistry. The relevance of crystal engineering to pharmaceutical science is particularly high since crystal forms of active pharmaceutical ingredients (APIs) are preferred by industry and regulatory bodies for use in oral dosage formulations of drugs.³ However, crystal forms of APIs have an Achilles' heel: their rate of dissolution is directly related to the thermodynamic (equilibrium) solubility of the crystal form,⁴ a physicochemical property that cannot be readily optimized for a particular clinical need. Indeed, the rate of dissolution may also be affected by particle size and diffusion phenomena, but thermodynamic solubility is a fixed property of the crystal form. Whereas controlled release technologies are available to modulate the dissolution rate of a highly soluble, highly permeable API (BCS class I, Scheme 1) or a highly soluble, poorly permeable API (BCS class III), there is little that can be done to control a poorly soluble, highly permeable API (BCS class II) or a poorly soluble, poorly permeable API (BCS class IV). Hence, the rate of dissolution of an API (BCS II and BCS IV) critically impacts the pharmacokinetic profile of orally delivered APIs, and the majority of new chemical entities in drug development (ca. 80%) suffer from poor solubility.⁵ Therefore, there is heightened interest in and awareness of the need to diversify the range of crystal forms exhibited by

APIs, which were traditionally limited to the pure API, its salts, solvates, and hydrates and polymorphs thereof. Pharmaceutical cocrystals,⁶ that is, cocrystals formed via complexation between different molecules, an API and a pharmaceutically acceptable "cocrystal former", have recently gained interest in this context as exemplified by bioavailability studies upon compounds such as fluoxetine hydrochloride (Prozac),⁷ a sodium channel blocker that was developed by Pfizer,⁸ and carbamazepine (Tegretol).⁹ Pharmaceutical cocrystals can be highly amenable to design because the very nature of APIs means that they contain exterior hydrogen bonding groups that will readily engage in supramolecular synthons¹⁰ with appropriate cocrystal formers. Furthermore, cocrystals that are highly soluble but form unstable complexes can produce a "spring-and-parachute" effect with APIs with low bioavailability that can modulate both T_{\max} and C_{\max} . In short, pharmaceutical cocrystals offer innovative approaches to controlling the bioavailability of APIs in ways that cannot be readily achieved through traditional approaches.¹¹

Hydrates represent another class of multiple-component crystal that is of relevance to both crystal engineering and pharmaceutical science. Water molecules readily incorporate into crystal lattices because of their small size and their versatile hydrogen bonding capabilities.¹² Indeed, water molecules can even stabilize crystal structures when there is an imbalance in the number of acceptors and donors¹³ by forming a diverse arrangement of supramolecular heterosynthons, and hydrates can be the preferred crystal form of an API¹⁴ if they are more stable to hydration than the corresponding anhydrate: the antiplatelet agent picotamide¹⁵ was found to be

*To whom correspondence should be addressed. E-mail: xtal@usf.edu. Fax: 813-974-3203. Tel: 813-974-3451.

Appendix 2 continued

Article

Crystal Growth & Design, Vol. 10, No. 5, 2010 2153

Scheme 1. Cocrystal Formers Used Herein, Abbreviated as Follows: CFA, FER, GAL, INM, NAM, ELA, QUE, HCT, TBR, CAF

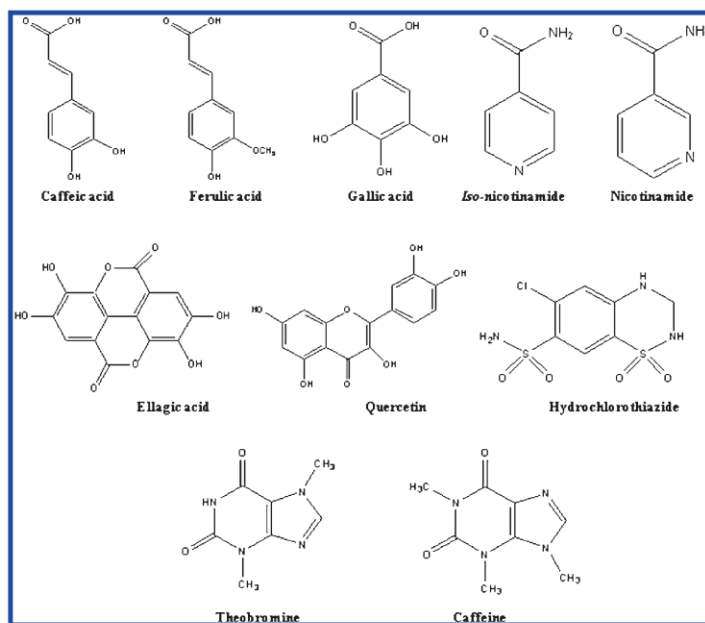


Table 1. Crystallographic Data and Structure Refinement Parameters for the 11 Cocrystal Hydrates Presented Herein

	FERINM·H ₂ O	FERNAM·H ₂ O	ELAINM·1.7H ₂ O	GALNAM·0.75H ₂ O	GALTBR·2H ₂ O	GALINM·H ₂ O
formula	C ₁₆ H ₁₈ N ₂ O ₆	C ₁₆ H ₁₈ N ₂ O ₆	C ₂₆ H _{21.4} N ₄ O _{11.7}	C ₁₃ H _{13.5} N ₂ O _{6.75}	C ₁₄ H ₁₆ N ₄ O ₉	C ₁₃ H ₁₄ N ₂ O ₇
MW	334.32	334.32	574.65	305.76	386.32	310.26
crystal system	monoclinic	monoclinic	triclinic	orthorhombic	monoclinic	monoclinic
space group	<i>P</i> 2 ₁ / <i>n</i>	<i>P</i> 2 ₁ / <i>n</i>	<i>P</i> $\bar{1}$	<i>P</i> 2 ₁ 2 ₁ 2 ₁	<i>C</i> 2/ <i>c</i>	<i>P</i> 2 ₁ / <i>n</i>
<i>a</i> (Å)	6.908 (1)	6.9389(2)	3.6207(2)	3.7606(1)	27.737(9)	17.448(1)
<i>b</i> (Å)	34.600(6)	33.460(1)	12.4908(6)	15.2613(3)	6.664(3)	3.709(4)
<i>c</i> (Å)	7.197(1)	7.3179(3)	13.5227(6)	22.7185(4)	17.345(8)	20.134(2)
α (deg)	90	90	72.641(3)	90	90	90
β (deg)	116.928(9)	116.652(2)	89.258(3)	90	92.962(9)	96.567(5)
γ (deg)	90	90	83.979(3)	90	90	90
<i>V</i> /Å ³	1533.7(4)	1518.51(9)	580.39(5)	1303.85(5)	3202(2)	1294.6(2)
<i>D</i> _c /g cm ⁻³	1.448	1.462	1.644	1.558	1.603	1.592
<i>Z</i>	4	4	1	4	8	4
2 θ range	2.55–63.61	2.64–67.35	3.42–65.36	3.49–68.09	2.35–25.03	3.18–65.52
Nref/Npara	2145/232	2680/234	1916/210	2295/218	2815/272	2174/219
<i>T</i> /K	100(2)	100(2)	100(2)	100(2)	173(2)	100(2)
<i>R</i> ₁ [<i>I</i> > 2 σ (<i>I</i>)]	0.0700	0.0336	0.0439	0.0323	0.0563	0.0376
<i>wR</i> ₂	0.1527	0.0878	0.1093	0.0815	0.1383	0.0942
GOF	0.996	1.026	1.037	1.085	1.076	1.044
abs coef	0.944	0.954	1.136	1.097	0.136	1.128

	GALCAF·0.5H ₂ O	QUETBR·2H ₂ O	ELACAF·H ₂ O	CFANAM·H ₂ O	HCTINM·H ₂ O
formula	C ₁₅ H ₁₇ N ₄ O _{7.5}	C ₂₂ H ₂₄ N ₄ O ₁₁	C ₂₂ H ₁₈ N ₄ O ₁₁	C ₁₅ H ₁₆ N ₂ O ₆	C ₁₃ H ₁₆ ClN ₅ O ₆ S ₂
MW	373.33	518.44	514.40	320.30	437.88
crystal system	monoclinic	triclinic	triclinic	triclinic	triclinic
space group	<i>C</i> 2/ <i>c</i>	<i>P</i> $\bar{1}$	<i>P</i> $\bar{1}$	<i>P</i> $\bar{1}$	<i>P</i> $\bar{1}$
<i>a</i> (Å)	19.966(4)	7.0113(3)	9.705(3)	6.2726(2)	7.3100(1)
<i>b</i> (Å)	15.800(3)	11.2981(4)	10.926(5)	7.2730(2)	9.3156(2)
<i>c</i> (Å)	13.111(3)	14.9611(6)	11.469(7)	16.4002(5)	13.5309(3)
α (deg)	90	106.545(2)	104.74(3)	98.430(2)	74.573(1)
β (deg)	130.780(3)	101.826(3)	95.68(3)	94.791(2)	87.442(1)
γ (deg)	90	94.794(3)	113.80(3)	95.896(2)	73.856(1)
<i>V</i> /Å ³	3131.8(11)	1099.15(8)	1047.9(9)	732.48(4)	852.76(3)
<i>D</i> _c /g cm ⁻³	1.584	1.566	1.630	1.452	1.705
<i>Z</i>	8	2	2	2	2
2 θ range	1.86–25.25	3.17–62.63	4.09–65.36	2.74–65.01	3.39–65.33
Nref/Npara	2825/291	3376/341	3301/349	2404/243	2805/268
<i>T</i> /K	100(2)	95(2)	100(2)	225(2)	100(2)
<i>R</i> ₁ [<i>I</i> > 2 σ (<i>I</i>)]	0.0383	0.0429	0.0549	0.0342	0.0349
<i>wR</i> ₂	0.1031	0.1163	0.1380	0.0934	0.0895
GOF	1.044	1.037	1.013	1.050	1.064
abs coef	0.129	1.097	1.150	0.964	4.702

Appendix 2 continued

2154 *Crystal Growth & Design*, Vol. 10, No. 5, 2010

Clarke et al.

Table 2. Hydrogen Bond Distances and Parameters for Cocrystal Hydrates

	hydrogen bond	$d(\text{H}\cdots\text{A})/\text{\AA}$	$D(\text{D}\cdots\text{A})/\text{\AA}$	$\angle(\text{DHA})$
FERINM·H₂O	O—H···O	1.91	2.681(5)	152.0
	O—H···O	2.29	2.733(5)	113.1
	O—H···O	1.77	2.578(5)	161.8
	O—H···O	2.26(3)	3.037(5)	149(5)
	O—H···N	1.98(3)	2.835(6)	165(6)
	N—H···O	2.10(5)	2.997(5)	167(5)
FERNAM·H₂O	N—H···O	2.19(5)	2.991(5)	147(5)
	O—H···O	1.84	2.624(2)	155
	O—H···O	2.26	2.687(1)	111
	O—H···O	1.66(2)	2.587(1)	171(2)
	N—H···O	2.10(2)	2.992(2)	168(2)
	N—H···O	2.26(2)	3.010(2)	158(2)
ELAINM·1.7H₂O	O—H···N	1.91(2)	2.777(2)	175(2)
	O—H···O	2.17(2)	2.973(2)	158(2)
	O—H···O	1.91	2.749(2)	177.1
	O—H···N	1.86	2.611(2)	147.8
	O—H···O	2.32	2.754(2)	112.8
	N—H···O	2.03(3)	2.930(3)	174(3)
GALNAM·0.75H₂O	N—H···O	2.06(3)	2.988(3)	173(3)
	N—H···O	1.98(3)	2.896(2)	169(2)
	N—H···O	2.06(3)	2.897(2)	157(2)
	O—H···O	1.82(3)	2.541(3)	145(4)
	O—H···O	2.04	2.793(2)	149.4
	O—H···O	2.29	2.732(2)	112.9
GALTBR·2H₂O	O—H···N	1.87	2.710(2)	175.5
	O—H···O	1.82	2.647(2)	169.4
	O—H···O	2.07(2)	2.877(3)	160(4)
	O—H···O	1.86(2)	2.688(4)	163(4)
	N—H···O	1.91	2.790(3)	174.9
	O—H···O	1.88	2.688(3)	161.2
	O—H···O	2.31	2.747(2)	113.0
	O—H···O	1.90	2.722(5)	166.1
	O—H···O	1.93	2.732(4)	158.1
	O—H···O	1.84	2.671(2)	170.5
	O—H···O	2.03	2.824(3)	158.6
	O—H···O	2.50(3)	2.862(3)	110(3)
	O—H···O	1.90(4)	2.807(3)	174(3)
	O—H···O	2.07(3)	2.902(5)	158(5)
GALINM·H₂O	O—H···N	2.13(2)	2.975(5)	162(3)
	O—H···O	2.01(3)	2.853(6)	156(5)
	O—H···N	2.13(2)	2.961(5)	151(3)
	N—H···O	2.17(3)	3.013(2)	162(2)
	N—H···O	2.04(3)	2.891(2)	171(2)
	O—H···N	1.81	2.645(2)	172.8
	O—H···O	1.92	2.756(2)	174.9
	O—H···O	2.13	2.832(2)	141.3
	O—H···O	2.28	2.722(2)	113.4
	O—H···O	1.97	2.803(2)	169.2
GALCAF·0.5H₂O	O—H···O	2.12(3)	2.888(2)	160(3)
	O—H···O	2.00(3)	2.853(2)	157(3)
	O—H···O	1.84(2)	2.703(2)	177(2)
	O—H···O	1.96(2)	2.750(2)	158(2)
	O—H···O	2.12(2)	2.857(1)	154(2)
	O—H···O	2.31(2)	2.712(2)	112(2)
	O—H···N	1.76(2)	2.705(2)	171(2)
	O—H···O	1.90(2)	2.752(2)	163(2)
	N—H···O	1.96	2.834(3)	172.5
	O—H···O	1.90	2.722(3)	165.2
QUETBR·2H₂O	O—H···O	1.86	2.615(2)	149.3
	O—H···O	2.26	2.709(2)	113.7
	O—H···O	1.89	2.705(2)	163.0
	O—H···O	1.92	2.753(2)	171.1
	O—H···O	1.83	2.582(2)	147.5
	O—H···N	1.89	2.822(3)	167.4
	O—H···O	1.97	2.909(3)	165.0
	O—H···O	1.92	2.860(3)	160.6
	O—H···O	2.15	3.115(3)	169.9
	O—H···N	1.93	2.702(4)	151.7
ELACAF·H₂O	O—H···O	2.30	2.742(3)	113.3
	O—H···O	1.90	2.708(3)	161.3

Table 2. Continued

	hydrogen bond	$d(\text{H}\cdots\text{A})/\text{\AA}$	$D(\text{D}\cdots\text{A})/\text{\AA}$	$\angle(\text{DHA})$
CFANAM·H₂O	O—H···O	1.78	2.608(3)	167.2
	O—H···O	1.93	2.701(3)	152.4
	O—H···O	2.27	2.706(3)	112.6
	O—H···O	2.08(2)	2.920(4)	164(4)
	O—H···O	1.99(2)	2.854(4)	162(4)
	O—H···O	1.68(3)	2.608(4)	177(2)
	O—H···O	1.75(3)	2.646(4)	161(2)
	O—H···O	2.07(2)	2.769(2)	135(2)
	O—H···O	2.19(2)	2.721(2)	118(2)
	O—H···O	1.61(2)	2.548(2)	166(2)
HCTINM·H₂O	N—H···O	2.16(2)	2.982(2)	157(2)
	N—H···O	2.04(2)	2.950(2)	171(2)
	O—H···N	1.90(1)	2.725(4)	160(2)
	O—H···O	1.89(2)	2.754(3)	166(5)
	O—H···O	2.05(3)	2.882(6)	159(5)
	N—H···O	2.48(3)	3.088(2)	130(2)
	N—H···O	2.17(3)	3.011(3)	161(2)
	N—H···O	2.12(2)	2.959(2)	164(3)
	N—H···O	2.08(2)	2.944(2)	168(3)
	N—H···O	2.45(2)	3.303(2)	168(3)
	N—H···O	2.178(2)	3.038(2)	174(3)
	O—H···N	1.94(2)	2.787(2)	163(3)
	O—H···O	2.23(2)	2.986(2)	148(3)

most stable as the monohydrate, and several drugs such as cephalixin,¹⁶ ampicillin,¹⁷ cromolyn sodium (disodium cromoglycate),¹⁸ and sildenafil citrate¹⁹ are being developed or are currently marketed as hydrates. It has been suggested that ca. 33% of organic compounds form hydrates, whereas solvates are less prevalent (10%).²⁰ However, a survey of the Cambridge Structural Database, v5.30 (CSD)²¹ reveals that only 8224 of the 159 565 molecular organic crystal structures that have had their 3D coordinates determined contain discrete water molecules. The corresponding numbers for organic, organometallic, and coordination compounds suggest that hydrates are more prevalent in general since 49 283 out of the 443 505 structures in the CSD are hydrates. Given their ubiquity, relevance, and that many hydrates occur from adventitious water, it should be unsurprising that a number of researchers have addressed the frequency,²² formation,²³ and the water environment of organic crystalline hydrates,²⁴ and crystalline hydrates have been classified according to their structure or energetics.²⁵ Morris and Rodriguez-Hornedo²⁶ proposed a classification system whereby hydrates are subdivided into three classes (1) channel hydrates in which water molecules interact with each other to form tunnels within the crystal lattice, (2) isolated site hydrates in which water molecules are not directly hydrogen bonded to each other, (3) metal ion associated hydrates in which water molecules form strong interactions with transition metals or alkali metals. Byrn et al. reported upon the macroscopic behavior of caffeine hydrate at room temperature and its dehydration, which was explained by the preferential escape of water molecules along a channel.²⁷ Other reports have discussed intermolecular interactions of water molecules in crystalline hydrates with other water molecules as well as interactions with APIs.²⁸ However, very little published research has addressed the thermal stability of hydrates in terms of why there is a variation in the temperature at which the water is lost from the crystal lattice, and cocrystal hydrates remain a largely unexplored class of compounds. In this contribution, we report 11 new cocrystal hydrates and analyze them to address

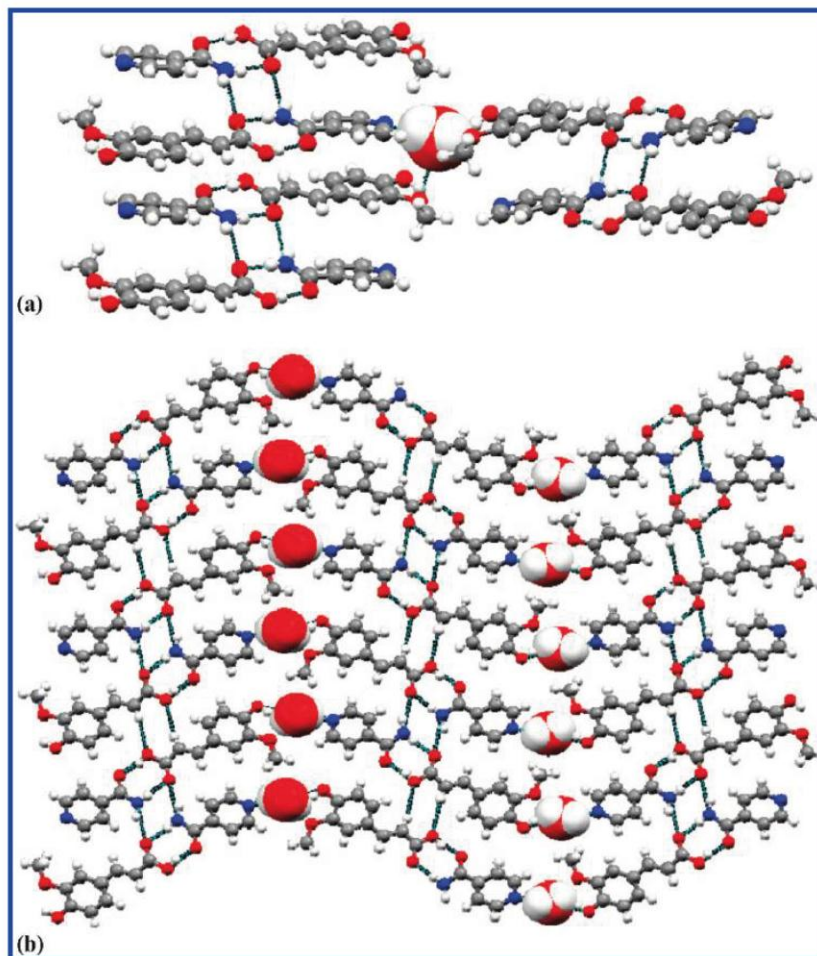


Figure 1. (a) Illustration of the water molecule in $\text{FERINM} \cdot \text{H}_2\text{O}$ that links three FER_2INM_2 tetramers. (b) Crystal packing in $\text{FERINM} \cdot \text{H}_2\text{O}$ reveals $2 + 2$ acid-amide hydrogen bonded tetramers that H-bond to water molecules so as to form H-bonded chains that pack as undulating sheets because of $\text{CH} \cdots \text{O}$ hydrogen bonds between adjacent chains.

whether or not there is any correlation between their structure and thermal stability.

Experimental Section

General. All reagents (Scheme 1) were purchased from commercial vendors and used as received. Solvents were obtained from commercial sources and distilled before use. Single crystals were obtained via slow evaporation of stoichiometric amounts of starting materials in an appropriate solvent. Cocrystals were characterized by infrared spectroscopy (IR), X-ray powder diffraction (PXRD), differential scanning calorimetry (DSC), thermogravimetric analysis (TGA), and single crystal X-ray analysis.

Ferulic Acid-Isonicotinamide Monohydrate, $\text{FERINM} \cdot \text{H}_2\text{O}$. Ferulic acid (19.9 mg, 0.1 mmol) and isonicotinamide (61.3 mg, 0.5 mmol) were dissolved in 3 mL of ethanol. The solution was left to slowly evaporate at room temperature and needles of $\text{FERINM} \cdot \text{H}_2\text{O}$ were harvested after 7 days. m.p.: 153 °C.

Ferulic Acid-Nicotinamide Monohydrate, $\text{FERNAM} \cdot \text{H}_2\text{O}$. Ferulic acid (19.9 mg, 0.1 mmol) and nicotinamide (61.3 mg, 0.5 mmol) were dissolved in 3 mL of ethanol. The solution was left to slowly evaporate at room temperature. Colorless needles of $\text{FERNAM} \cdot \text{H}_2\text{O}$ were harvested after 7 days. m.p.: 127 °C.

Ellagic Acid-Isonicotinamide Hydrate, $\text{ELAINM} \cdot 1.7\text{H}_2\text{O}$. Ellagic acid dihydrate (20.0 mg, 0.06 mmol) was dissolved in 2 mL of *N,N*-dimethylacetamide, and isonicotinamide (290 mg, 2.37 mmol) was dissolved in 1 mL of deionized water. The resulting solutions were mixed and left for slow evaporation. Yellow plates were harvested after one month. m.p.: 300 °C.

Gallic Acid-Nicotinamide Monohydrate, $\text{GALNAM} \cdot 0.75\text{H}_2\text{O}$. Gallic acid (59.5 mg, 0.348 mmol) and nicotinamide (49.9 mg, 0.405 mmol) were dissolved in 5 mL of ethanol and allowed to slowly evaporate at room temperature. Colorless needles were harvested after 3 days. m.p.: 210 °C.

Gallic Acid-Theobromine Dihydrate, $\text{GALTBR} \cdot 2\text{H}_2\text{O}$. Gallic acid (50.5 mg, 0.297 mmol) and theobromine (53.3 mg, 0.296 mmol) were dissolved in 6 mL of water/ethanol (1:1 volume ratio) by heating and allowed to slowly evaporate at room temperature. Colorless prisms were harvested after 6 days. m.p.: 270 °C.

Gallic Acid-Isonicotinamide Monohydrate, $\text{GALINM} \cdot \text{H}_2\text{O}$. Gallic acid (59.5 mg, 0.348 mmol) and isonicotinamide (49.9 mg, 0.405 mmol) were dissolved in 5 mL of ethanol until a clear solution was obtained. The solvent was allowed to slowly evaporate at room temperature. Colorless needles were harvested after 3 days. m.p.: 203 °C.

Gallic Acid-Caffeine Hemihydrate, $\text{GALCAF} \cdot 0.5\text{H}_2\text{O}$. Gallic acid (50.3 mg, 0.296 mmol) and caffeine anhydrous (57.4 mg,

Appendix 2 continued

2156 *Crystal Growth & Design*, Vol. 10, No. 5, 2010

Clarke et al.

0.296 mmol) were dissolved in 5 mL of methanol and allowed to slowly evaporate at room temperature. Colorless prisms were harvested after 14 days. m.p.: 242 °C.

Quercetin·Theobromine Dihydrate, QUETBR·2H₂O. Quercetin dihydrate (33.8 mg, 0.0999 mmol) and theobromine (18.0 mg,

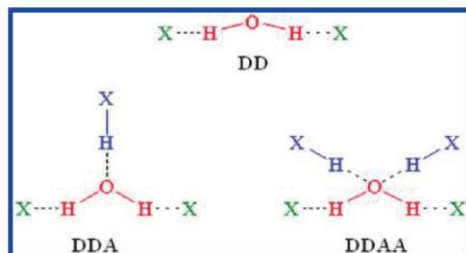
0.0999 mmol) were dissolved in 5 mL of ethanol and 10 mL of 1:1 mixture of water and ethanol respectively by heating. Resulting solutions were filtered together and placed in the refrigerator for slow evaporation. Colorless needles were harvested after 4 days. m.p.: 293 °C.

Ellagic Acid·Caffeine Monohydrate, ELACAF·H₂O. Ellagic acid dihydrate (10.0 mg, 0.0296 mmol) and caffeine (29.0 mg, 0.148 mmol) were dissolved in 5 mL of 1,2-propanediol/ethanol (6:4 volume ratio) by heating, filtered, and allowed to slowly evaporate at room temperature. Yellow plates were harvested after a week. m.p.: 299 °C.

Caffeic Acid·Nicotinamide Monohydrate, CFANAM·H₂O. Caffeic acid (9 mg, 0.04995 mmol) and nicotinamide (30 mg (0.1000 mmol) were dissolved in 3 mL of ethanol/water (1:1 volume ratio) by heating and allowed to slowly evaporate at room temperature. Colorless needles were harvested after two days. m.p.: 108 °C.

Hydrochlorothiazide·Isonicotinamide Monohydrate, HCTINM·H₂O. Hydrochlorothiazide (15 mg, 0.05 mmol) and isonicotinamide (6.1 mg (0.049 mmol) were dissolved in 4 mL of ethyl acetate by heating, filtered, and allowed to slowly evaporate at room temperature. Colorless plates were harvested after two days. m.p.: 127 °C.

Scheme 2. The Water H-Bond Environments That Have Been Observed in Cocrystal Hydrates (D: donor; A: acceptor)^a



^a Only strong H-bonds were included (i.e., no C–H···O H-bonds).

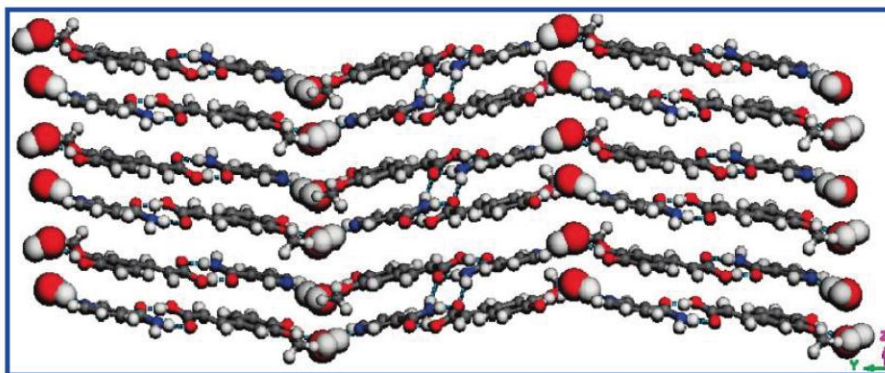


Figure 2. Crystal packing in FERNAM·H₂O exhibits 2 + 2 acid-amide tetramers that are cross-linked by H-bonded water molecules.

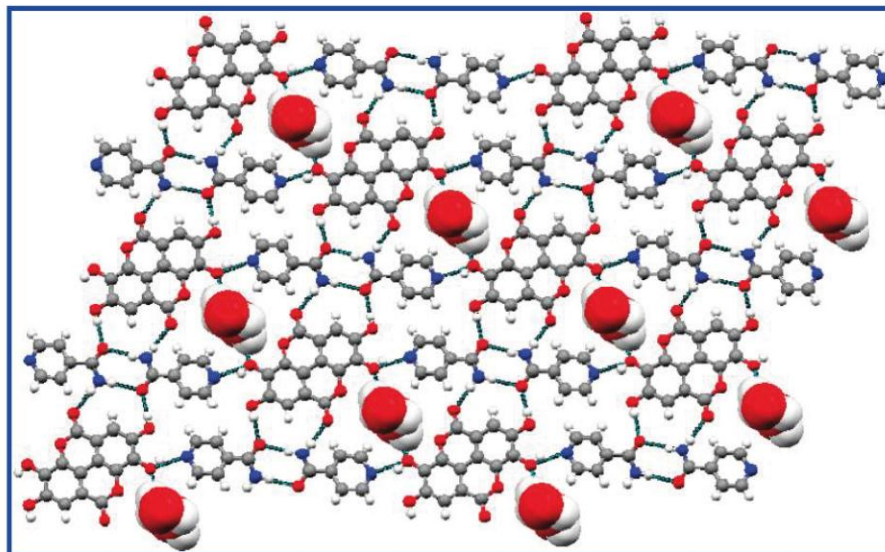


Figure 3. Crystal packing of ELAINM·1.7H₂O reveals molecular tapes of INM dimers with lateral H-bonding to phenol and carbonyl moieties of ELA. Water molecules form channels perpendicular to the aromatic rings and donate H-bonds to the phenol moieties of ELA.

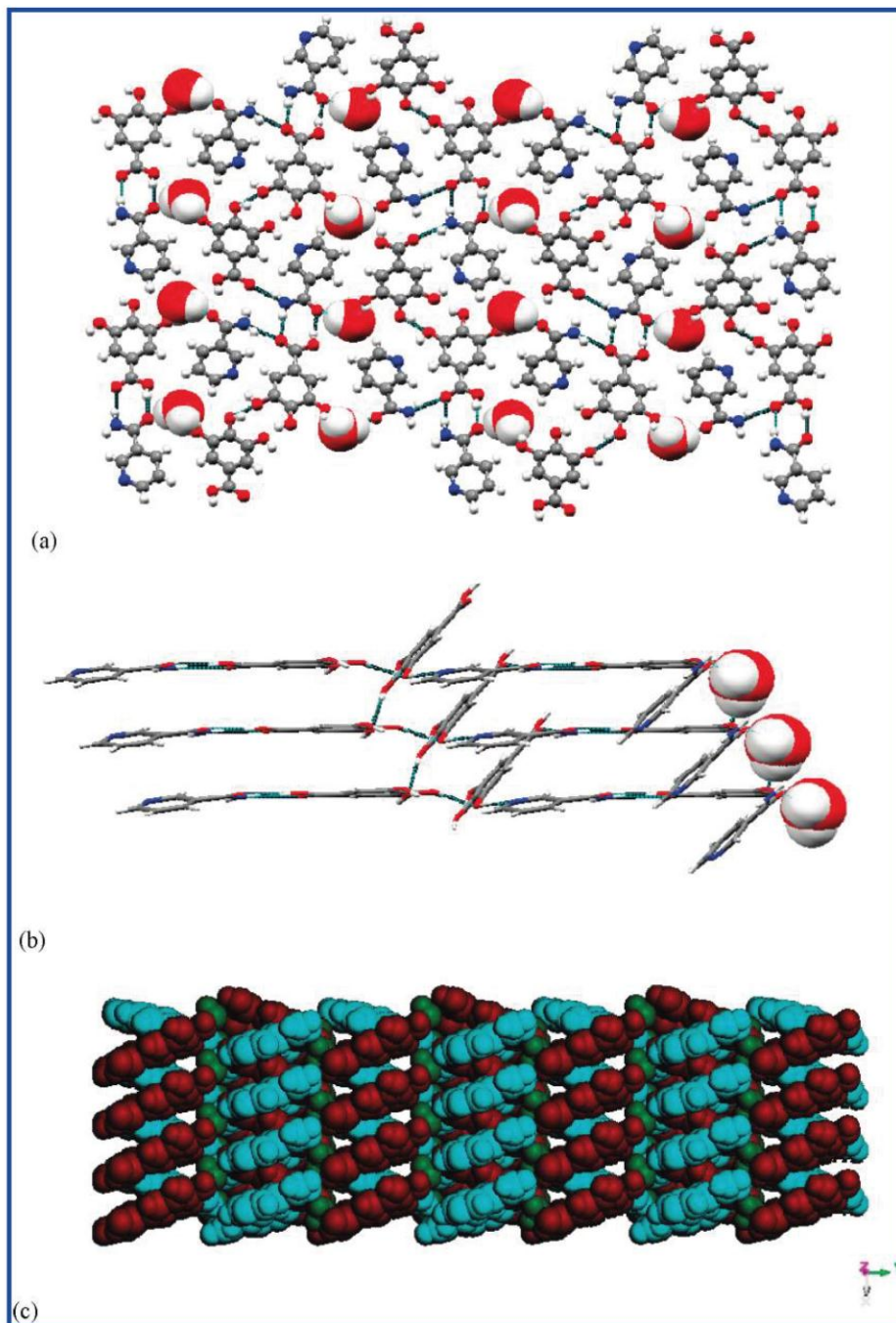


Figure 4. (a) Crystal packing in $\text{GALNAM}\cdot 0.75\text{H}_2\text{O}$ reveals molecular tapes of heterodimers of GAL and NAM with disordered water molecules cross-linking each dimer. (b) Lateral view of heterodimers. (c) Crystal packing shows heterodimers forming an interwoven 3D network.

Differential Scanning Calorimetry (DSC). Thermal analysis was carried out employing a TA Instruments DSC 2920 differential scanning calorimeter. Aluminum pans were used for all samples and temperature calibrations were made using indium as a standard. An empty pan, sealed in the same way as the sample, was used as a

reference. The thermograms were run at a scanning rate of $2\text{--}10\text{ }^\circ\text{C}/\text{min}$ from $30\text{ }^\circ\text{C}$ on $3\text{--}5\text{ mg}$ crystalline samples.

Thermogravimetric Analysis (TGA). TGA was performed with a Perkin-Elmer STA 6000 simultaneous thermal analyzer. Open alumina crucibles were used for analysis in the temperature range

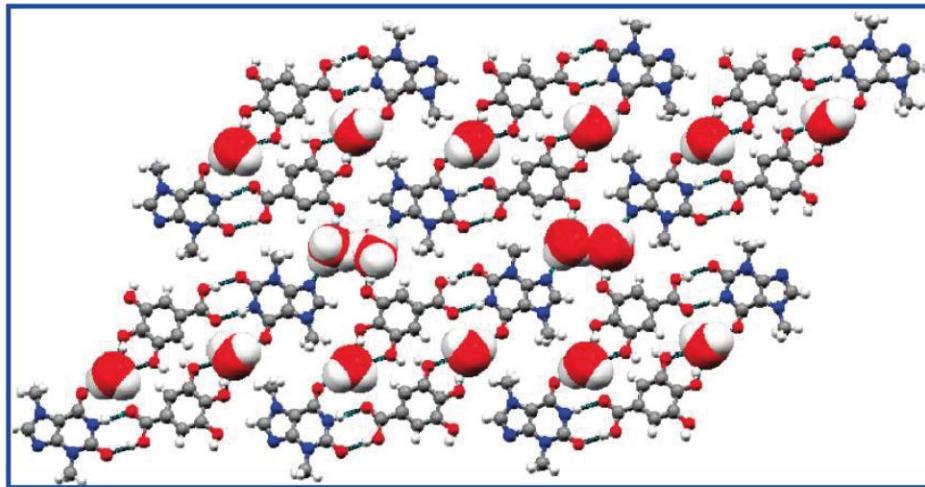


Figure 5. Crystal packing of $\text{GALTBR} \cdot 2\text{H}_2\text{O}$ reveals that GAL:TBR dimers are connected by water molecules so as to form H-bonded sheets.

30 °C to the appropriate temperature at 2–10 °C/min scanning rate under nitrogen stream.

Infrared Spectroscopy (FT-IR). All crystalline samples were characterized by infrared spectroscopy using a Nicolet Avatar 320 FT-IR instrument. 2–3 mg of material was used for all samples. Spectra were measured over the range of 4000–400 cm^{-1} and data were analyzed using EZ Omnic software.

Powder X-ray Diffraction (PXRD). Bulk samples were analyzed by X-ray powder diffraction with a Bruker AXS D8 powder diffractometer. Experimental conditions: Cu $K\alpha$ radiation ($\lambda = 1.54056 \text{ \AA}$); 40 kV; 30 mA; scanning interval 3–40° 2 θ ; time per step 0.5 s. The experimental PXRD patterns and calculated PXRD patterns from single crystal structures were compared to confirm the composition of materials.

Single-Crystal X-ray Data Collection and Structure Determinations. Crystalline products were examined under a microscope, and suitable crystals were selected for single crystal X-ray crystallography. Data were collected on single crystals of $\text{GALCAF} \cdot 0.5\text{H}_2\text{O}$ and $\text{GALTBR} \cdot 2\text{H}_2\text{O}$ on a Bruker-AXS SMART APEX CCD diffractometer with monochromatized Mo $K\alpha$ radiation ($\lambda = 0.71073 \text{ \AA}$), whereas data for single crystals of the hydrates of $\text{FERINM} \cdot \text{H}_2\text{O}$, $\text{FERNAM} \cdot \text{H}_2\text{O}$, $\text{ELAINM} \cdot 1.7\text{H}_2\text{O}$, $\text{GALNAM} \cdot 0.75\text{H}_2\text{O}$, $\text{GALINM} \cdot \text{H}_2\text{O}$, $\text{QUETBR} \cdot 2\text{H}_2\text{O}$, $\text{ELACAF} \cdot \text{H}_2\text{O}$, $\text{CFANAM} \cdot \text{H}_2\text{O}$, and $\text{HCTINM} \cdot 2\text{H}_2\text{O}$ were collected on a Bruker-AXS SMART APEX 2 CCD diffractometer with monochromatized Cu $K\alpha$ radiation ($\lambda = 1.54178 \text{ \AA}$). Both diffractometers were connected to a KRYO-FLEX low temperature device. Indexing was performed using SMART v5.625²⁹ or using APEX 2008v1-0.³⁰ Frames were integrated with SaintPlus 7.51³¹ software package. Absorption corrections were performed by a multiscan method implemented in SADABS.³² The structures were solved using SHELXS-97 and refined using SHELXL-97 contained in SHELXTL v6.10³³ and WinGX v1.70.01³⁴ program packages. All non-hydrogen atoms were refined anisotropically. Hydrogen atoms were placed in geometrically calculated positions or found in the Fourier difference map and included in the refinement process using riding model or without constraints. Occupancy factors were refined for disordered water molecules of $\text{ELAINM} \cdot 1.7\text{H}_2\text{O}$ and $\text{GALNAM} \cdot 0.75\text{H}_2\text{O}$. For $\text{ELAINM} \cdot 1.7\text{H}_2\text{O}$, it was not possible to locate all hydrogen atoms attached to disordered water molecules.

Crystallographic data are presented in Table 1. Hydrogen bond parameters are given in Table 2.

Results

$\text{FERINM} \cdot \text{H}_2\text{O}$. $\text{FERINM} \cdot \text{H}_2\text{O}$ crystallizes in the monoclinic space group $P2_1/n$, and the asymmetric unit contains

one molecule of each component. The crystal structure is sustained by a 2-point supramolecular heterosynthon between the carboxylic acid moiety of FER and the amide moiety of INM ($\text{O} \cdots \text{O}$: 2.578(5) \AA , $\text{N} \cdots \text{O}$: 2.997(6) \AA). The acid-amide supramolecular heterosynthon³⁵ further dimerizes to form an $R^2_4(8)$ tetramer sustained by $\text{N}-\text{H} \cdots \text{O}$ hydrogen bonding ($\text{N} \cdots \text{O}$: 2.991(5) \AA , Figure 1a,b). The water molecules exhibit DDA H-bonding (Scheme 2): they link tetramers by donating bifurcated hydrogen bonds to the methoxy moieties ($\text{O} \cdots \text{O}$: 3.037(5) \AA) and the pyridyl moieties ($\text{OH} \cdots \text{N}$: 2.835(6) \AA) and accepting $\text{OH} \cdots \text{O}$ hydrogen bonds from phenolic moieties ($\text{O} \cdots \text{O}$: 2.681(5) \AA , Figure 1a). $\text{CH} \cdots \text{O}$ hydrogen bonds ($\text{C} \cdots \text{O}$: 3.608 \AA) cross-link the resulting zigzag chains to form an undulating sheet. Adjacent water molecules lie in tunnels parallel to the c axis, but they are not hydrogen bonded to each other.

$\text{FERNAM} \cdot \text{H}_2\text{O}$. $\text{FERNAM} \cdot \text{H}_2\text{O}$ crystallizes in the monoclinic space group $P2_1/n$, and it exhibits a crystal packing similar to that of $\text{FERINM} \cdot \text{H}_2\text{O}$. Indeed, the versatility of the water molecule compensates for the different orientations of the pyridyl moieties in NAM and INM , and $\text{FERNAM} \cdot \text{H}_2\text{O}$ is isostructural with $\text{FERINM} \cdot \text{H}_2\text{O}$. Water molecules form tunnels along the c axis and are hydrogen bonded in the DDA environment (Figure 2).

$\text{ELAINM} \cdot 1.7\text{H}_2\text{O}$. The crystal structure reveals that $\text{ELAINM} \cdot 1.7\text{H}_2\text{O}$ contains one ELA molecule, two INM molecules, and disordered water molecules in the unit cell. $\text{ELAINM} \cdot 1.7\text{H}_2\text{O}$ exhibits hydrogen bonding between the pyridyl group of INM and the phenolic hydrogen atoms of ELA ($\text{O} \cdots \text{N}$: 2.611(2) \AA). The neutral nature of INM is supported by the C–N–C angle of 118.07° in the pyridyl moiety. Two INM molecules further interact through amide–amide supramolecular homosynths ($\text{N} \cdots \text{O}$: 2.988(3) \AA). The phenol–pyridine supramolecular heterosynthon³⁶ and the amide dimer supramolecular homosynthon³⁷ generate a tape (Figure 3). The amide dimer also acts as both a hydrogen bond donor and acceptor toward the carbonyl moiety ($\text{NH} \cdots \text{O}$: 2.930(3) \AA) and phenolic hydrogen atom of ELA ($\text{OH} \cdots \text{O}$: 2.749(2) \AA) to form an $R^3_3(10)$ trimer that links the INM – ELA chains. Disordered water molecules form channels

Appendix 2 continued

Article

Crystal Growth & Design, Vol. 10, No. 5, 2010 2159

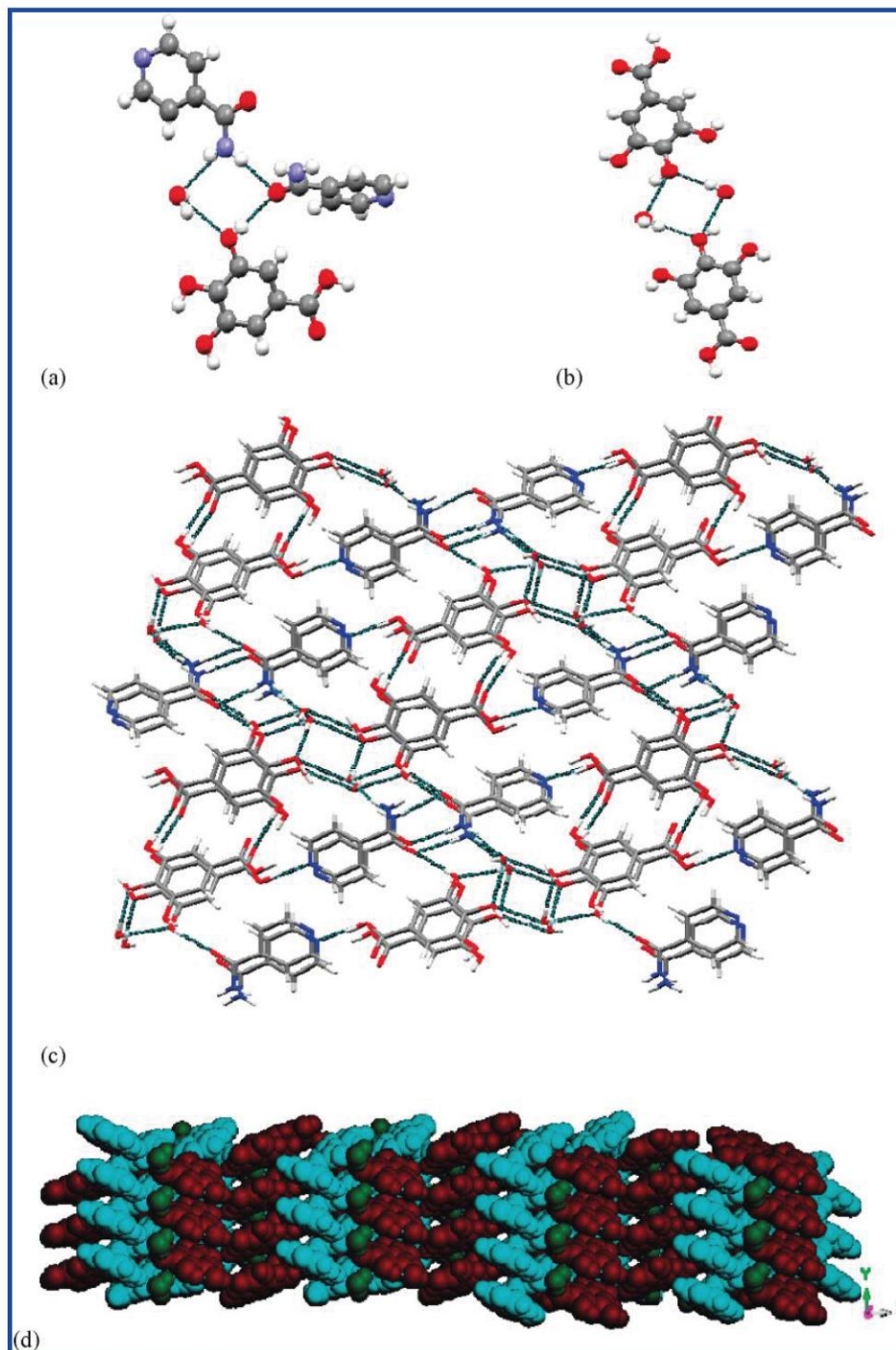


Figure 6. (a) $R^3_4(8)$ tetrameric motif involving two INM molecules, a GAL molecule, and a water molecule; (b) $R^4_4(8)$ tetrameric motif involving phenolic moieties of two GAL molecules and two water molecules. (c) The crystal packing of $\text{GALINM} \cdot \text{H}_2\text{O}$ reveals sheets sustained by $\text{COOH} \cdots \text{N}$ supramolecular heterosynths. (d) Crystal packing is that of a 3D network with water molecules (green) parallel to the b axis.

parallel to the crystallographic a axis and exist in DDA environments.

$\text{GALNAM} \cdot 0.75\text{H}_2\text{O}$. GAL and NAM crystallize with a disordered water molecule in the orthorhombic space group

Appendix 2 continued

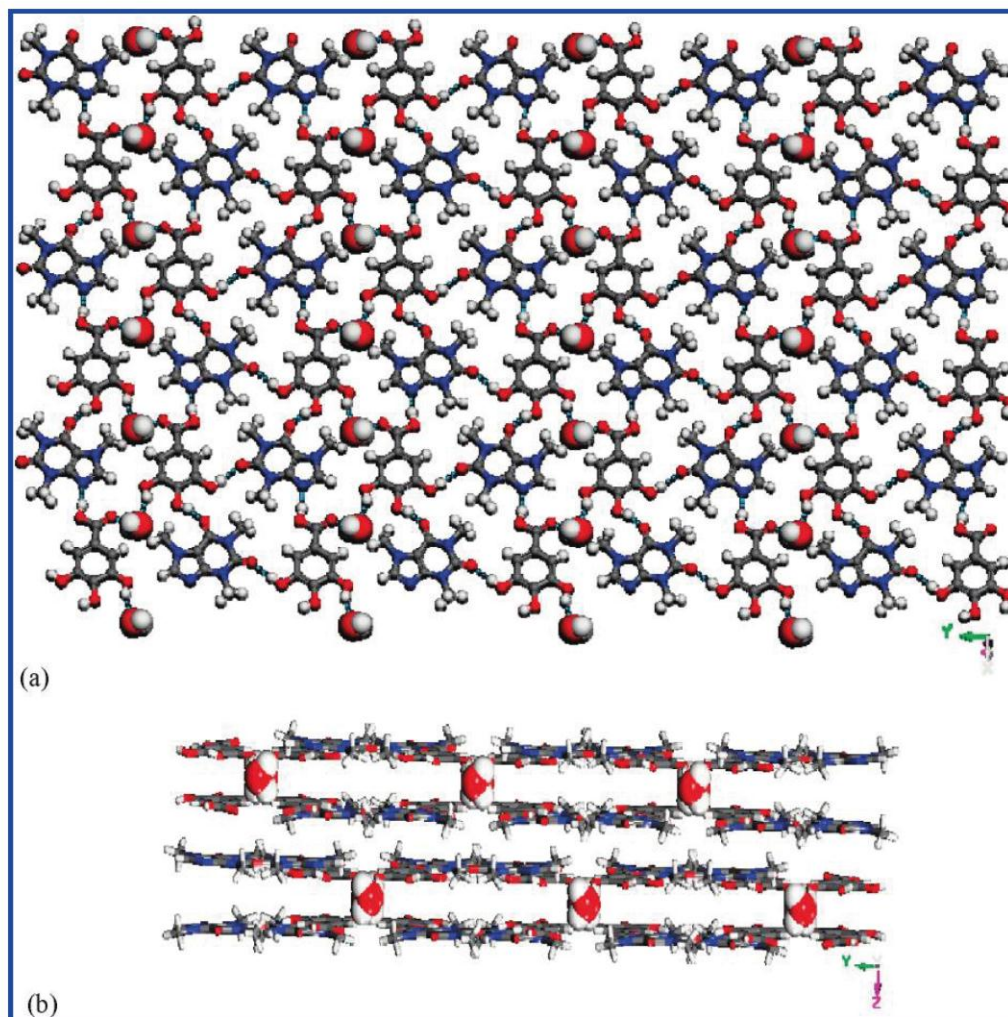


Figure 7. (a) Crystal packing of GALCAF·0.5H₂O tapes cross-linked by water molecules. (b) The water molecules sustain bilayers that pack ABAB.

*P*2₁2₁2₁. GAL and NAM form a 1:1 complex sustained by acid-amide supramolecular heterosynthons³⁵ (N···O: 2.896(2) Å, O···O: 2.647(2) Å, Figure 4a). The heterodimers link to one another via OH···N_{arom} H-bonds (2.710(2) Å) to adjacent heterodimers that are at dihedral angles of 46.3 °C. In addition, the carbonyl moiety of GAL accepts a hydrogen bond from the NH₂ moiety of an adjacent heterodimer at a dihedral angle of 46.83 °C (N···O: 2.897(2) Å). The disordered water molecule is in a DDA environment and connects three heterodimers as follows: accepting a bifurcated H-bond from the phenolic moieties of contiguous heterodimers; donating an H-bond to the carbonyl moiety of an adjacent heterodimer in an offset manner (Figure 4b); H-bonding with phenolic moieties so as to form tunnels parallel to the *a*-axis. The crystal packing is that of an interwoven 3D H-bonded network (Figure 4c).

GALTBR·2H₂O. The crystal structure of GALTBR·2H₂O reveals a 1:1 cocrystal dihydrate which crystallizes in the monoclinic space group *C*2/*c*. The crystal structure

consists of GAL and TBR molecules that form acid-imide supramolecular heterosynthons (N···O: 2.790(3) Å, O···O: 2.671(2) Å) interconnected by ordered water molecules to form 6-component assemblies that are further connected by disordered water molecules into sheets (Figure 5). The GAL:TBR dimers are also connected through water molecules to GAL:TBR dimers that lie above and below the sheets (O···O: 2.902(5) Å) and by π - π stacking so that the overall crystal packing can be described as a 3D network. The disordered water molecules exist in a DDAA environment, whereas the ordered water molecules H-bond in a DDA environment.

GALINM·H₂O. The crystal structure of GALINM·H₂O reveals a 1:1 cocrystal monohydrate that crystallizes in space group *P*2₁/*n* with one molecule of each component in the asymmetric unit. The crystal structure is sustained by the COOH···N_{arom} supramolecular heterosynthons,³⁸ but the amide-amide supramolecular homosynthon is absent. Instead, the carbonyl moiety of INM H-bonds to the amide moiety of an adjacent molecule of INM (N···O: 2.891(2) Å),

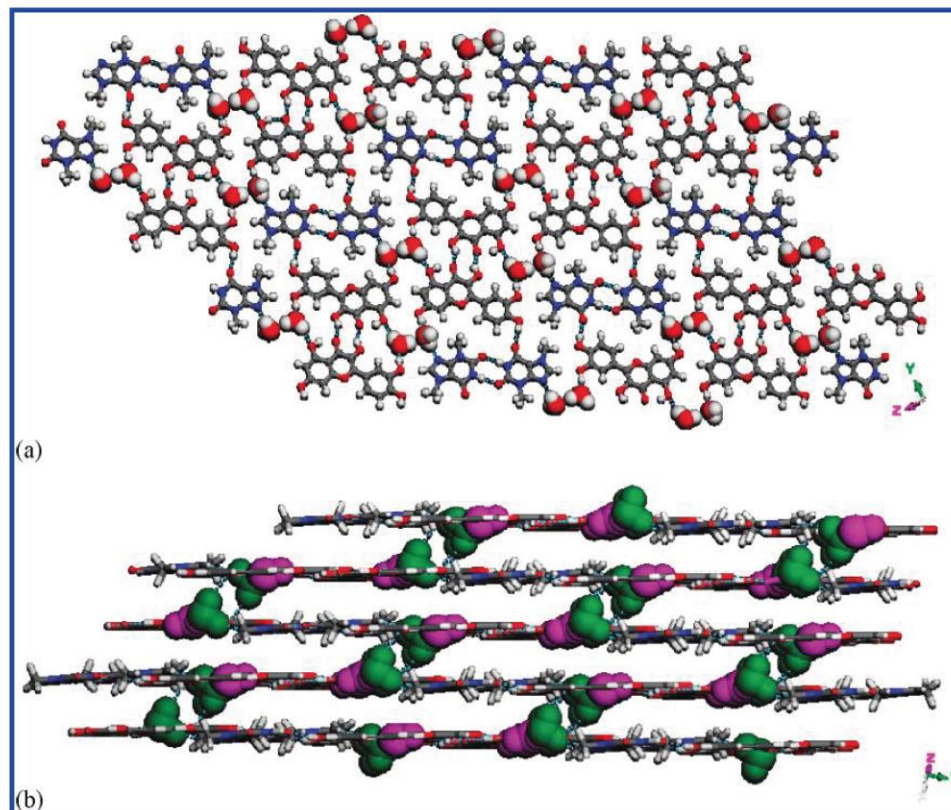


Figure 8. (a) Crystal packing in $\text{QUETBR} \cdot 2\text{H}_2\text{O}$ is sustained by dimers of **QUE** and **TBR** molecules linked by pairs of water molecules. (b) Lateral view of the sheets that are sustained by $R_6^6(12)$ motifs.

a water molecule and a **GAL** molecule to generate a tetrameric ring motif (Figure 6a). A centrosymmetric $R_4^4(8)$ tetrameric ring motif occurs between phenolic moieties of two different **GAL** molecules and two water molecules, ($\text{O} \cdots \text{O} = 2.853(2)$ and $2.833(2)$ Å, Figure 6b). Overall, the crystal packing can be described as a 3D H-bonded network with water molecules in DDAA environments that form tunnels parallel to the b axis.

GALCAF·0.5H₂O. The crystal structure of **GALCAF·0.5H₂O** reveals a 1:1:0.5 ratio of gallic acid, caffeine, and water molecules. **GAL** and **CAF** molecules form H-bonded tapes that are sustained by $\text{COOH} \cdots \text{N}^{38}$ supramolecular heterosynthons ($\text{O} \cdots \text{N}$: $2.705(2)$ Å) and $\text{OH} \cdots \text{O}$ supramolecular heterosynthons formed between adjacent phenolic moieties of **GAL** molecules and carbonyl moieties of adjacent **CAF** molecules ($\text{O} \cdots \text{O}$: $2.703(2)$, $2.750(2)$ Å). These tapes lie parallel to the a axis and are cross-linked by water molecules that H-bond with the third phenolic moiety of each **GAL** molecule ($\text{O} \cdots \text{O}$: $2.857(1)$ Å, Figure 7a). The neutral nature of the molecules is supported by the C–O bond distances, 1.320 and 1.224 Å and the C–N–C bond angle, 103.49° . The water molecules exist in DDAA environments and generate bilayers that stack in an ABAB manner sustained by π – π interactions.

QUETBR·2H₂O. The crystal structure of **QUETBR·2H₂O** reveals supramolecular homosynthons of **QUE** dimers ($\text{O} \cdots \text{O}$: $2.615(2)$ Å) and **TBR** dimers ($\text{N} \cdots \text{O}$: $2.834(3)$ Å). These dimers interact via donation of H-bonds from the phenolic moiety of **QUE** molecules to the carbonyl moiety of

TBR molecules ($\text{O} \cdots \text{O}$: $2.753(2)$ Å). The **QUE** and **TBR** homodimers alternate to form molecular tapes (Figure 8a). The two crystallographically independent water molecules (DDA and DDAA environments) cross-link the homodimers through an $R_6^6(12)$ ring motif involving four water molecules and the phenolic moieties of two **QUE** molecules (Figure 8b).

ELACAF·H₂O. Analysis of the crystal structure reveals that **ELACAF·H₂O** contains two **ELA** molecules, two **CAF** molecules, and two water molecules in the unit cell. The phenolic hydrogen atoms of **ELA** act as H-bond donors to basic nitrogen and carbonyl moieties of **CAF** molecules at $2.702(4)$ and $2.708(3)$ Å so as to form straight chains of alternating **ELA** and **CAF** molecules. Adjacent chains are linked via $\text{OH}(\text{ELA}) \cdots \text{O} = \text{C}(\text{CAF})$ H-bonds ($2.708(3)$ Å) and water molecules at ($2.609(3)$ and $2.854(4)$ Å) that H-bond to two **ELA** molecules, thereby forming a sheet (Figure 9a). Adjacent sheets are cross-linked by H-bonds between water molecules and carbonyl oxygen atoms of **ELA** ($2.920(4)$ Å). Water molecules are isolated and sit in DDAA environments (Figure 9b).

CFANAM·H₂O. The crystal structure of **CFANAM·H₂O** reveals that **CFA** and **NAM** molecules form carboxylic acid-amide supramolecular heterosynthons ($\text{O} \cdots \text{O}$: $2.548(2)$ Å; $\text{N} \cdots \text{O}$: $2.950(2)$ Å) that self-assemble to form tapes rather than 2 + 2 tetramers. These tapes are cross-linked by phenolic dimer supramolecular homosynthons ($\text{O} \cdots \text{O}$: $2.769(2)$ Å, Figure 10). Disordered water molecules

Appendix 2 continued

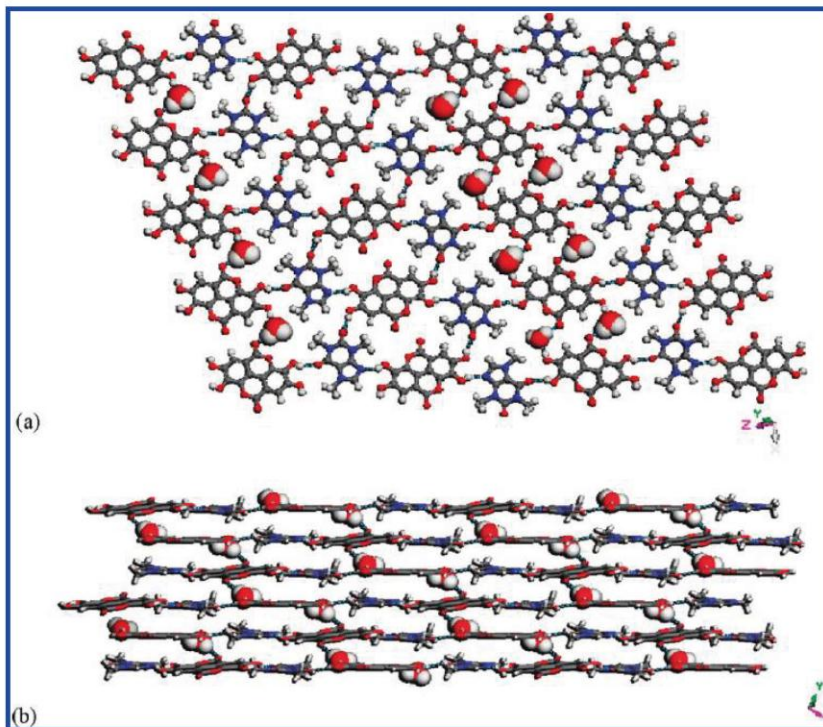


Figure 9. (a) Crystal packing in $\text{ELACAF}\cdot\text{H}_2\text{O}$ reveals H-bonding between ELA and CAF molecules via $\text{OH}\cdots\text{N}$ supramolecular heterosynthons. (b) View along the c axis illustrates isolated water molecules.

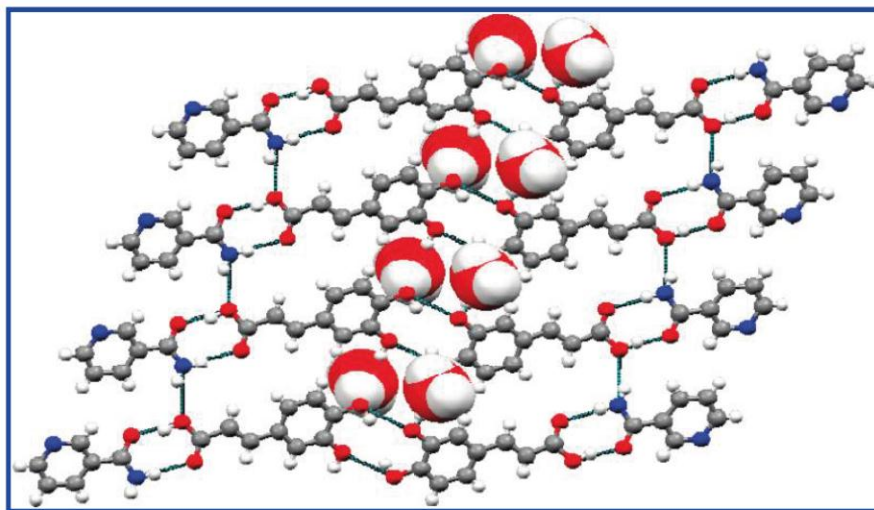


Figure 10. Molecular tapes of $\text{CFANAM}\cdot\text{H}_2\text{O}$ cross-linked by phenol–phenol interactions.

exist in DDAA environments as they H-bond with the phenolic dimers via $R_6^6(12)$ motifs and form tunnels parallel to the b axis.

HCTINM·H₂O. The crystal structure of $\text{HCTINM}\cdot\text{H}_2\text{O}$ reveals that it is a monohydrate of the 1:1 cocrystal of **HCT** and **INM**. **INM** molecules form amide–amide supramolecular homosynthons ($\text{N}\cdots\text{O}$: 3.038(2) Å) that are linked to **HCT** molecules by water molecules that donate H-bonds

to the pyridyl moieties of **INM** molecules and the sulfonamide groups of **HCT** molecules ($\text{O}\cdots\text{N}$: 2.787(2) Å, $\text{O}\cdots\text{O}$: 2.986(2) Å, Figure 11). Water molecules are in DDAA environments since they accept H-bonds from two different **HCT** molecules and they form tunnels in which they are not H-bonded to each other. The overall crystal packing consists of H-bonded sheets that pack via π - π stacking.

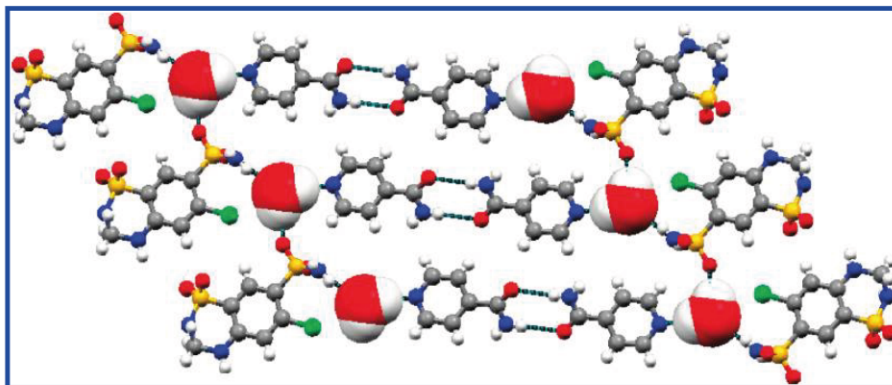


Figure 11. The crystal packing of $\text{HCTINM}\cdot\text{H}_2\text{O}$ is sustained by amide–amide supramolecular homosynths between INM molecules that are in turn H-bonded to HCT molecules via water molecules.

Discussion

Table 3 tabulates selected structural features of the 11 cocrystal hydrates reported herein and 8 cocrystal hydrates involving zwitterions that have been reported elsewhere.³⁹ The following structural features were addressed: local water environment in terms of strong H-bond donors and acceptors, whether water molecules are isolated or in tunnels, and packing efficiency index. Table 3 also provides parameters related to thermal stability: temperature at which water loss occurs, melting point, and result of dehydration. In terms of thermal stability, the cocrystal hydrates in Table 3 can be grouped as follows: (1) water is lost at $< 100\text{ }^\circ\text{C}$ for loosely held water or channel hydrates; (2) water is lost between 100 and $120\text{ }^\circ\text{C}$ for water molecules exhibiting the hydrogen bonding patterns of bulk water; (3) water is lost at $> 120\text{ }^\circ\text{C}$ for tightly bound crystalline water molecules; (4) dehydration occurs concurrently with the melt of the cocrystal. This is grouped according to the classification of hydrates proposed by Morris and Rodriguez-Hornedo²⁶ where the dehydration temperature is related to the degree of how tightly the water molecule is bound, that is, whether the water molecule is an integral part of the crystal structure or loosely held. Each group is discussed individually and then collectively.

Group 1. Inspection of group 1 reveals that all the cocrystal hydrates in this group exhibit water molecules that lie in tunnels and they are not hydrogen bonded with each other except for $\text{ELAINM}\cdot 1.7\text{H}_2\text{O}$, in which water molecules form H-bonded chains parallel to the a axis. The dehydration of Group 1 cocrystal hydrates occurs at temperatures ranging from 58 to $98\text{ }^\circ\text{C}$. Group 1 cocrystal hydrates exist in the DDA environment except for $\text{CITINA}\cdot 2\text{H}_2\text{O}$, which contains water molecules that lie in both DDA and DDAA environments. Interestingly, in $\text{CITINA}\cdot 2\text{H}_2\text{O}$ the dehydration of the water molecules occurs in two steps, at temperatures of 93 and $136\text{ }^\circ\text{C}$. These water molecules exhibit a D2 water motif,⁴⁰ which indicates that there are two water molecules connected by hydrogen bonding in a discrete chain. The packing indices calculated using Platon⁴¹ were in the range 71.7 – 74.0 . The dehydration of these cocrystal hydrates revealed new crystal forms for $\text{FERINM}\cdot\text{H}_2\text{O}$, $\text{FERNAM}\cdot\text{H}_2\text{O}$, and $\text{CITINA}\cdot 2\text{H}_2\text{O}$, whereas an isostructural anhydrate occurred following dehydration of $\text{ELAINM}\cdot 1.7\text{H}_2\text{O}$.

Group 2. The Group 2 hydrates exhibit dehydration temperatures from 109 to $118\text{ }^\circ\text{C}$. Tunnels of water molecules not H-bonded to each other are exhibited in $\text{GALNAM}\cdot 0.75\text{H}_2\text{O}$, $\text{GALINA}\cdot\text{H}_2\text{O}$, $\text{GALNAC}\cdot\text{H}_2\text{O}$, and $\text{GALTBR}\cdot 2\text{H}_2\text{O}$, whereas in $\text{PCAINA}\cdot\text{H}_2\text{O}$ and $\text{GALNAC}\cdot 1.5\text{H}_2\text{O}$ isolated water molecules are observed. The water molecules are H-bonded in DDA environments in all Group 2 cocrystal hydrates. However, in $\text{GALTBR}\cdot 2\text{H}_2\text{O}$ and $\text{GALNAC}\cdot 1.5\text{H}_2\text{O}$, DDAA environments are also exhibited by a second crystallographically independent water molecule. Packing indices range from 68.5 to 75.9 . Dehydration of Group 2 hydrates afforded crystal forms with new crystal packing according to PXRD patterns.

Group 3. With the exceptions of $\text{CITINA}\cdot 2\text{H}_2\text{O}$, $\text{QUEINA}\cdot\text{H}_2\text{O}$, and $\text{GALINM}\cdot\text{H}_2\text{O}$, crystal structures in Group 3 contain waters of crystallization that lie in isolated sites. $\text{GALINM}\cdot\text{H}_2\text{O}$, $\text{QUEINA}\cdot\text{H}_2\text{O}$, and $\text{CITINA}\cdot 2\text{H}_2\text{O}$ exhibit water loss at 124 , 175 , and $136\text{ }^\circ\text{C}$, respectively. These crystal structures displayed tunnels of water molecules not hydrogen bonded to each other. The crystal structures of Group 3 hydrates reveal DDA water environments except $\text{GALCAF}\cdot 0.5\text{H}_2\text{O}$, $\text{CITINA}\cdot 2\text{H}_2\text{O}$, and $\text{QUETBR}\cdot 2\text{H}_2\text{O}$, which display DDAA environments, and $\text{BTNRES}\cdot\text{H}_2\text{O}$, which display a DD environment. The packing indices range from 70.4 to 75.6 . PXRD of the dehydrated crystal forms reveals new crystal packing for $\text{BTNRES}\cdot\text{H}_2\text{O}$, $\text{GALINM}\cdot\text{H}_2\text{O}$, $\text{CITINA}\cdot 2\text{H}_2\text{O}$, $\text{ELACAF}\cdot\text{H}_2\text{O}$, and $\text{QUEINA}\cdot\text{H}_2\text{O}$. However, dehydration of $\text{GALCAF}\cdot 0.5\text{H}_2\text{O}$ and $\text{QUETBR}\cdot 2\text{H}_2\text{O}$ resulted in isostructural anhydrates.

Group 4. In Group 4, water loss occurs concurrently with melt of the cocrystal. The water molecules in $\text{CFANAM}\cdot\text{H}_2\text{O}$ and $\text{HCTINM}\cdot\text{H}_2\text{O}$ sit in DDAA environments, whereas in $\text{FERBAC}\cdot 0.5\text{H}_2\text{O}$ it sits in a DDA environment. Tunnels of water molecules not hydrogen bonded to each other are observed in $\text{CFANAM}\cdot\text{H}_2\text{O}$, $\text{FERBAC}\cdot 0.5\text{H}_2\text{O}$, and $\text{HCTINM}\cdot\text{H}_2\text{O}$ and packing indices range from 68.8 to 73.3 .

In summary, there appears to be little or no correlation between structure and thermal stability in the 11 new cocrystal hydrates reported herein other than for tunnel hydrates, which exhibit a tendency to lose water at or around the boiling point of water. Isolated water molecules that form at least three H-bonds were observed to exhibit greater thermal stability, and it might be anticipated that the presence of strong hydrogen bonding (short hydrogen bond

Appendix 2 continued

Table 3. Structural and Thermal Stability Properties of Selected Cocrystal Hydrates^a

Group 1: Thermal Loss of Water of Crystallization $T < 100$ °C									
cocrystal	stoichiometric ratio (T:CF:H ₂ O)	disordered water molecule	thermal loss of water	melting point of cocrystal	water environment	type of hydrate	packing index	energy of dehydration per mole of water (J/g, kJ/mol)	result after dehydration
CITINA·2H ₂ O	1:2:2	no	93	187	DDA, DDAA	tunnels D2 motif	72.7		new crystal form
FERINM·H ₂ O	1:1:1	no	58	153	DDA	tunnels of water molecules not H-bonded	74.0		new crystal form
FERNAM·H ₂ O	1:1:1	no	98	127	DDA	tunnels of water molecules not H-bonded	71.7		new crystal form
ELAINM·H ₂ O	1:1:2	yes	< 100	300	DDA	channel			new crystal form
Group 2: Thermal Loss of Water of Crystallization $100 > T > 120$ °C									
cocrystal	stoichiometric ratio (T:CF:H ₂ O)	disordered water molecule	thermal loss of water	melting point of cocrystal	water environment	type of hydrate	packing index	energy of dehydration per mole of water (J/g, kJ/mol)	result after dehydration
GALNAM·0.75H ₂ O	1:1:1	no	109	210	DDA	tunnels of water molecules not H-bonded	74.4	92.58, 37.74	new crystal form
GALINA·H ₂ O	1:1:1	no	115	234	DDA	tunnels of water molecules not H-bonded	73.3	87.25, 27.15	new crystal form
GALTBR·2H ₂ O	1:1:2	yes	115	270	DDA, DDAA	tunnels of water molecules not H-bonded		283.8, 54.81	new crystal form
PCANAC·H ₂ O	1:1:1	no	115	224	DDA	isolated	68.5	106.2, 31.35	new crystal form
GALNAC·1.5H ₂ O	2:2:3	no	118	211	DDAA, DDA	isolated, tunnels of water molecules not H-bonded D2-motif	75.9	236.2, 50.42	new crystal form
Group 3: Thermal Loss of Water of Crystallization $T > 120$ °C									
cocrystal	stoichiometric ratio (T:CF:H ₂ O)	disordered water molecule	thermal loss of water	melting point of cocrystal	water environment	type of hydrate	packing index	energy of dehydration per mole of water (J/g, kJ/mol)	result after dehydration
BTNRES·H ₂ O	2:1:1	no	~120	188	DD	isolated	70.4		new crystal form
GALINM·H ₂ O	1:1:1	yes	124	203	DDA	tunnels of water molecules not H-bonded	73.3		new crystal form
GALCAF·0.5H ₂ O	1:1:0.5	no	135	242	DDAA	isolated	74.7	69.7, 52.04	isostructural
CITINA·2H ₂ O	1:2:2	no	136	187	DDA, DDAA	tunnel D2-Motif	72.7		new crystal form
QUETBR·2H ₂ O	1:1:2	no	142	293	DDA, DDAA	isolated D2 motif	73.1	176.0, 45.62	isostructural
ELACAF·H ₂ O	2:1:1	no	175	299	DDA	isolated	75.6	124.8, 64.20	new crystal form
QUEINA·H ₂ O	1:1:1	no	196	282	DDA	tunnels of water molecules not H-bonded	74.2		new crystal form
Group 4: Thermal Loss of Water of Crystallization Occurs at Melt of the Cocrystal									
cocrystal	stoichiometric ratio (T:CF:H ₂ O)	disordered water molecule	thermal loss of water	melting point of cocrystal	water environment	type of hydrate	packing index		
CFANAM·H ₂ O	1:1:1		yes	occurs at melt	108	DDAA	tunnels of water molecules not H-bonded		71.7
FERBAC·0.5H ₂ O	1:1:0.5		no	occurs at melt	156	DDA	tunnels of water molecules not H-bonded		68.8
HCTINM·H ₂ O	1:1:1		no	occurs at melt	127	DDAA	tunnels of water molecules not H-bonded		73.3

^a Energies of dehydration are only reported for compounds with a well-resolved endotherm in the DSC thermogram.

distances) would afford the high degree of thermal stability. However, this does not seem to be the case since the same environment from a structural perspective can exhibit a dramatically different thermal stability. Indeed, even the number of hydrogen bonds between the host molecules and the water molecules is not necessarily a good predictor of thermal stability. Likewise, packing indices show no correlations with thermal stability. In addition, the enthalpy of dehydration was calculated for the eight cocrystal hydrates that exhibited a well-defined DSC endotherm associated with dehydration. The range of values is wide,

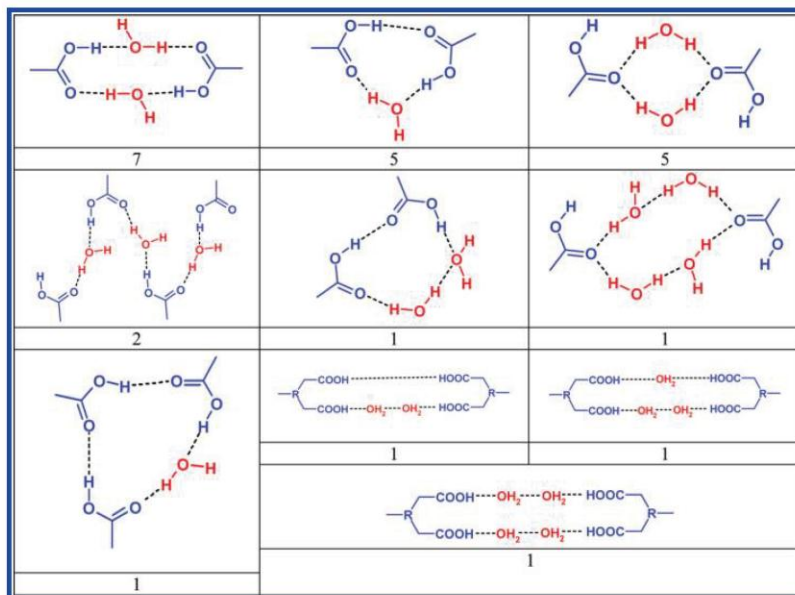
27.15–64.20 kJ/mol, and in general the enthalpy of dehydration increases with thermal stability of the hydrate. However, there is a great deal of variability from compound to compound. That we are in a sense “comparing apples with oranges”, that is, the cocrystal hydrates reported herein exhibit variable hydrate stoichiometry, multiple hydrate packing environments, and several possible outcomes of dehydration (i.e., melting, isostructural anhydrate, anhydrate is a new crystal form), makes it hard to correlate thermal stability of the cocrystal hydrate and its enthalpy of dehydration.

Appendix 2 continued

Article

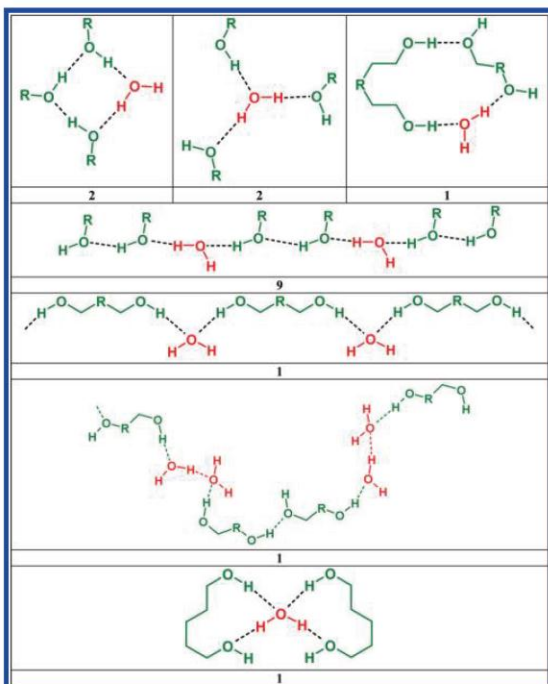
Crystal Growth & Design, Vol. 10, No. 5, 2010 2165

Chart 1. Supramolecular Heterosynthons Observed in Hydrates of Carboxylic Acids That Contain No Additional H-Bonding Groups^a



^a The number given under each scheme indicates the times of occurrence.

Chart 2. Supramolecular Heterosynthons Observed in Hydrates of Phenols That Contain No Additional H-Bonding Groups^a



^a The number given under each schematic indicates the times of occurrence in the CSD.

CSD Analysis. The persistence of supramolecular heterosynthons is a feature of cocrystals that makes them particularly

Table 4. CSD Statistics of Polymorphs of Single and Multicomponent (Cocrystals and Hydrates) Organic Structures^a

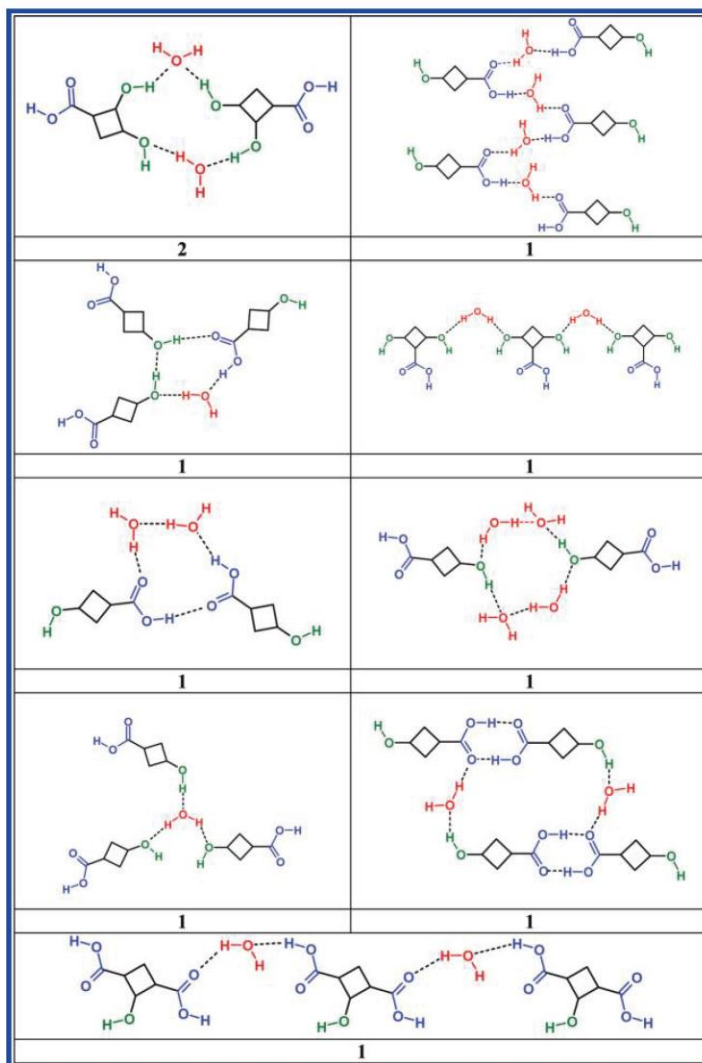
	no. of entries	% of organic structures
organic crystal structures	196575 ^b	100 ^c
single component molecular organic structures	141350	71.9 ^c
single component polymorphic structures	2319 ^c	1.6 ^f
hydrates	15938	8.1 ^e
molecular organic hydrates ^d	6351	3.2 ^e
polymorphic molecular organic hydrates ^d	65	1.0 ^h
cocrystals ^d	2415 ^d	1.2 ^e
polymorphic cocrystals ^d	48	1.9 ^g

^a CSD May 09 update, 483 021 entries. ^b Structures containing Na, Li, K, As were excluded. ^c Only one refcode was counted for each polymorphic compound. ^d Cocrystals sustained by strong hydrogen bonds. ^e Percentages with respect to organic crystal structures only. ^f Percentages with respect to 141 350 subtotals. ^g Percentages with respect to 2415 subtotals. ^h Percentages with respect to 6351 entries only. ⁱ Conquest 1.11, only organics, 3D coordinates known, $R \leq 7.5$, no ions.

amenable to crystal engineering studies. For example, carboxylic acids and phenols both form persistent supramolecular synthons with pyridines³⁷ even in the presence of competing H-bond acceptors. However, as revealed by Charts 1–3, water molecules are rather promiscuous in terms of their H-bond interactions with carboxylic acids and phenols. These charts summarize a CSD analysis of the supramolecular heterosynthons that exist when at least one water molecule is present in a crystal that contains a carboxylic acid or a phenol in the absence of competing functional groups. There are just 23 hydrates of simple carboxylic acids and remarkably 10 supramolecular heterosynthons exist between the carboxylic acid moieties and the water molecules (Chart 1). Supramolecular heterosynthons between water molecules and phenols are also diverse with 7 different supramolecular heterosynthons out of

Appendix 2 continued

Chart 3. Supramolecular Heterosynthons Observed in Hydrates of Carboxylic Acids and Phenols^a



^aThe numbers given under each schematic indicate the times of occurrence in the CSD.

just 17 crystal structures (Chart 2). There are only 10 crystal structures in which a carboxylic acid moiety, a phenol moiety and a water molecule are involved in the absence of competing H-bonding groups, and remarkably nine different supramolecular heterosynthons occur in this subset (Chart 3). These structural observations beg the question of whether or not the promiscuity in supramolecular synthons and polymorphs exhibited is general for multicomponent crystals or an artifact of the water molecules of hydration and their promiscuity. A CSD analysis (Table 4) reveals that structurally characterized polymorphs remain rare in single-component molecular crystals (2319/141350, 2.0%) and in multicomponent crystals such as hydrates (65/6351, 1.0%) and cocrystals (48/2415, 2.0%). However, there are enough compounds for which 3D coordinates are known on both polymorphic cocrystals (38 compounds) and polymorphic hydrates (44 compounds) to address polymorphism in multicomponent crystals. Analysis

of the 38 polymorphic cocrystals reveals that in 35 polymorphic pairs polymorphism is the result of conformational flexibility and/or structural changes in the overall packing; that is, the hydrogen bonded supramolecular synthons are persistent as had been previously suggested.³⁸ The remaining three cocrystals exhibit different supramolecular heterosynthons: carbamazepine and saccharin, ref codes: UNEZAO and UNEZAO01; bis(4-hydroxybenzoic acid) and 2,3,5,6-tetramethylpyrazine, ref codes: ODOBIT and ODOBIT01; urea and barbituric acid, ref codes: EFOZAB, EFOZAB 01 and EFOZAB02. However, this is not the case with polymorphic hydrates: 28 out of 44 polymorphic hydrates for which the 3D coordinates are known exhibit different supramolecular synthons with respect to the water molecules.

In conclusion, there are numerous structural features that might influence the thermal stability of organic crystalline hydrates, and the promiscuity of water molecules in

Appendix 2 continued

Article

terms of supramolecular synthons mean that their composition, structure, and thermal stability remain largely unpredictable with the exception that channel hydrates tend to exhibit low thermal stability. It would therefore be appropriate to assert that water is indeed in many ways the nemesis of crystal engineering.

Supporting Information Available: X-ray crystallographic information in CIF format, IR, DSC, TGA, PXRD are available free of charge via the Internet at <http://pubs.acs.org>.

References

- (1) (a) Pepinsky, R. *Phys. Rev.* **1955**, *100*, 971. (b) Schmidt, G. M. *J. Pure Appl. Chem.* **1971**, *27*, 647–678. (c) Desiraju, G. R. *Crystal Engineering: The Design of Organic Solids*; Elsevier: Amsterdam, 1989. (d) Etter, M. C. *J. Am. Chem. Soc.* **1982**, *104*, 1095–1096.
- (2) (a) Moulton, B.; Zaworotko, M. *J. Chem. Rev.* **2001**, *101*, 1629–1658. (b) Zaworotko, M. *J. Cryst. Growth Des.* **2007**, *7*, 4–9.
- (3) Vippagunta, S. R.; Brittain, H. G.; Grant, D. J. W. *Adv. Drug Delivery Rev.* **2001**, *48*, 3–26.
- (4) Noyes, A. A.; Whitney, R. R. *J. Am. Chem. Soc.* **1897**, *19*, 930–934.
- (5) Amidon, G. L.; Lennernas, H.; Shah, V. P.; Crison, J. R. *Pharm. Res.* **1995**, *12*, 413–420.
- (6) (a) Vishweshwar, P.; McMahon, J. A.; Bis, J. A.; Zaworotko, M. J. *J. Pharm. Sci.* **2006**, *95*, 499–516. (b) Special issue on Pharmaceutical Cocrystals. *Mol. Pharmaceutics* **2007**, *4*, 299–486. (c) Shan, N.; Zaworotko, M. *J. Drug. Discov. Today* **2008**, *13*, 440–446. (d) Meanwell, N. A. *Annu. Rep. Med. Chem.* **2008**, *43*, 373–404. (e) Schultheiss, N.; Newman, A. *Cryst. Growth Des.* **2009**, *9*, 2950–2967. (f) Stanton, M. K.; Bak, A. *Cryst. Growth Des.* **2008**, *8*, 3856–3862. (g) Stahly, G. P. *Cryst. Growth Des.* **2009**, *9*, 4212–4229. (h) Aakeröy, C. B.; Desper, J.; Fasulo, M.; Hussain, I.; Levin, B.; Schultheiss, N. *CrystEngComm* **2008**, *10*, 1816–182.
- (7) Childs, S. L.; Chyall, L. J.; Dunlap, J. T.; Smolenskaya, V. N.; Stahly, B. C.; Stahly, G. P. *J. Am. Chem. Soc.* **2004**, *126*, 13335–13342.
- (8) McNamara, D. P.; Childs, S. L.; Giordano, J.; Iarriccio, A.; Cassidy, J.; Shet, M. S.; Mannion, R.; O'Donnell, E.; Park, A. *Pharm. Res.* **2006**, *23*, 1888–1897.
- (9) Hickey, M. B.; Peterson, M. L.; Scopettuolo, L. A.; Morrisette, S. L.; Vetter, A.; Guzman, H.; Remenar, J. F.; Zhang, Z.; Tawa, M. D.; Haley, S.; Zaworotko, M. J.; Almarsson, O. *Eur. J. Pharm. Biopharm.* **2007**, *67*, 112.
- (10) Walsh, R. D. B.; Bradner, M. W.; Fleischman, S.; Morales, L. A.; Moulton, B.; Rodriguez-Hornedo, N.; Zaworotko, M. *J. Chem. Commun.* **2003**, 186.
- (11) (a) Almarsson, O.; Zaworotko, M. *J. Chem. Commun.* **2004**, 1889–1896. (b) McNamara, D. P.; Childs, S. L.; Giordano, J.; Iarriccio, A.; Cassidy, J.; Shet, M. S.; Mannion, R.; O'Donnell, E.; Park, A. *Pharm. Res.* **2006**, *23*, 1888–1897. (c) Variankaval, N.; Wenslow, R.; Murry, J.; Hartman, R.; Helmy, R.; Kwong, E.; Clas, S. D.; Dalton, C.; Santos, I. *Cryst. Growth Des.* **2006**, *6*, 690–100.
- (12) Gillon, A. L.; Feeder, N.; Davey, R. J.; Storey, R. *Cryst. Growth Des.* **2003**, *3*, 663–673.
- (13) Desiraju, R. G. *J. Chem. Soc., Chem. Commun.* **1991**, 426–428.
- (14) (a) Stahl, H. P. In *Towards Better Safety of Drugs and Pharmaceutical Products*; Braimar, D. D., Ed.; Biomedical Press: Elsevier North Holland, 1980; pp 265–280. (b) Jeffrey, G. A. *An Introduction to Hydrogen Bonding*; Oxford University Press: New York, 1997.
- (15) Bettinetti, G.; Mura, P.; Sorrenti, M.; Faucci, M. T.; Negri, A. *J. Pharm. Sci.* **1999**, *88*, 1133–1139.
- (16) Stephenson, G. A.; Groleau, E. G.; Kleeman, R. L.; Xu, W.; Rigsbee, D. R. *J. Pharm. Sci.* **1998**, *87*, 536–542.
- (17) Khankari, R. K.; Law, D.; Grant, D. J. W. *Int. J. Pharm.* **1992**, *82*, 117–127.
- (18) Chen, L. R.; Young, V. G., Jr.; Lechuga-Ballesteros, D.; Grant, D. J. W. *J. Pharm. Sci.* **1999**, *88*, 1191–1200.
- (19) (a) Apperly, D. C.; Basford, P. A.; Dallman, C. I.; Harris, R. K.; Kinns, M.; Marshall, P. V.; Swanson, A. G. *J. Pharm. Sci.* **2005**, *94*, 516–523. (b) Zegarac, M.; Mestrovic, E.; Dumbovic, A.; Devic, M.; Tudja, P. WO 2007/080362 A1.
- (20) Henck, J. O.; Griesser, U. J.; Burger, A. *Pharm. Ind.* **1997**, *59*, 165–169.
- (21) (a) Allen, F. H.; Kennard, O. *Chem. Des. Automat. News* **1993**, *8*, 31–37. (b) Allen, F. H. *Acta Crystallogr.* **2002**, *B58*, 380–388.
- (22) Infantes, L.; Fábrián, L.; Motherwell, W. D. S. *CrystEngComm* **2007**, *9*, 65–71.
- (23) (a) Khankari, R. K.; Grant, D. J. *Thermochim. Acta* **1995**, *248*, 61–79. (b) Morris, K. R. *Polymorphism in Pharmaceutical Solids*; Brittain, H. G., Ed.; Marcel Dekker, Inc.: New York, 1999; Vol. 95, pp 125–181.
- (24) (a) Infantes, L.; Chisholm, J.; Motherwell, S. *CrystEngComm* **2003**, *5*, 480–486. (b) Hickey, M. B.; Peterson, M. L.; Manas, E. S.; Alvarez, J.; Haeflner, F.; Almarsson, Ö. *J. Pharm. Sci.* **2007**, *96*, 1090–1099. (c) Kiang, Y.-H.; Xu, W.; Stephens, P. W.; Ball, R. G.; Yasuda, N. *Cryst. Growth Des.* **2009**, *9*, 1833–1843. (d) Bak, A.; Cooke, M.; Kleppe, M. *Am. Pharm. Rev.* Sep/Oct **2008**.
- (25) (a) Falk, M.; Knop, O. *Water: A Comprehensive Treatise*; Franks, F., Ed.; Plenum Press: New York, 1973; Vol. 2, pp 55–113. (b) Authelin, J. R. *Int. J. Pharm.* **2005**, *303*, 37–53.
- (26) Morris, K. R.; Rodriguez-Hornedo, N. *Encyclopedia of Pharmaceutical Technology*; Swarbrick, J.; Boylan, J., Eds; Marcel Dekker, Inc: New York, 1993; Vol. 7, pp 393–440.
- (27) Byrn, S. R.; Lin, C. T. *J. Am. Chem. Soc.* **1976**, *98*, 4004.
- (28) (a) Reutzel-Edens, S. M.; Bush, J. K.; Magee, P. A.; Stephenson, G. A.; Byrn, S. R. *Cryst. Growth Des.* **2003**, *3*, 897–907. (b) Britain, H. G.; Morris, K. G.; Boerrigter, S. X. M. *Polymorphism in Pharmaceutical Solids*; Brittain, H. G., Ed.; Informa Healthcare, Inc.: New York, 2009; Vol. 192, pp 233–279.
- (29) SMART-V5.625. *Data Collection Software*; Bruker-AXS: Madison, Wisconsin, USA, 2001.
- (30) APEX2 (Version 2008.1–0); Bruker: Madison, Wisconsin, USA, 2008.
- (31) SAINT-V7.51A, *Data Reduction Software*, Bruker-AXS: Madison, Wisconsin, USA, 2008.
- (32) Sheldrick, G. M. *SADABS. Program for Empirical Absorption Correction*; University of Göttingen: Germany, 1996.
- (33) Sheldrick, G. M. *SHELXTL, v. 6.10*; Bruker-AXS Madison: Wisconsin, USA, 2000.
- (34) (a) Farrugia, L. *J. Appl. Crystallogr.* **1999**, *32*, 837–838. (b) Sheldrick, G. M. *Acta Crystallogr.* **2008**, *A64*, 112–122. (c) Sheldrick, G. M. *Acta Crystallogr.* **1990**, *A46*, 467–473.
- (35) (a) Fleischman, S. G.; Kuduva, S. S.; McMahon, J. A.; Moulton, B.; Walsh, R. B.; Rodriguez-Hornedo, N.; Zaworotko, M. *J. Cryst. Growth Des.* **2003**, *3*, 909–919. (b) Aakeröy, C. B.; Beatty, A. M.; Helfrich, B. A. *Angew. Chem., Int. Ed.* **2001**, *40*, 3240. (c) Reddy, L. S.; Nangia, A.; Lynch, V. M. *Cryst. Growth Des.* **2004**, *4*, 89–94. (d) Aakeröy, C. B.; Desper, J.; Scott, B. M. T. *Chem. Commun.* **2006**, *13*, 1445. (e) Vishweshwar, P.; Nangia, A.; Lynch, V. M. *Cryst. Growth Des.* **2003**, *3*, 783. (f) Videnova-Adrabsinska, V.; Etter, M. C. *J. Chem. Crystallogr.* **1995**, *25*, 823–829. (g) Leiserowitz, L.; Nader, F. *Acta Crystallogr., Sect. B: Struct. Sci.* **1977**, *33*, 2719–2733.
- (36) (a) Bis, J. A.; Vishweshwar, P.; Weyna, D.; Zaworotko, M. *J. Mol. Pharmaceutics* **2007**, *4*, 401–416. (b) Vishweshwar, P.; Nangia, A.; Lynch, V. M. *CrystEngComm* **2003**, *5*, 164–168. (c) Papaefstathiou, G. S.; MacGillivray, L. R. *Org. Lett.* **2001**, *3*, 3835–3838.
- (37) (a) McMahon, J. A.; Bis, J. A.; Vishweshwar, P.; Shattock, T. R.; McLaughlin, O. L.; Zaworotko, M. *J. Z. Kristallogr.* **2005**, *220*, 340–350. (b) Jagadeesh Babu, N.; Sreenivas Reddy, L.; Nangia, A. *Mol. Pharmaceutics* **2007**, *4*, 417–434. (c) Leiserowitz, L.; Hagler, A. T. *Proc. R. Soc. London Series A* **1983**, *388*, 133–175.
- (38) (a) Shattock, T. R.; Arora, K. K.; Vishweshwar, P.; Zaworotko, M. *J. Cryst. Growth Des.* **2008**, *8*, 4533–4545. (b) Aakeröy, C. B.; Beatty, A. M.; Helfrich, B. A. *J. Am. Chem. Soc.* **2002**, *124*, 14425. (c) Vishweshwar, P.; Nangia, A.; Lynch, V. M. *J. Org. Chem.* **2002**, *67*, 556–565.
- (39) Kavuru, P.; Aborayes, D.; Arora, K. K.; Clarke, H. D.; Kennedy, A.; Marshall, L.; Ong, T. T.; Pujari, T.; Wojtas, L.; Zaworotko, M. J.; Perman, J. A.; *Cryst. Growth Des.* submitted for publication.
- (40) Infantes, L.; Motherwell, S. *CrystEngComm* **2002**, *4* (75), 454–461.
- (41) Spek, A. L. *PLATON, Molecular Geometry Program*; University of Utrecht: The Netherlands, May, 1997.

Appendix 3: Publication 2: Polymorphism in Multiple Component Crystals: Forms III and IV of Gallic Acid Monohydrate

Note to Reader

Reprinted with permission from *Cryst. Growth Des.*, 2011, 11 (4), pp 964–966
Copyright 2011, American Chemical Society.

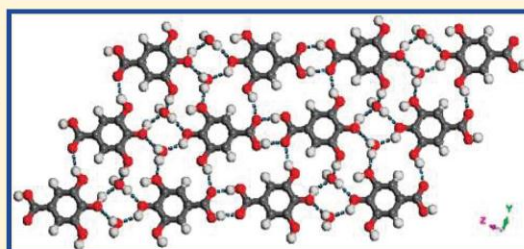
Polymorphism in Multiple Component Crystals: Forms III and IV of Gallic Acid Monohydrate

Heather D. Clarke, Kapildev K. Arora, Łukasz Wojtas, and Michael J. Zaworotko*

Department of Chemistry, University of South Florida, CHE205, 4202 East Fowler Avenue, Tampa, Florida 33613, United States

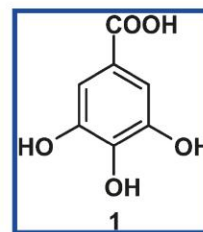
Supporting Information

ABSTRACT: Gallic acid monohydrate is the first tetramorphic hydrate for which fractional coordinates have been determined, and analysis of the hydrogen bonding patterns in these and other polymorphic hydrates suggests that waters of hydration are a nemesis to crystal engineers.



Crystal engineering^{1,2} is predicated upon the assumption that crystalline solids are *de facto* manifestations of self-assembly. It has evolved in such a manner that a wide range of new compounds can be generated without the need to invoke covalent bond breakage or formation. Rather, the resulting crystal forms are regarded as “supermolecules”³ that are stabilized by a series of weak, directional, and, in certain cases, predictable supramolecular synthons.⁴ The persistence of supramolecular synthons between different but complementary functional groups, i.e. supramolecular heterosynthons, is exemplified by carboxylic acids, which form supramolecular heterosynthons with primary amides⁵ and aromatic heterocycles,⁶ and the persistence of the supramolecular heterosynthon between carboxylate and weakly acidic hydroxyl moieties such as phenols.⁷ Supramolecular heterosynthons are key to understanding and designing cocrystals, a long known⁸ but little studied class of compounds. Pharmaceutical cocrystals⁹ composed of an active pharmaceutical ingredient, API, and a pharmaceutically acceptable cocrystal former are of topical and growing interest, as they diversify the number of crystalline forms available for a given API and can profoundly affect clinically relevant physicochemical properties such as stability¹⁰ and solubility.¹¹ Whereas cocrystals exemplify how the solid state chemist can design and prepare multicomponent crystals with a reasonable degree of control over structure and stoichiometry, hydrates represent a class of multiple component crystal that lies at the other extreme. Hydrates, crystalline compounds in which solute and water molecules coexist, represent ca. 10% of the crystal structures that have been deposited in the Cambridge Structural Database, CSD.¹² Desiraju et al. have reported the use of the water molecule as a design element in crystal engineering.¹³ Indeed, the water molecule can be used as a structural glue to fill a void in the case of an imbalance of the number of hydrogen bond donors and

acceptors. However, it would be fair to assert that little if anything is predictable about hydrates,¹⁴ from their preparation (water of hydration is often adventitious), to their stoichiometry (multiple hydrates of different stoichiometry can occur), to their stability (water of hydration might be removed below the boiling point of water or well above the boiling point of water), to the consequences of dehydration (anhydrides might be isostructural with the hydrate from which they are prepared, i.e. pseudopolymorphs,¹⁵ or exhibit very different crystal packing). In this contribution we address this matter by systematically studying polymorphism¹⁶ in a hydrate that could represent a microcosm of the special challenges and opportunities represented by hydrates: gallic acid monohydrate.



Gallic acid, **1**, is a dietary polyphenol found in *Choerospondiatis fructus*, a Mongolian medicinal herb used to treat disorders such as angina pectoris.¹⁷ It contains two of the most ubiquitous functional groups present in APIs: carboxylic acids and phenols. It is also one of only 61 hydrates of molecular organics in the

Received: February 8, 2011

Published: March 16, 2011

Appendix 3 continued

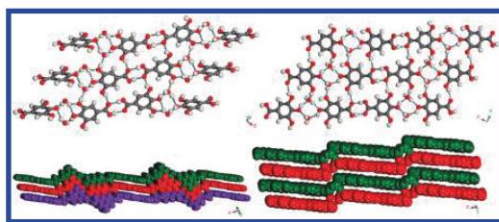


Figure 1. Crystal packing of forms I (left) and III (right) of $1 \cdot \text{H}_2\text{O}$ reveal layered structures formed from carboxylic acid dimers and phenol \cdots water interactions.

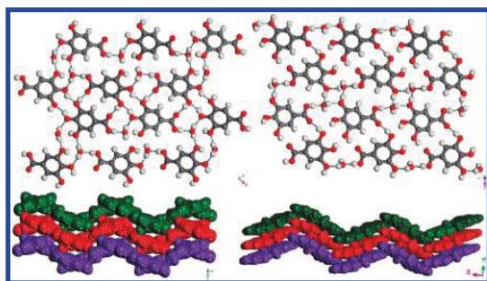


Figure 2. Crystal packing in forms II (left) and IV (right) of $1 \cdot \text{H}_2\text{O}$ reveals corrugated sheet structures in which water molecules link acid and phenol moieties.

CSD that exhibit polymorphism via forms I¹⁸ and II¹⁹ of its monohydrate, $1 \cdot \text{H}_2\text{O}$. We report herein two new polymorphs of the monohydrate of gallic acid, forms III and IV, which makes $1 \cdot \text{H}_2\text{O}$ the first hydrate that exhibits more than two polymorphs for which 3D coordinates are defined. We also report the crystal structure of the anhydrate of gallic acid and address general issues about hydrates by coupling our structural study of $1 \cdot \text{H}_2\text{O}$ with CSD analysis of polymorphism in molecular hydrates.

Forms I and II of $1 \cdot \text{H}_2\text{O}$ crystallize in monoclinic space groups $P2_1/c$ and $P2_1/n$, respectively. Form III is a high Z' triclinic form obtained via attempted cocrystallization of **1** and sarcosine in aqueous methanol.²⁰ Monoclinic form IV was harvested by crystallizing **1** from water. In addition to single crystal X-ray crystallography, all crystal forms were characterized by PXRD, IR, DSC, and TGA.

Forms I and III (Figure 1) of $1 \cdot \text{H}_2\text{O}$ are related in that molecules of **1** form carboxylic acid dimers that are linked into sheets through $\text{O}-\text{H}_{(\text{ph})} \cdots \text{O}_{(\text{water})}$ hydrogen bonding. In form II, **1** and water molecules form linear tapes via acid \cdots water \cdots phenol hydrogen bonds. These tapes are in turn connected via $\text{OH}_{(\text{ph})} \cdots \text{OH}_{(\text{ph})}$ supramolecular homosynthons and $\text{O}-\text{H}_{(\text{ph})} \cdots \text{O}=\text{COH}_{(\text{acid})}$ supramolecular heterosynthons to afford corrugated sheets. Forms II and IV are related in terms of their supramolecular synthons (Figure 2) but different from forms I and III. In form IV, molecules of **1** and water form linear tapes; however, these tapes are connected through $\text{OHC}=\text{O}_{(\text{acid})} \cdots \text{O}-\text{H}_{(\text{ph})}$ supramolecular heterosynthons. These double tapes form a herringbone pattern by interacting with adjacent double tapes via $\text{O}-\text{H}_{(\text{ph})} \cdots \text{O}_{(\text{water})}$ hydrogen bonds. Form II displays similar crystal packing to Form IV in that it forms linear tapes between **1** and water molecules. However, its supramolecular heterosynthons differ in that form II exhibits phenolic 2-point

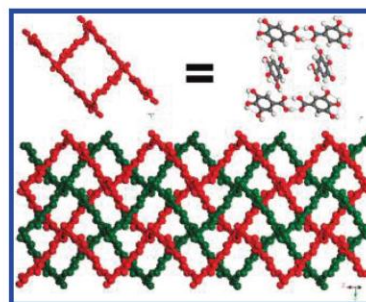


Figure 3. Doubly interpenetrated nets exhibited by **1**.

supramolecular homosynthons and $R^4_4(10)$ motifs consisting of a carboxylic acid moiety, two phenolic moieties, and a water molecule. In form IV, these supramolecular synthons are absent and are replaced by a $R^4_4(8)$ tetrameric motif involving two molecules of **1** and two water molecules. In summary, the four structurally characterized polymorphs of $1 \cdot \text{H}_2\text{O}$ can be categorized as packing polymorphs in which forms I/III exhibit the same supramolecular synthons but different crystal packing and forms II/IV exhibit different supramolecular synthons. This makes $1 \cdot \text{H}_2\text{O}$ quite different from ROY, the most promiscuous single component polymorphic compound, which exhibits eight conformational polymorphs.²¹ To our knowledge, $1 \cdot \text{H}_2\text{O}$ is the first tetramorphic hydrate for which 3D coordinates have been determined. The API olanzapine has three polymorphs of its dihydrate for which coordinates have been reported (forms B, D, and E).²²

A recent paper published by our group addressed structure and stability issues in hydrates of cocrystals and asserted that the promiscuity of hydrates in terms of the supramolecular synthons they exhibit makes them a nemesis of crystal engineering.²³ A CSD survey reveals that there are 61 polymorphic hydrates: 10 of carboxylic acids and 7 of phenols. 7/10 and 6/7 polymorphic pairs, respectively, exhibit different supramolecular synthons with respect to the water molecule. These observations coupled with our study on cocrystal hydrates suggest that hydrates are indeed promiscuous and unpredictable in terms of their supramolecular synthons.

The stability of hydrates to dehydration and the nature of the resulting anhydrate are of practical relevance to the pharmaceutical industry given that APIs are prone to form hydrates and that hydrates are sometimes the preferred crystal form for drug delivery.^{14c} Form I has only been obtained from extracts of the plant *Geum japonicum* and was not studied. The thermal stability of forms II–IV of $1 \cdot \text{H}_2\text{O}$ was studied by PXRD, DSC, and TGA. PXRD reveals that heating forms II–IV affords an anhydrate, **1**, that melts at 266–269 °C. **1** is the commercially available form of **1**, yet its crystal structure is not archived in the CSD. Colorless crystals of **1** were obtained from a saturated solution of **1** in EtOH. The single crystal structure of **1** reveals centrosymmetric carboxylic acid dimers that hydrogen bond to form an open 3D net that is doubly interpenetrated (Figure 3). DSC and TGA data reveal that II–IV convert cleanly to the anhydrate but that their thermal stabilities with respect to water loss are different (119.7, 99.4, and 114 °C for II–IV, respectively).

In summary, water is a frequent participant in multiple component crystalline solids. However, unlike cocrystal formers, which can induce predictable structural and physicochemical

properties, waters of hydration tend to be highly promiscuous in terms of the supramolecular synthons they exhibit and unpredictable in terms of thermal stability. This has the sometimes desirable consequence of opening up new routes to anhydrate crystal forms that cannot be obtained directly from solution but indicates that water is indeed a nemesis from the perspective of crystal design and crystal structure prediction. In the context of the latter, forms III and IV of $1 \cdot H_2O$ were incorporated into the most recent crystal structure prediction competition organized by the CCDC.²⁴

■ ASSOCIATED CONTENT

Supporting Information. X-ray crystallographic information in CIF format, IR, DSC, TGA, and PXRD spectra, hydrogen bond table, and CSD refcode listings. This material is available free of charge via the Internet at <http://pubs.acs.org>.

■ AUTHOR INFORMATION

Corresponding Author

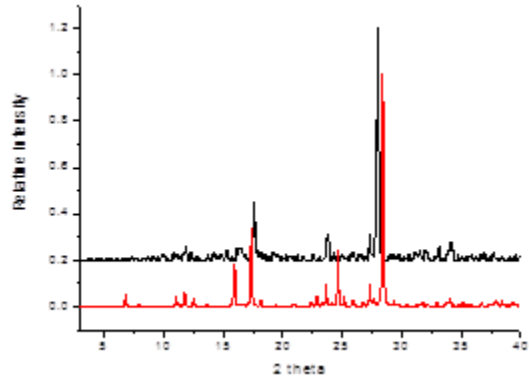
*E-mail address: xtal@usf.edu.

■ REFERENCES

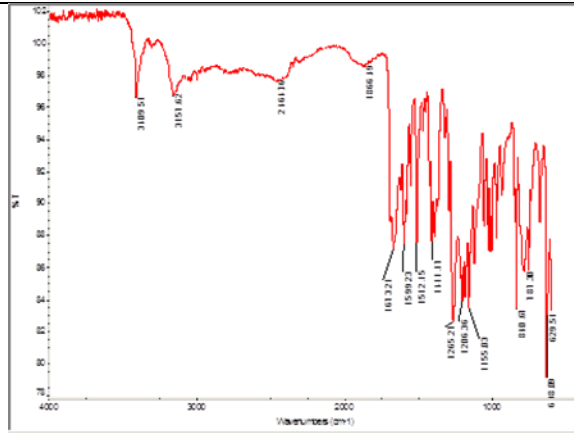
- (1) (a) Pepinsky, R. *Phys. Rev.* **1955**, *100*, 971. (b) Schmidt, G. M. J. *Pure Appl. Chem.* **1971**, *27*, 647–678. (c) Desiraju, G. R. *Crystal Engineering: The Design of Organic Solids*; Elsevier: Amsterdam, 1989. (d) Etter, M. C. *J. Am. Chem. Soc.* **1982**, *104*, 1095–1096.
- (2) (a) Moulton, B.; Zaworotko, M. J. *Chem. Rev.* **2001**, *101*, 1629–1658. (b) Zaworotko, M. J. *Cryst. Growth Des.* **2007**, *7*, 4–9.
- (3) Dunitz, J. D. *Perspect. Supramol. Chem.* **1996**, *2*, 1.
- (4) Desiraju, G. R. *Angew. Chem., Int. Ed.* **1995**, *34*, 2311–2327.
- (5) (a) Fleischman, S. G.; Kuduva, S. S.; McMahon, J. A.; Moulton, B.; Walsh, R. B.; Rodriguez-Hornedo, N.; Zaworotko, M. J. *Cryst. Growth Des.* **2003**, *3*, 909–919. (b) Vishweshwar, P.; McMahon, J. A.; Peterson, M. L.; Hickey, M. B.; Shattock, T. R.; Zaworotko, M. J. *Chem. Commun.* **2005**, 4601–4603. (c) Aakeroy, C. B.; Beatty, A. M.; Helfrich, B. A.; Nieuwenhuyzen, M. *Cryst. Growth Des.* **2003**, *3*, 159. (d) Reddy, L. S.; Nangia, A.; Lynch, V. M. *Cryst. Growth Des.* **2004**, *4*, 89–94.
- (6) (a) Vishweshwar, P.; Nangia, A.; Lynch, V. M. *J. Org. Chem.* **2002**, *67*, 556–565. (b) Shattock, T. R.; Arora, K. K.; Vishweshwar, P.; Zaworotko, M. J. *Cryst. Growth Des.* **2008**, *8*, 4533–4545.
- (7) Kavuru, P.; Aboarayas, D.; Arora, K. K.; Clarke, H. D.; Kennedy, A.; Marshall, L.; Ong, T.; Perman, J.; Pujari, T.; Wojtas, L.; Zaworotko, M. J. *Cryst. Growth Des.* **2010**, *10*, 3568–3584.
- (8) Wöhler, F. *Justus Liebigs Ann. Chem.* **1844**, *51*, 153.
- (9) (a) Vishweshwar, P.; McMahon, J. A.; Bis, J. A.; Zaworotko, M. J. *J. Pharm. Sci.* **2006**, *95*, 499–516. (b) Special issue on Pharmaceutical cocrystals *Mol. Pharmaceutics* **2007**, *4*, 299–486. (c) Shan, N.; Zaworotko, M. J. *Drug. Discovery Today* **2008**, *13*, 440–446. (d) Meanwell, N. A. *Annu. Rev. Med. Chem.* **2008**, *43*, 373–404.
- (10) Trask, A. V.; Motherwell, W. D. S.; Jones, W. *Cryst. Growth Des.* **2005**, *5*, 1013–1021.
- (11) (a) Good, D. J.; Rodriguez-Hornedo, N. *Cryst. Growth Des.* **2010**, *10*, 1028–1032. (b) Blagden, N.; de Matas, M.; Gavan, P. T.; York, P. *Adv. Drug. Delivery Rev.* **2007**, *59*, 617–630. (c) Childs, S. L.; Chyall, L. J.; Dunlap, J. T.; Smolenskaya, V. N.; Stahly, B. C.; Stahly, G. P. *J. Am. Chem. Soc.* **2004**, *126*, 13335–13342. (d) Remenar, J. F.; Morissette, S. L.; Peterson, M. L.; Moulton, B.; MacPhee, J. M.; Guzmán, H. R.; Almarsson, Ö. *J. Am. Chem. Soc.* **2003**, *125*, 8456–8457.
- (12) Allen, F. H. *Acta Crystallogr.* **2002**, *B58*, 380–388.
- (13) Varughese, S.; Desiraju, G. R. *Cryst. Growth Des.* **2010**, *10*, 4184–4196.
- (14) (a) Khankari, R. K.; Grant, D. J. *Thermochim. Acta* **1995**, *248*, 61–79. (b) Morris, K. In *Structural aspects of hydrates and solvates*; Brittain, H. G., Ed.; Polymorphism in Pharmaceutical Solids, Vol. I; Marcel Dekker: 1999; pp 125–226. (c) Hickey, M. B.; Peterson, M. L.; Manas, E. S.; Alvarez, J.; Haeflner, F.; Almarsson, Ö. *J. Pharm. Sci.* **2007**, *96*, 1090–1099. (d) Authelin, J.-R. *Int. J. Pharm.* **2005**, *303*, 37–53.
- (15) Halebian, J.; McCrone, W. C. *J. Pharm. Sci.* **1969**, *58*, 911–929.
- (16) (a) Bernstein, J. *Polymorphism in Molecular Crystals*; Clarendon Press: Oxford, 2002. (b) Hilfiker, R. *Polymorphism: in the Pharmaceutical Industry*; Wiley VCH: New York, 2006. (c) Nangia, A. *Acc. Chem. Res.* **2008**, *41*, 595–604.
- (17) Zhao, X.; Zhang, W.; Kong, S. J. *Liq. Chromatogr. Relat. Technol.* **2007**, *30*, 235–244.
- (18) Jiang, R.; Ming, D.; But, P. P. H.; Mak, T. C. W. *Acta Crystallogr., Sect. C* **2000**, *56*, 594–595.
- (19) Okabe, N.; Kyoyama, H. *Acta Crystallogr., Sect. E* **2002**, *58*, 565–567.
- (20) Rafilovich, M.; Bernstein, J. *J. Am. Chem. Soc.* **2006**, *128*, 12185–12191.
- (21) Yu, L. *Acc. Chem. Res.* **2010**, *43*, 1257–1266.
- (22) Reutzel-Edens, S. M.; Bush, J. K.; Magee, P. A.; Stephenson, G. A.; Byrn, S. R. *Cryst. Growth Des.* **2003**, *3*, 897–907.
- (23) Clarke, H. D.; Arora, K. K.; Bass, H.; Kavuru, P.; Ong, T.; Pujari, T.; Wojtas, L.; Zaworotko, M. J. *Cryst. Growth Des.* **2010**, *10*, 2152–2167.
- (24) www.ccdc.cam.ac.uk/aboutccdc/scienceprofile/structureprediction/

Appendix 4: Supplementary Information: A Crystal Engineering Study of Gallic Acid and Ferulic Acid as Cocrystal Formers

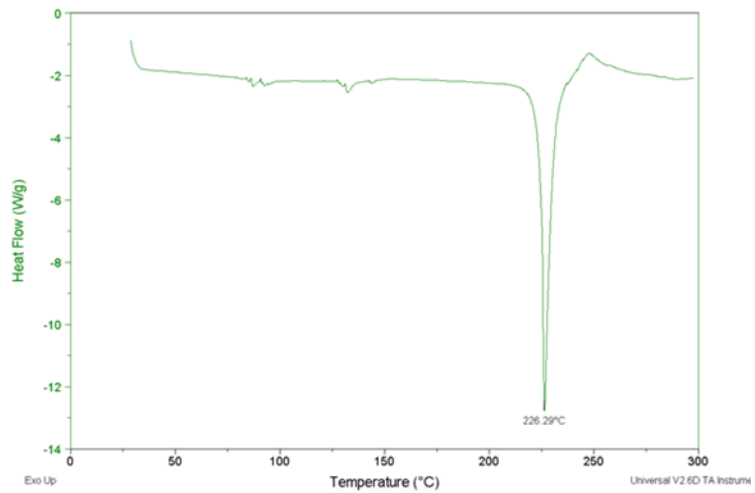
Gallic Acid•Isoniazid, GALINZ



PXRD of GALINZ

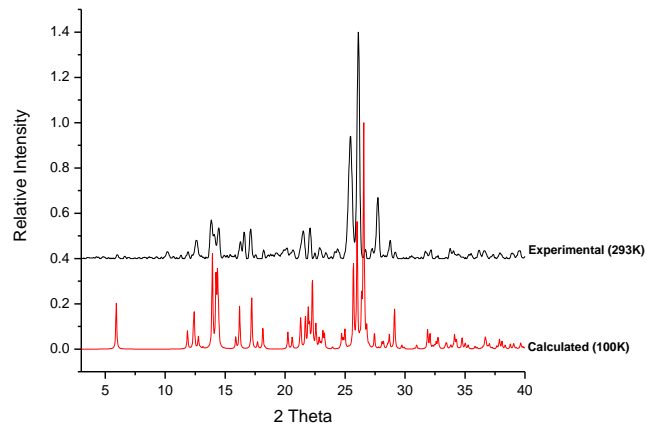


IR of GALINZ

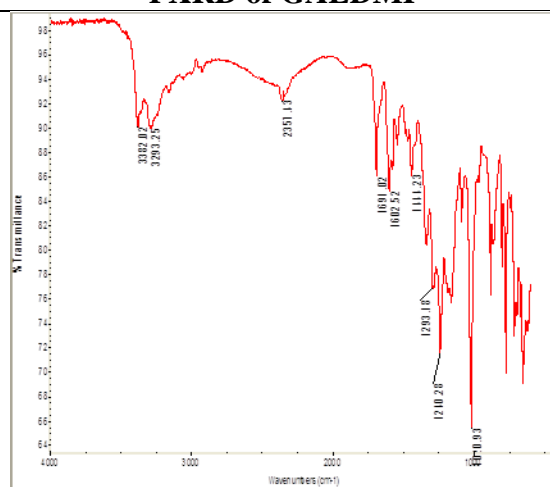


DSC of GALINZ

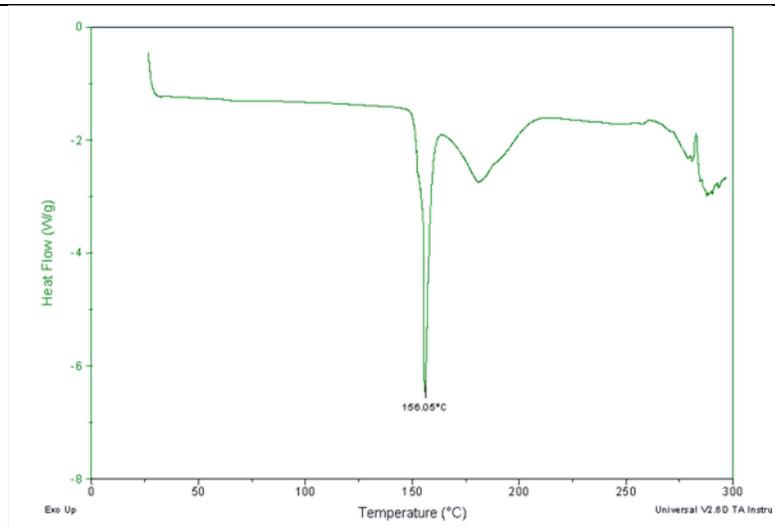
Gallic Acid•Dimethylpyrazole, GALDMP



PXRD of GALDMP

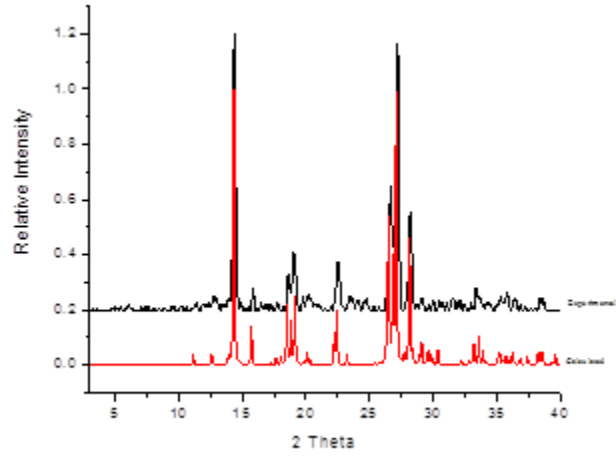


IR of GALDMP

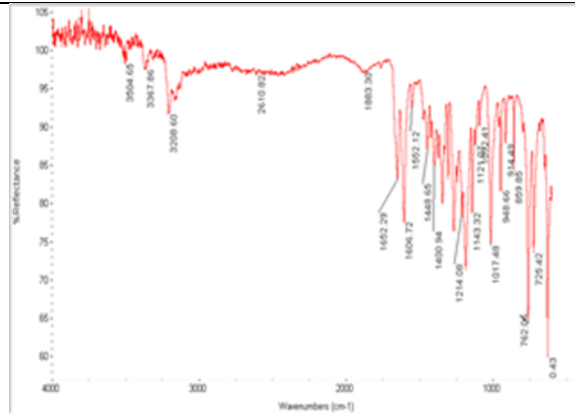


DSC of GALDMP

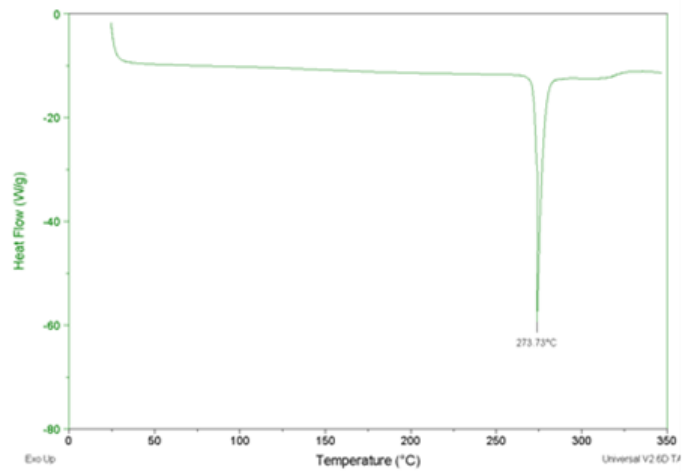
Gallic Acid•Adenine, GALADN



PXRD of GALADN

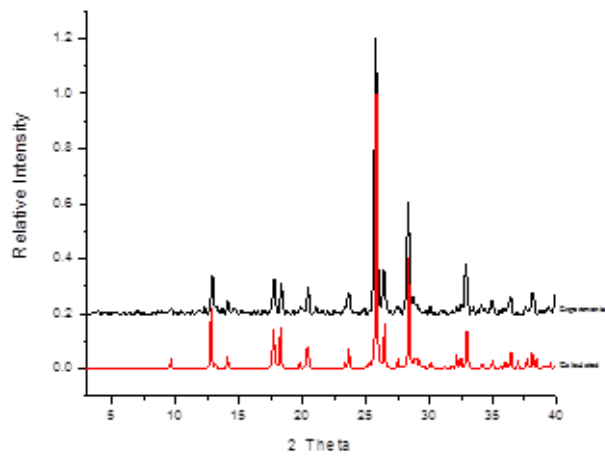


IR of GALADN

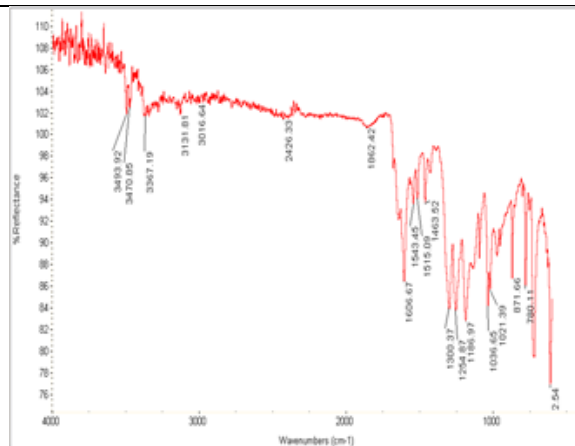


DSC of GALADN

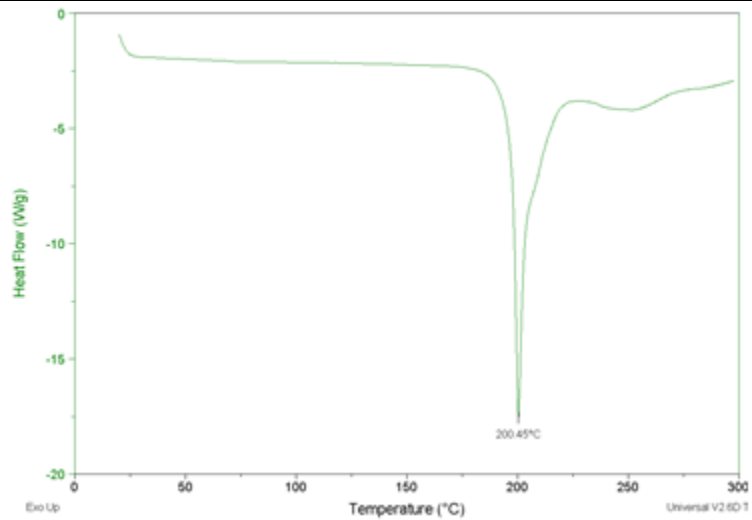
Gallic Acid•Urea, GALURE



PXRD of GALURE

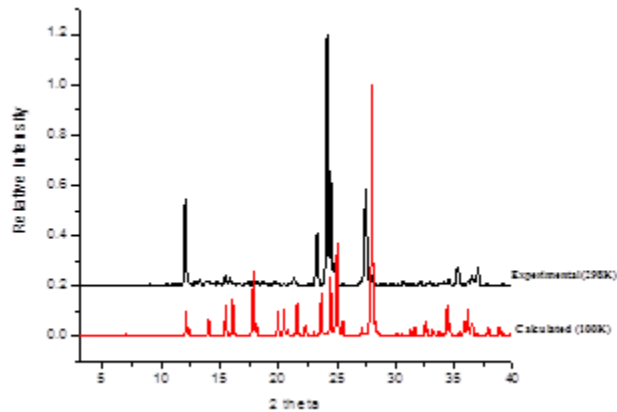


IR of GALURE

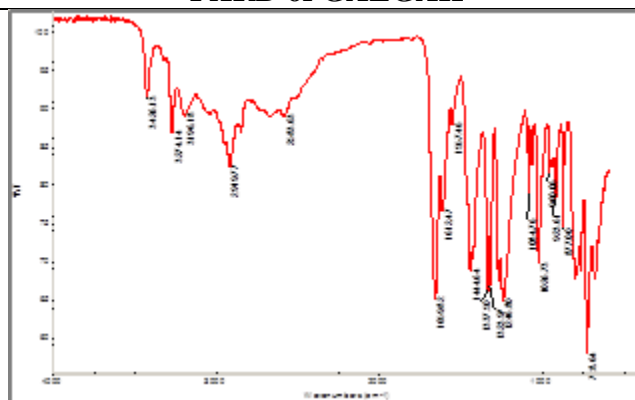


DSC of GALURE

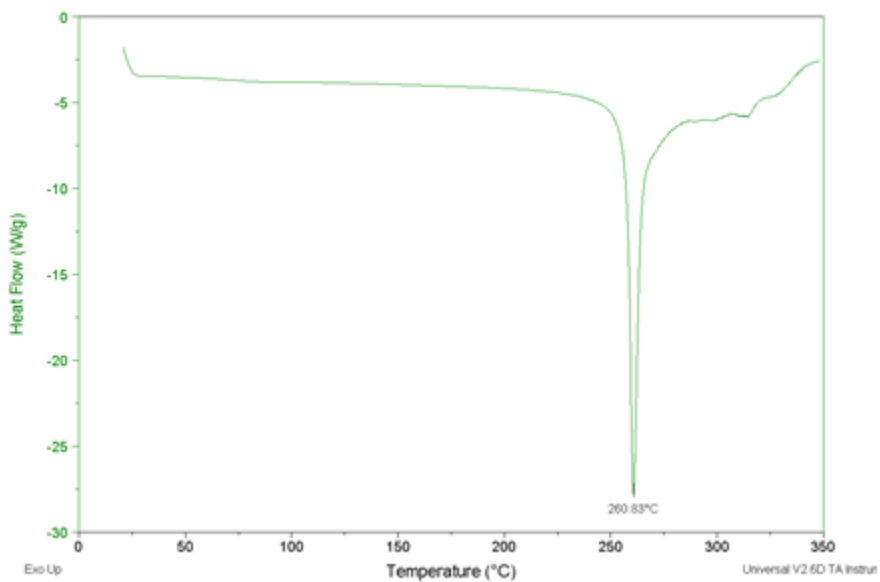
Gallic Acid•Glycine Anhydride, GALGAH



PXRD of GALGAH

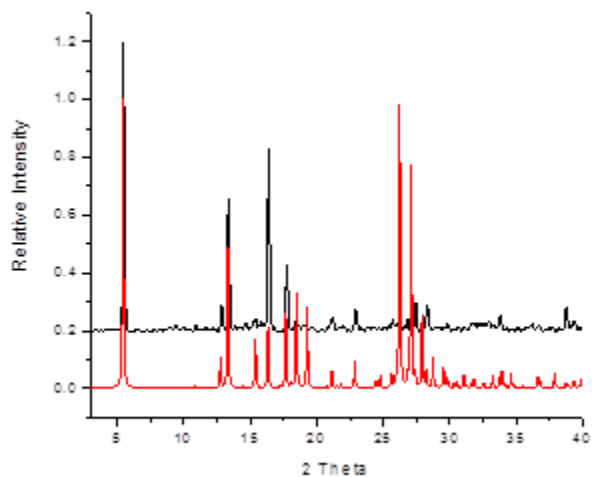


IR of GALGAH

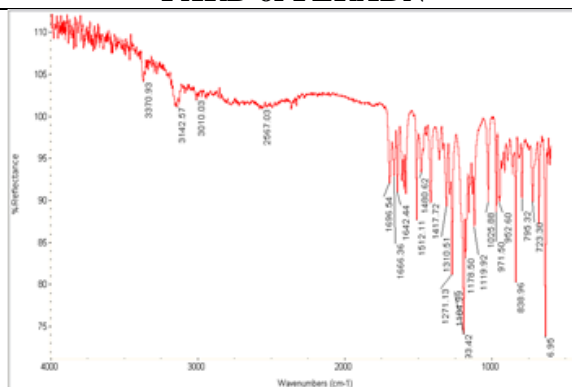


DSC of DSC

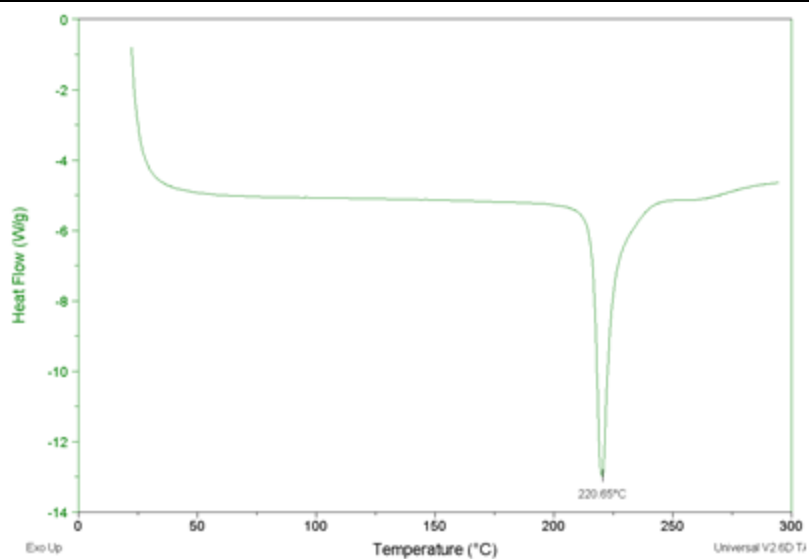
Ferulic Acid• Adenine, FERADN



PXRD of FERADN

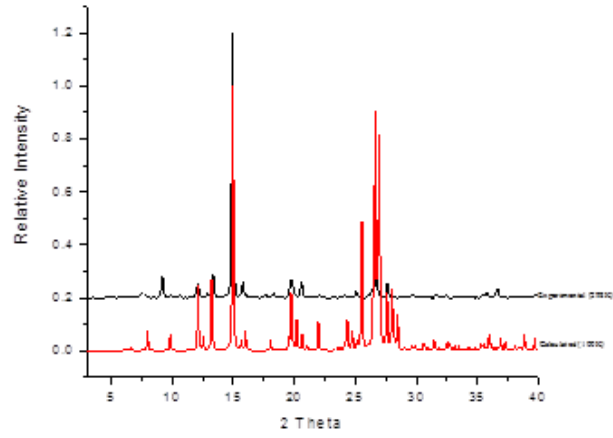


IR of FERADN

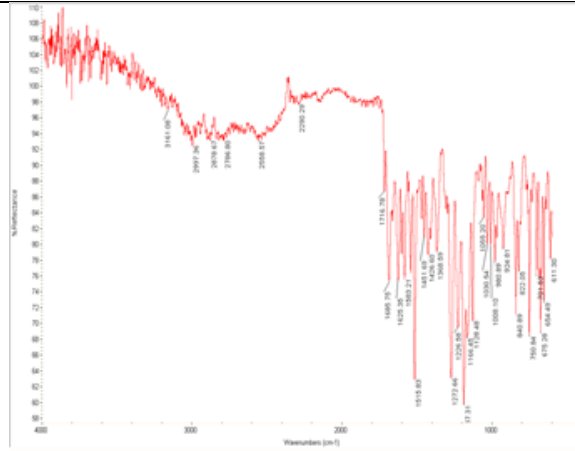


DSC of FERADN

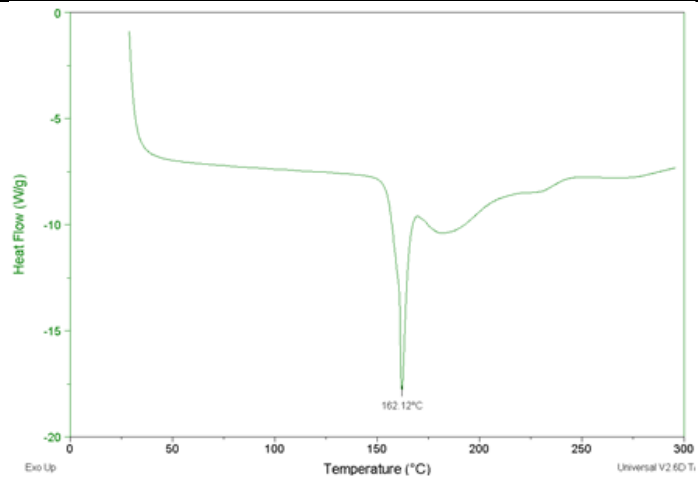
Ferulic Acid•Isoniazid, FERINZ



PXRD of FERINZ

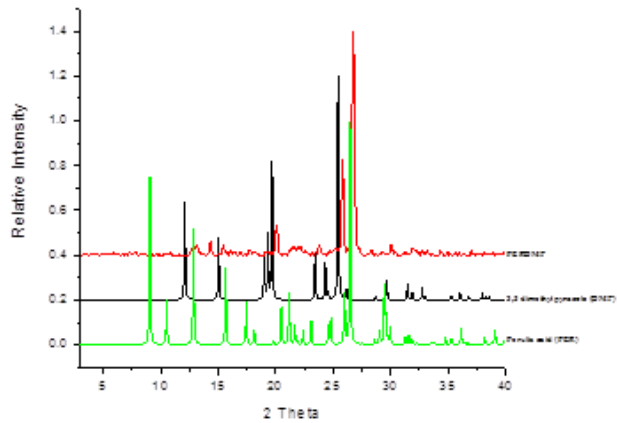


IR of FERINZ

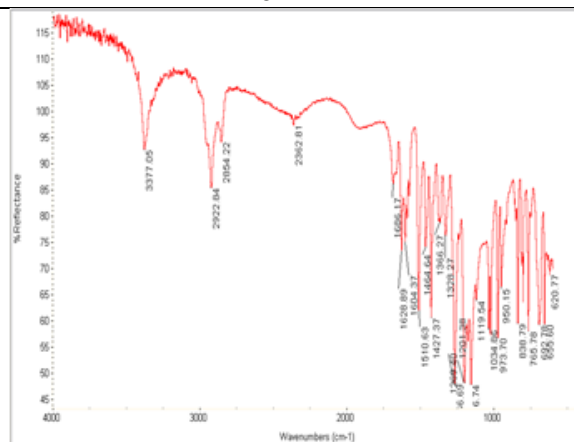


DSC of FERINZ

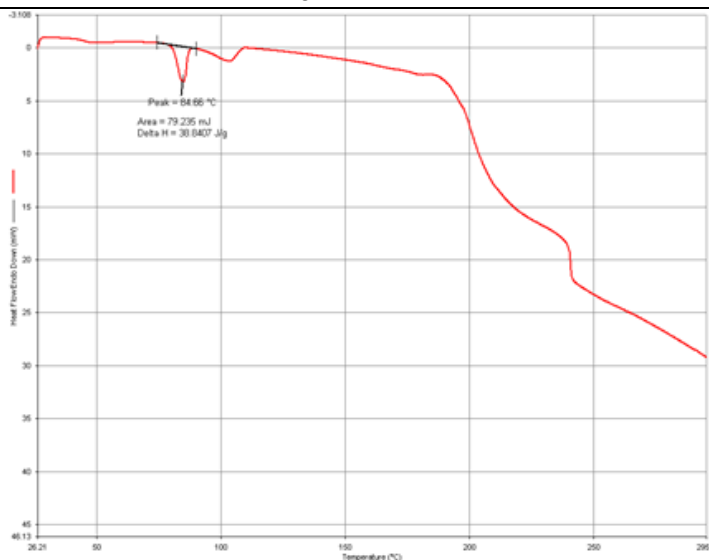
Ferulic Acid•Dimethylpyrazole, FERDMP



PXRD of FERDMP

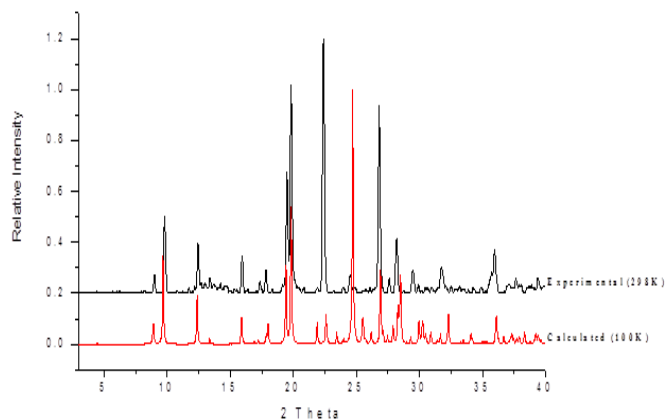


IR of FERDMP

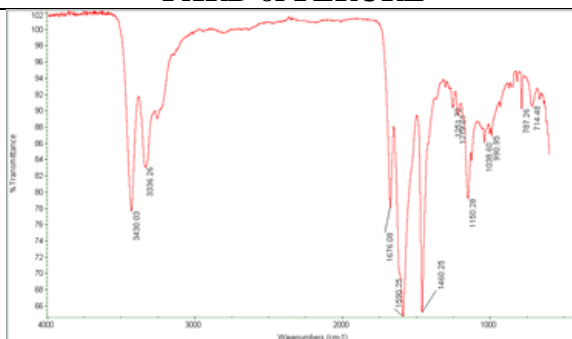


DSC of FERDMP

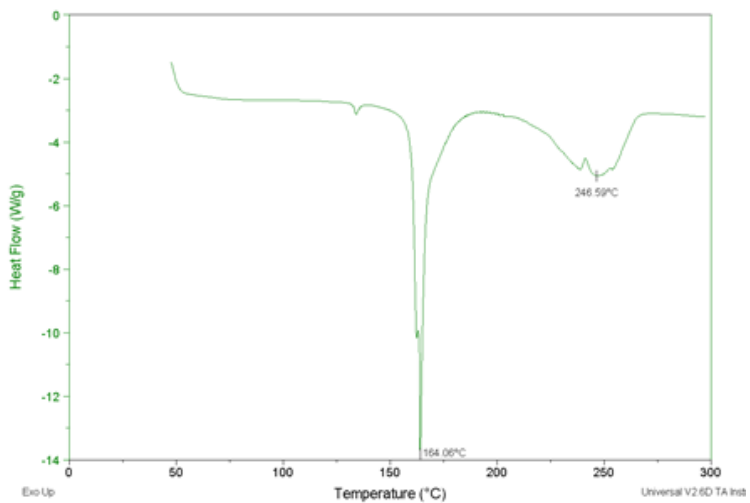
Ferulic Acid•Urea, FERURE



PXRD of FERURE

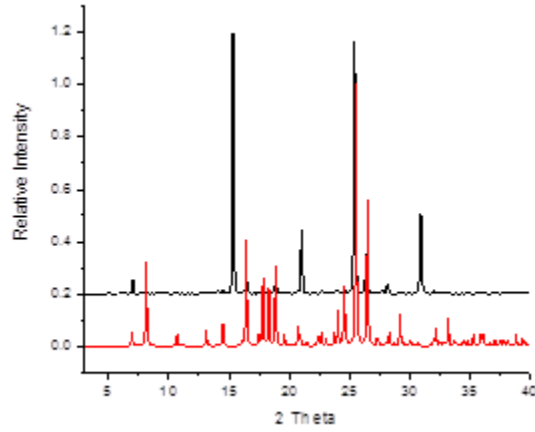


IR of FERURE

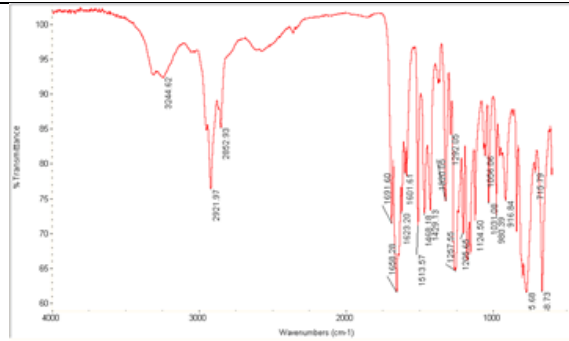


DSC of FERURE

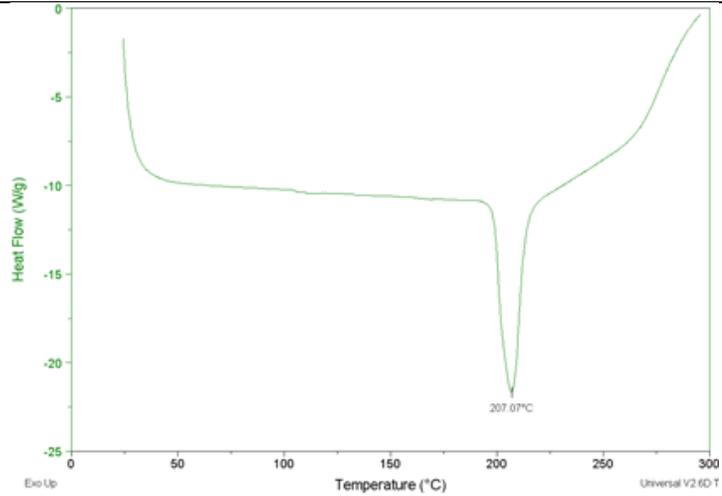
Ferulic Acid•Glycine Anhydride, FERGAH



PXRD of FERGAH

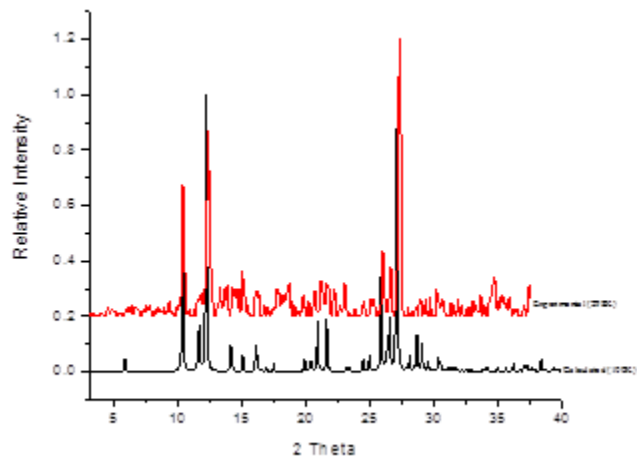


IR of FERGAH

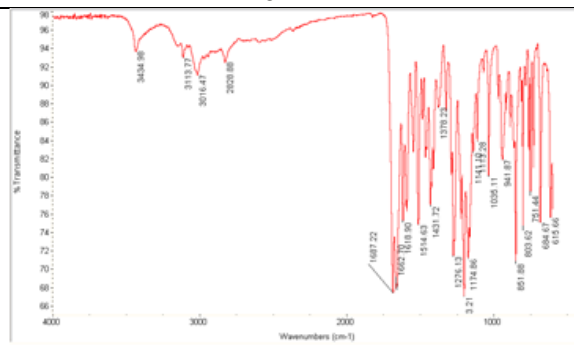


DSC of FERGAH

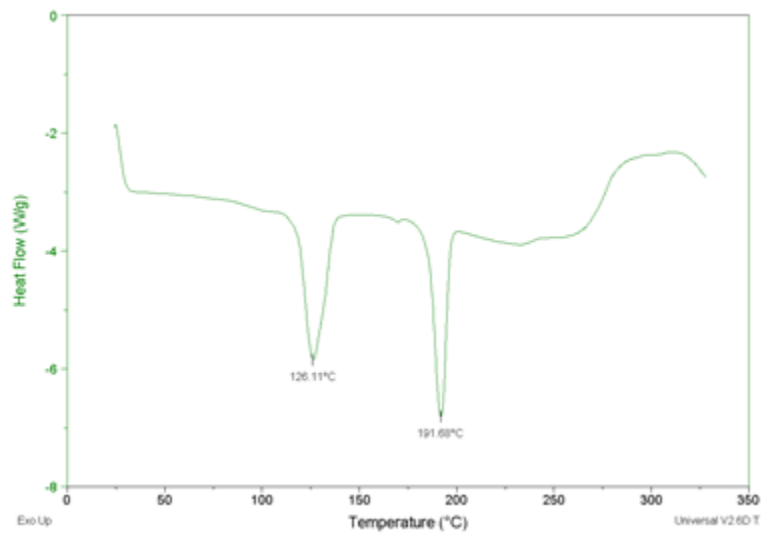
Ferulic Acid• Theobromine, FERTBR



PXRD of FERTBR

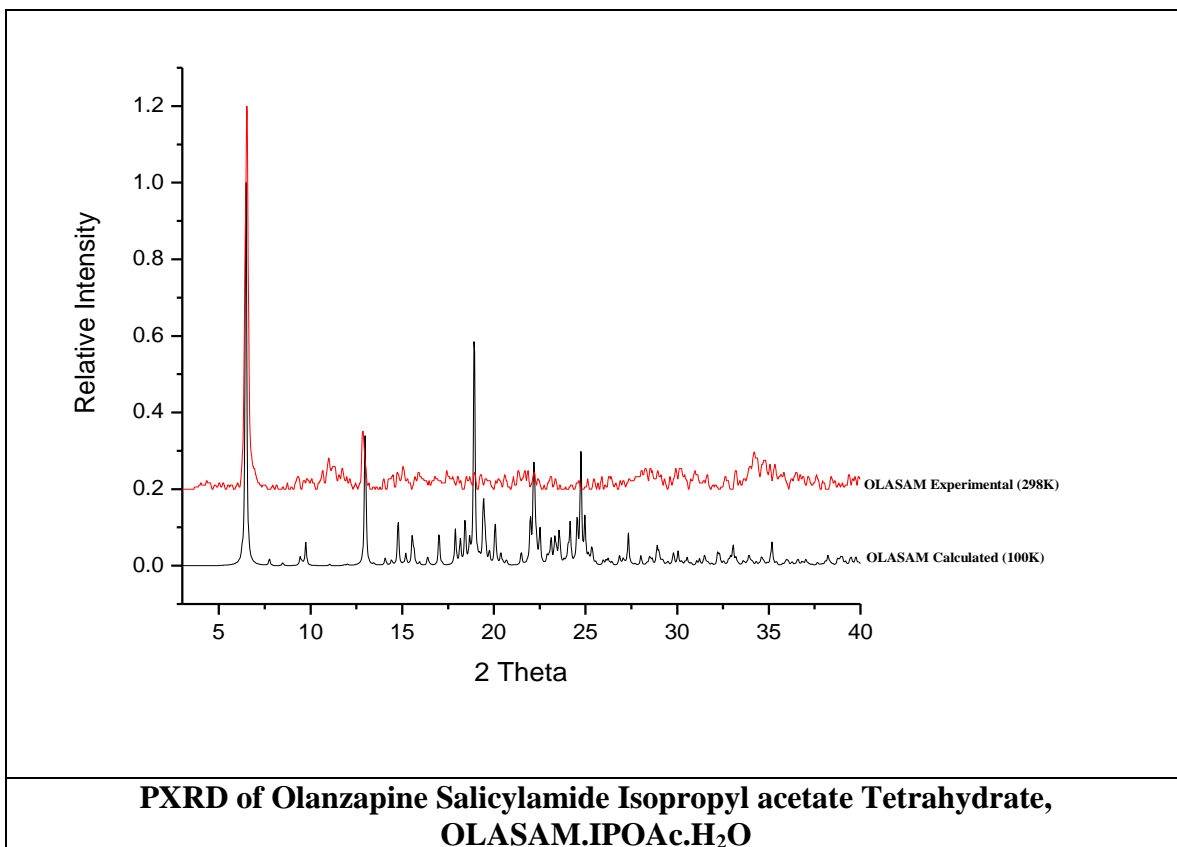
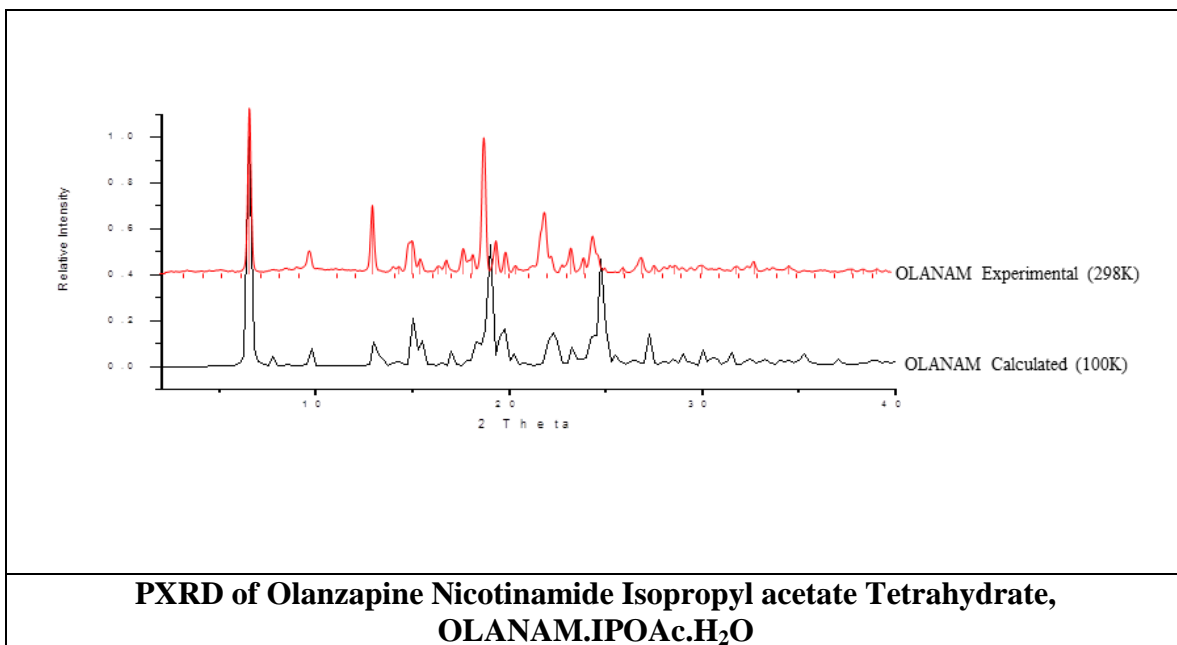


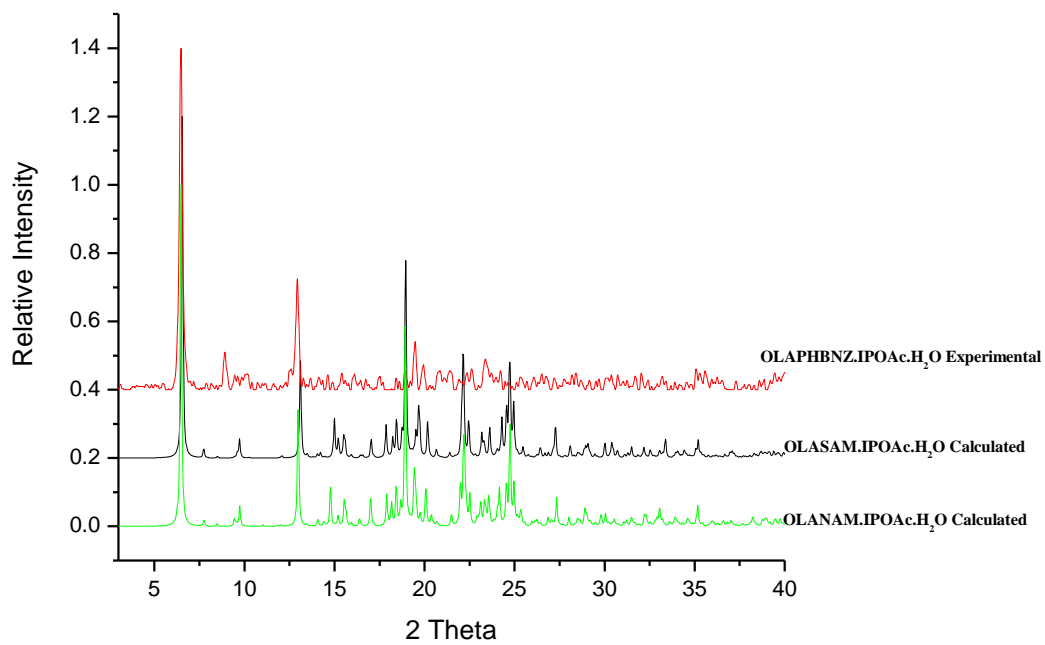
IR of FERTBR



DSC of FERTBR

Appendix 5: Supplementary Information: Crystal Engineering of Isostructural Quaternary Multi-Component Crystal Forms of Olanzapine.





**PXRD of Olanzapine *p*-Hydroxybenzamide Isopropyl acetate Tetrahydrate,
OLAPHBNZ.IPOAc.H₂O**

	OLANAM.IPA.4H₂O	OLASAM.IPA.4H₂O
Formula	C ₄₅ H ₆₄ N ₁₀ O ₇ S ₂	C ₄₅ H ₆₄ N ₁₀ O ₈ S ₂
MW (g/mol)	921.18	937.17
Crystal system	monoclinic	monoclinic
Space group	<i>P2₁/c</i>	<i>P2₁/c</i>
a (Å)	14.0961 (12)	14.1966(7)
b (Å)	12.5984 (10)	12.5375(6)
c (Å)	27.219 (2)	27.4599(15)
α (deg)	90	90
β (deg)	97.396 (2)	96.579(3)
γ (deg)	90	90
V / Å³	4793.6 (7)	4855.4
D_c/g cm⁻³	1.276	
Z	4	4
2θ range	1.46 to 25.04	3.13 to 67.47
Nref./Npar	8457/620	8186 / 594
T /K	100(2)	100(2)
R₁ [I>2σ (I)]	0.0676	0.0698
wR₂	0.1687	0.2120
GOF	1.018	1.010
Abs coef	0.171	1.492

Table 1: Crystallographic data and structure refinement parameters for cocrystals of olanzapine.

	Hydrogen bond	d (H···A) /Å	D (D···A)/Å	\angle (DHA)
OLANAM.IPOAc.H₂O	N-H···O	2.01(2)	2.878(4)	170(4)
	N-H···O	1.99(2)	2.865(4)	168(3)
	N-H···O	1.91(2)	2.829(4)	172(4)
	N-H···O	2.02(2)	2.926(4)	173(4)
	O-H···O	2.034(18)	2.909(4)	175(4)
	O-H···O	1.916(18)	2.771(4)	168(3)
	O-H···O	2.110(18)	2.956(4)	172(4)
	O-H···O	1.99(2)	2.840(4)	160(4)
	O-H···N	1.94(2)	2.764(4)	168(3)
	O-H···N	1.901(18)	2.772(4)	175(4)
	O-H···N	2.043(18)	2.896(4)	173(4)
	O-H···N	2.07(2)	2.939(4)	173(4)
OLASAM.IPOAc.H₂O	N-H···O	2.02(2)	2.894(4)	169(5)
	N-H···O	2.03(3)	2.881(4)	160(4)
	N-H···O	2.068(2)	2.958(5)	177(6)
	N-H···O	1.94(3)	2.812(5)	161(6)
	O-H···O	1.90	2.620(5)	143.7
	O-H···O	2.061(1)	2.922(4)	173(4)
	O-H···O	2.08(3)	2.847(4)	146(5)
	O-H···O	1.924(1)	2.783(4)	172(4)
	O-H···O	2.142(2)	2.976(5)	162(4)
	O-H···N	1.890(2)	2.750(4)	168(4)
	O-H···N	2.16(2)	2.984(5)	160(4)
	O-H···N	1.926(1)	2.790(5)	176(5)
O-H···N	2.049(2)	2.899(4)	167(5)	

Table 2: Selected hydrogen bond distances and parameters of cocrystals